STATUS OF THESIS

Title of thesis: The Effect of Acetic Acid on Film Formation in Carbon Dioxide Corrosion

I BUDI AGUNG KURNIAWAN

hereby allow my thesis to be placed at the Information Resource Center (IRC) of Universiti Teknologi PETRONAS (UTP) with the following conditions:

1. The thesis becomes the properties of UTP.
2. The IRC of UTP may make copies of the thesis for academic purposes only.
3. This thesis is classified as

☐ Confidential

☑ Non-confidential

If this thesis is confidential, please state the reason:

\-

The contents of the thesis will remain confidential for - years.

Remarks on disclosure:

\-

Endorsed by

Signature of Author	Signature of Supervisor
Permanent Address:	Name of Supervisor:
Perumdos ITS U-108	Ap.Ir.Dr. Mokhtar Che Ismail
60111 Surabaya, Indonesia	
Date: July 25, 2009	Date:

UNIVERSITI TEKNOLOGI PETRONAS

Approval by Supervisor (s)

The undersigned certify that they have read, and recommend to The Postgraduate Studies Programme for acceptance, a thesis entitled **"The Effect of Acetic Acid on Film Formation in Carbon Dioxide Corrosion"** submitted by **Budi Agung Kurniawan** for the fulfillment of the requirements for the degree of (Master of Science in Mechanical Engineering).

Date : July 25, 2009

Signature : ____________________________________

Main supervisor : Associate Prof. Ir. Dr. Mokhtar Che Ismail

Date : ____________________________________

Co-Supervisor 1 : Associate Prof. Dr. Mustafar bin Sudin___

Co-Supervisor 2 : ____________________________________

TITLE PAGE

UNIVERSITI TEKNOLOGI PETRONAS

The Effect of Acetic Acid on Film Formation in Carbon Dioxide Corrosion

By

Budi Agung Kurniawan

A THESIS

SUBMITTED TO THE POSTGRADUATE STUDIES PROGRAMME

AS A REQUIREMENT FOR THE

DEGREE OF MASTER OF SCIENCE IN MECHANICAL ENGINEERING

DEPARTMENT OF MECHANICAL ENGINEERING

BANDAR SERI ISKANDAR,

PERAK

JULY 2009

DECLARATION

I hereby declare that the thesis is based on my original work except for quotations and citations which have been duly acknowledged. I also declare that it has not been previously or concurrently submitted for any other degree at UTP or other institutions.

Signature : ____________________

Name : BUDI AGUNG KURNIAWAN

Date : July 25, 2009

ACKNOWLEDGEMENT

First and foremost, all praises and gratitude are due to Allah, the almighty God, for the blessing and guidance to me in my life.

First of all I would like to thank my supervisor Dr. Mokhtar Che Ismail for his fabulous support, guidance and excellent mentorship. I am very fortunate that he has supervised me. His enthusiasm and knowledge encouraged me to pursue higher level. May Allah bless him. And I would like to thank my co-supervisor Ass.Prof. Mustafar Sudin for advice and help during my research here.

I would also like to acknowledge my indebtedness to UTP technologists: En. Zairi, En. Anuar, En. Shairul, En. Faisal and En. Irwan for their invaluable assistance in technical matter. My sincere thank is also due to postgraduate office staffs for their assistance during my study. My postgraduate friends, thanks for everything.

Last but not least, I would like to thank to my family, especially my beloved wife Betta Handaru Liestyaningsih, for her patience and affection, and my beloved mother for endless support.

ABSTRACT

CO_2 corrosion is one of the main concerns in upstream oil and gas particularly during material selection process. The presence of other multi-corrosive species mainly acetic acid (CH_3COOH) further complicates the CO_2 corrosion mechanism, due to possible interaction between iron(II) carbonate ($FeCO_3$) and iron(II) acetate ($Fe(CH_3COO)_2$) film formation. This is important since most of the CO_2 prediction modeling is affected by the protectiveness nature of $FeCO_3$ film. Most of film formation studies in CO_2 environment were done by adding Fe^{2+} ions to induce the formation of a dense iron carbonate film. However, this methodology is not representing the operational condition where $FeCO_3$ film naturally formed. Thus, the objective of this research is to investigate the effect of acetic acid in CO_2 environment on the corrosion rate in natural filming condition. Electrochemical corrosion experiments and surface morphology investigation were performed to study the effect of 10-400 ppm acetic acid on mild steel in CO_2-saturated 3-wt% NaCl at pH 5.5, 90^oC in stagnant natural filming condition. Linear Polarization Resistance of 96 hours showed that in blank test (without acetic acid), the effect of $FeCO_3$ film formation was observed to decrease corrosion rate of 2.13 mm/yr at beginning to 0.25 mm/yr at the end of the test. Based on the morphology of film, there is small amount of $FeCO_3$ film formed and partially covered the steel surface at the end of test. The presence of a small amount of acetic acid below 60 ppm did not change corrosion rate as compared to the blank test. Corrosion rate increases significantly in the range of 2.26-2.65 mm/yr with 60-400 ppm acetic acid and affect the $FeCO_3$ film formation. The existence of acetate and bicarbonate ions in the solution caused a competition among them to react with Fe^{2+} ions, resulting delay the formation of $FeCO_3$ film and delay stability of corrosion rate. However, there was no evidence of iron(II) acetate film since the solubility of iron(II) acetate is high. There is no variation in the thickness of $FeCO_3$ film with more than 60 ppm acetic acid. This due to the longer time needed to reach saturation limit with the increase of acetic acid concentration. Polarization sweeps result show no difference in mechanism of corrosion. However the kinetics of corrosion varies with different concentration of acetic acid. Comparison with prediction tools showed an agreement about trend of corrosion rate at high temperature. There is no sufficient information on prediction tool regarding the effect of film formation to corrosion rate. In conclusion, the presence of acetic acid increases corrosion rate of mild steel in CO_2 environment, especially above concentration of 60-ppm. Acetic acid delays $FeCO_3$ film formation by reacting with Fe^{2+} ions and forms soluble iron(II) acetate. Iron carbonate film which found in both blank and acetic acid added corrosion samples was not fully protective.

Keywords: *CO_2 corrosion, acetic acid, mild steel, stagnant, natural filming condition, saturation, iron carbonate*

ABSTRAK

Korosi yang disebabkan oleh karbondioksida adalah sangat dititikberatkan dalam industri petroleum dan gas terutama semasa proses pemilihan bahan. Kehadiran pelbagai ejen korosi terutama asid asetik (CH_3COOH) merumitkan mekanisma korosi karbondioksida, terutama dalam kemungkinan interaksi antara besi karbonat ($FeCO_3$) dan besi(II) asetat ($Fe(CH_3COO)_2$). Ini penting kerana kebanyakan model ramalan korosi karbondioksida dipengaruhi oleh sifat dasar lapisan perlindungan $FeCO_3$. Kebanyakan penelahan pembetukan lapisan dalam suasana karbondioksida dilakukan dengan menambah ion Fe^{2+} untuk membentuk lapisan besi karbonat padat. Metodologi ini tidak menggambarkan keadaan operasional dimana lapisan lapisan $FeCO_3$ terbentuk semula jadi. Jadi, tujuan penyelidikan ini adalah menyelidik kesan asid asetat dalam persekitaran karbondioksida pada kadar korosi dan keadaan pembentukan lapisan semula jadi. Eksperimen korosi elektrokimia dan penyelidikan morfologi muka telah dijalankan untuk memerhatikan kesan 10-400 ppm asid asetik kepada mild steel dalam karbondioksida tepu, menggunakan 3-wt% NaCl pada pH 5.5, 90^{o}C, tidak mengalir dan kondisi pembentukan lapisan semula jadi. Hasil Linear Polarization Resistance selama 96 jam menunjukkan bahawa pada ujian menggunakan larutan tanpa asid asetik, pembentukan lapisan $FeCO_3$ menyusutkan kadar korosi 2.13 mm/yr pada awal ujian dan turun kepada 0.25 mm/yr pada akhir ujian. Berdasarkan morfologi lapisan, hanya sedikit sahaja lapisan $FeCO_3$ yang terbentuk dan ianya meliputi hanya separuh permukaan besi. Kehadiran sedikit asid asetik kurang daripada 60 ppm tidak mengubah laju korosi jika dibandingkan dengan larutan tanpa asid asetik. Kadar korosi meningkat secara nyata (2.26-2.65 mm/yr) ditunjukkkan dengan kepekatan asid asetic 60-400 ppm dan mempengaruhi pembentukan lapisan $FeCO_3$. Kewujudan ion asetat dan ion bikarbonat dalam larutan menyebabkan persaingan di antara kedua-duanya untuk bertindak balas dengan ion Fe^{2+} yang menghasilkan penundaan pembentukan lapisan $FeCO_3$ dan menunda stability kadar korosi. Bagaimanapun, tidak ada bukti pembentukan lapisan besi(II) asetat dikeranakan keterlarutan besi(II) asetat yang tinggi. Tidak ada keragaman ketebalan lapisan $FeCO_3$ dengan asid asetat 60 ppm atau lebih. Ini dikeranakan masa lebih lama untuk mencapai keadaan tepu dengan kenaikan kepekatan asid asetat. Data polarization sweep menunjukkan tidak ada perbezaan dalam mekanisme korosi. Akan tetapi, kinetic korosi berubah dengan kepekatan asid asetat yang berbeza. Perbandingan dengan alat peramalan menunjukkan kesesuaian trend kadar korosi pada suhu tinggi. Tidak ada kecukupan maklumat perihal pengaruh pembentukan lapisan film berkenaan dengan kadar korosi. Kesimpulannya, kehadiran asid asetik meningkatkan kadar korosi besi dalam persekitaran karbondioxida, terutama pada kepekatan 60 ppm atau lebih. Asid asetik melambatkan pembentukan lapisan $FeCO_3$ dengan bertindak balas dengan ion Fe^{2+} dan membentuk besi(II) asetat terlarutkan. Lapisan $FeCO_3$ yang terdapat pada semua sampel dengan dan tanpa asid asetik tidak sepenuhnya melindungi permukaan

Kata kunci: *korosi CO_2, asid asetik, mild steel, statik, keadaan pembentukan lapisan semula jadi, tepu, besi karbonat*

TABLE OF CONTENTS

CHAPTER V

LIST OF FIGURES

LIST OF TABLES

CHAPTER I
INTRODUCTION

1.1. Background

CO_2 corrosion of carbon steel has been one of the main concerns in oil and gas industry since 1940. CO_2 exists as dissolved gas in the formation water and corrodes mild steel pipelines. This CO_2 corrosion affects the materials used in production, transportation system and processing facilities. Recent issue in CO_2 corrosion is the presence of organic acid such as acetic acid, which is commonly found in oilfield, leads to an increase in corrosion rate of carbon steel pipelines[1-7].

Historically, CO_2 corrosion was discovered in 1940 and the presence of organic acid in oil and gas was first discovered in 1944. Certain correlation was found between the corrosivity of oil and gas fields and the presence of organic acids[1]. Many researchers [2-9] have performed an investigation on CO_2 corrosion as there are many interacting factors particularly operating parameters, kinetics, corrosion mechanism and electrochemical process. According to Fajardo *et.al*[2], severity of CO_2 corrosion depends particularly on temperature, CO_2 partial pressure, pH and surface film and organic acid. According to Schmidt and Hörstemeier[3], the rate of general corrosion mainly depends on the formation of protective, semi-protective or non-protective corrosion product scales which were affected by temperature, CO_2 partial pressure, pH, flow, alloy composition and mechanical stress.

In CO_2 corrosion when the concentrations of Fe^{2+} and CO_3^{2-} ions exceed the solubility limit, they combine to form iron carbonate ($FeCO_3$) film and precipitate on steel surface. Saturated condition of both species was needed for precipitation[8,10]. The existence of precipitated $FeCO_3$ film is an important factor in corrosion prediction and modeling since the coverage of the film affects corrosion rate and degree of protectiveness[11]. The effect of organic acid such as acetic acid on $FeCO_3$

film formation is one of great research interests due to the possibility of interaction between iron carbonate and iron(II) acetate films. Most studies on film formation in CO_2 corrosion are done by adding Fe^{2+} ion to induce $FeCO_3$ film formation. This method was used to obtain a dense iron carbonate layer and observe its protectiveness against corrosion.

1.2. Problem Statement

The existence of organic acid such as acetic acid in oil and gas pipelines becomes an important factor besides other known parameters of temperature, pressure and pH. Acetic acid mainly acts as source of hydrogen ion (H^+) and acetate ion (CH_3COO^-). The most important concern of acetic acid is on the possibility to affect $FeCO_3$ film formation. Acetate ion could react with Fe^{2+} ion and forms iron(II) acetate ($Fe(CH_3COO)_2$). This competition among carbonate/ bicarbonate and acetate ions yields thinning effect on film formed and formation of iron acetate could impair the protectiveness of $FeCO_3$ film layer. Further investigation is needed to observe CO_2 corrosion product characteristic with the presence of acetic acid and in natural filming condition.

1.3. Research Objective

The objective of this research is to investigate the effect of various concentrations of acetic acid in CO_2 environment on the corrosion rate, in stagnant (without effect of flow), high temperature and natural filming condition. This research investigates the morphology of $FeCO_3$ film as main corrosion product, precipitation rate and chemical reaction involved during corrosion process.

1.4. Scope of Study

The investigation is focused on the effect of different acetic acid concentrations to corrosion rate of mild steel. A stagnant condition (0 rpm of stirring rate) is chosen to ensure $FeCO_3$ film precipitation on steel surface without any removal effect from flow. This experiment is performed in natural film formation condition without any addition of Fe^{2+} to induce $FeCO_3$ film precipitation simulating typical service or operation condition. The corrosion mechanism and kinetics will be measured electrochemically by Linear Polarization Resistance and Potentiodynamic Sweep. Characterization of the film formation will be determined by Scanning Electron Microscope, Energy Dispersive X-Ray Spectroscopy and X-Ray Diffraction.

1.5. Organization of the Thesis

Five chapters are presented to produce a systematic investigation of CO_2 corrosion rate and film formation with the presence of acetic acid.

Chapter 1 describes the research background related to the CO_2 corrosion phenomena, parameters involved in corrosion process and film formation. Problem statement, research objectives and scopes of recent research are described in this chapter as well.

Chapter 2 reviews the corrosion theory and measurements, general CO_2 corrosion, species involved in CO_2 corrosion, mechanism and kinetic of corrosion process and effect of film formation and acetic acid on corrosion rate. This chapter describes previous findings especially related to parameter used, which are temperatures, pressure, pH, chemical species and concentration of acetic acid as well.

Chapter 3 describes experimental setup and methodology, consists of sample preparations, solution preparation, test matrix and parameters setting. This chapter also describes procedure of each experiment and goals that will be achieved.

At chapter 4, all results obtained from experiments are presented. Graph and tables will be given here, followed with chemical and precipitation calculations. There will be two types of results, which is qualitative and quantitative results. These results then will be analyzed and discussed to obtain main understanding and finding about the entire research.

At last, in chapter 5, conclusions and recommendations as result of analysis are presented. This chapter contains summarize of experiment's finding, goals achieved and recommendation for future work which might still be possible for development.

CHAPTER II

LITERATURE REVIEW

2.1. Corrosion Theory and Corrosion Rate Measurements

Corrosion is defined as the destructive attack of a material by reaction with its environment, by chemical or electrochemical reaction. Corrosion is electrochemical reaction consists of a set of reduction and oxidation reactions. Consider the case of a metal M dissolves in an acid. The metal is oxidized at anodic sites:

$$M \rightarrow M^{2+} + 2e^- \tag{1}$$

and hydrogen is reduced at the cathodic sites,

$$2H^+ + 2e^- \rightarrow H_2 \tag{2}$$

Due to the electrochemical nature of most corrosion processes, electrochemical methods can be used to measure the kinetics of electrochemical processes. An example of current and potential relationship of a mixed-couple system is shown in Figure (2.1). The equilibrium potentials of the couples in Equations (1) and (2) are labeled $E_{eq,M}$ and $E_{eq,H2}$, respectively. The corrosion potential is the potential at which the rate of oxidation of M (defined by current i_{Ox} is equal to the rate of reduction of H^+ (defined by current i_{red}).

$$i_{app} = i_{Ox} - i_{Red} = 0 \qquad \text{at } E_{corr} \tag{3}$$

and

$$i_{corr} = i_{Ox} = i_{Red} \tag{4}$$

$$\Delta E = b_a \log\left(\frac{i_{Ox}}{i_{corr}}\right) \text{ and}$$

$$\Delta E = b_c \log\left(\frac{i_{Red}}{i_{corr}}\right) \tag{5}$$

Since

$$\Delta E = E_{app} - E_{corr} \tag{6}$$

$$\log\left(\frac{i_{Ox}}{i_{corr}}\right) = \frac{\Delta E}{b_a} \text{ and}$$

$$\log\left(\frac{i_{Red}}{i_{corr}}\right) = -\frac{\Delta E}{b_c} \tag{7}$$

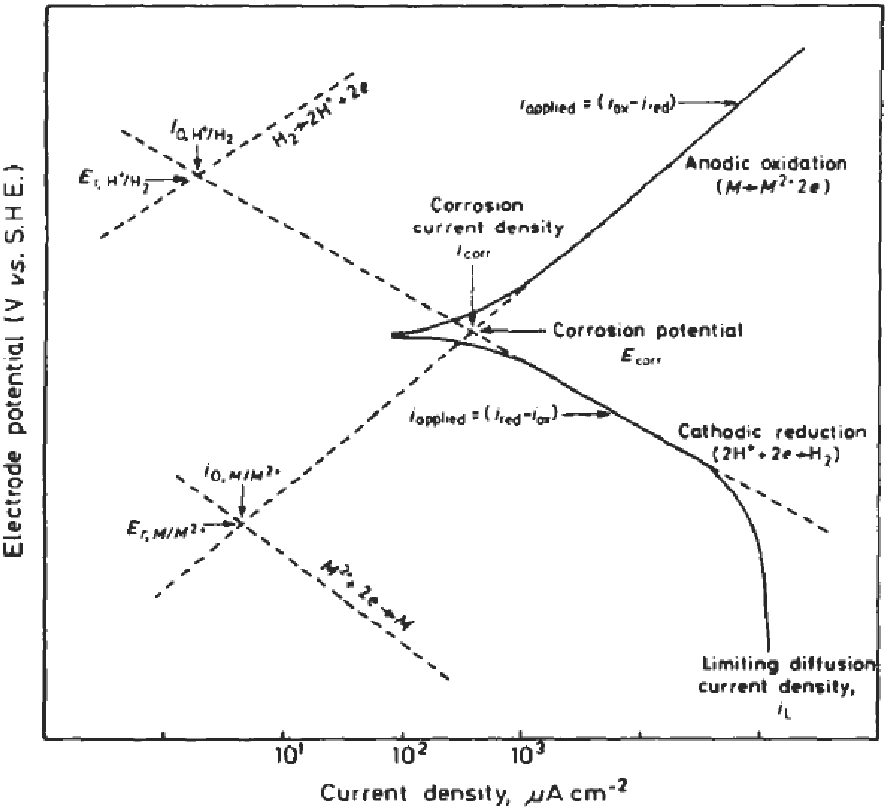

Figure 2.1 Potential vs log I for mixed electrode system[9]

$$10^{\frac{\Delta E}{b_a}} = \frac{i_{Ox}}{i_{corr}} \text{ and}$$

$$10^{-\frac{\Delta E}{b_c}} = \frac{i_{Red}}{i_{corr}} \tag{8}$$

Equation (8) can be simplified mathematically from an approximation of Taylor Series:

$$10^{x} = 1 + 2.3x + \left[\frac{(2.3x)^2}{2!}\right] + \ldots \left[\frac{(2.3x)^n}{n!}\right] \tag{9}$$

$$10^{\frac{\Delta E}{b_a}} = 1 + \frac{2.3\Delta E}{b_a} \text{ and}$$

$$10^{-\frac{\Delta E}{b_c}} = 1 - \frac{2.3\Delta E}{b_c} \tag{10}$$

Substituting equation (10) to equation (3) yields:

$$i_{app} = \frac{2.3 i_{corr} \Delta E (b_a + b_c)}{b_a b_c} \tag{11}$$

Where b_a and b_c are anodic and cathodic Tafel constants.

$$\frac{\Delta E}{i_{app}} = \frac{b_a b_c}{2.3 i_{corr} (b_a + b_c)} \tag{12}$$

$$i_{corr} = \frac{b_a b_c}{2.3(b_a + b_c)} \frac{\Delta i}{\Delta E} \tag{13}$$

Polarization resistance R_p is determined as the slope of the polarization curve near the corrosion potential.

$$R_p = \frac{\Delta E}{\Delta i} \text{ at } \Delta E = 0 \tag{14}$$

Hence, the equation can be rewritten to

$$i_{corr} = \frac{b_a b_c}{2.3(b_a + b_c)} \frac{1}{R_p} \tag{15}$$

Corrosion of a metal can be determined using equation related to Faraday's Law as:

$$CR = 3.27 \times 10^{-3} \frac{i_{corr} EW}{\rho} \tag{16}$$

Which

CR = corrosion rate (mm/yr)

i_{corr} = corrosion current density (μA/cm^2)

EW = equivalent weight (grams)

ρ = density of metal (g/cm^3)

2.2. CO_2 Corrosion on Steel

In CO_2 corrosion of steel, a number of chemical, electrochemical and transport processes occur simultaneously. When dissolved in water, CO_2 is hydrated to form carbonic acid (H_2CO_3) :

$$CO_2(g) \rightarrow CO_2(aq) \tag{17}$$

Concentration of dissolved CO_2 can be calculated using Henry's law for ideal gases and ideal solutions in equilibrium,

$$[CO_2(aq)] = p_{CO_2} \times K_d \tag{18}$$

Which p_{CO_2} is partial pressure of CO_2 and K_d is CO_2 solubility constant.

Dissolved CO_2 then hydrates to produce a weak acid called carbonic acid (H_2CO_3),

$$CO_2(aq) + H_2O \rightleftharpoons H_2CO_3(aq) \tag{19}$$

Carbonic acid concentration is only a small fraction (1/600) of the CO_2(aq) concentration[10]. Furthermore, H_2CO_3 dissociates in two steps to form bicarbonates and then carbonate ion:

$$H_2CO_3 \rightleftharpoons H^+ + HCO_3^- \tag{20}$$

$$HCO_3^- \rightleftharpoons H^+ + CO_3^{2-} \tag{21}$$

The concentration for each species at different pH can be illustrated on Figure below:

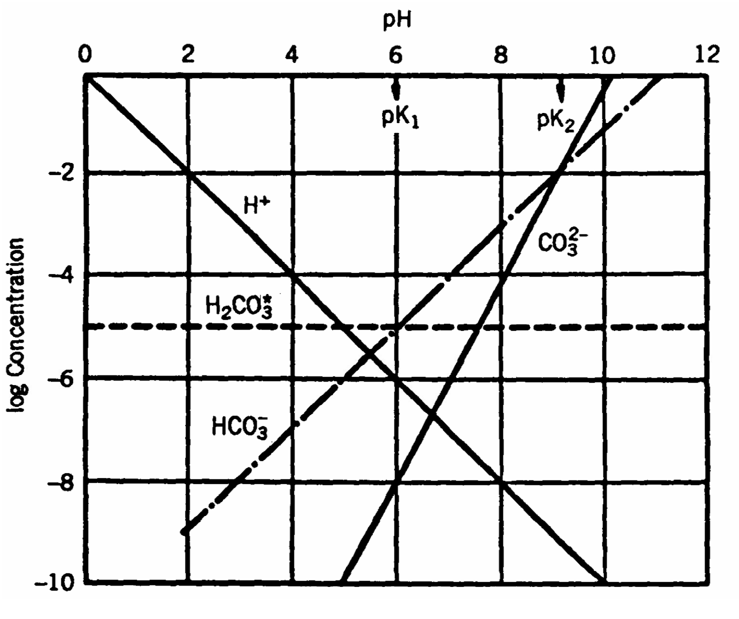

Figure 2.2. Carbonate species of seawater (20°C) in equilibrium at different pH[11]

Figure 2.2 above shows the concentration of H^+, H_2CO_3, HCO_3^- and CO_3^{2-} with respect to pH. The decreasing of H^+ concentration at high pH is followed by the increasing of bicarbonate (HCO_3^-) and carbonate (CO_3^{2-}) species according to chemical equilibrium however, carbonic acid (H_2CO_3) shows constant concentration for entire pH. HCO_3^- and CO_3^{2-} species are important at high pH values.

In practical CO_2 corrosion situations, many other species are present in the water solution. Therefore a large number of additional chemical reactions can occur which also depends on pH, temperatures, pressure[13].

The electrochemical dissolution of iron in CO_2 environment:

$$Fe \rightarrow Fe^{2+} + 2e^- \qquad (22)$$

Hence the overall reaction in CO_2 environment is:

$$Fe^{2+} + CO_2(aq) + H_2O \rightleftharpoons FeCO_3(aq) + H_2(g) \qquad (23)$$

Another equilibrium condition was offered by Mendoza and Turgoose [14] for pH below 7, since CO_3^{2-} species is considered minority (refer to Figure 2.1), HCO_3^- act as the species involved with Fe^{2+} for precipitation. Then, the formation of iron carbonate occurs according to:

$$Fe^{2+} + HCO_3^- \rightleftharpoons FeCO_3(s) + H^+ \qquad (24)$$

As shown in the equation (8) above, $FeCO_3$ precipitation is a function of Fe^{2+} concentration, bicarbonate ion concentration and pH.

The corrosion product in CO_2 corrosion is known as $FeCO_3$ film which is formed at high temperature and high pH[1-8,10,11]. This film becomes very important because lifetime of material used in services and corrosion predictions depend on the protectiveness of this film. Iron carbonate scales can reduce the corrosion process by presenting a diffusion barrier for the species involved in the corrosion process and by covering up a portion of the steel surface and preventing the underlying steel from further dissolution[15]. Schematic of CO_2 corrosion process of a metal under conditions where $FeCO_3$ film is present on metal surface is shown on Figure 2.3 below:

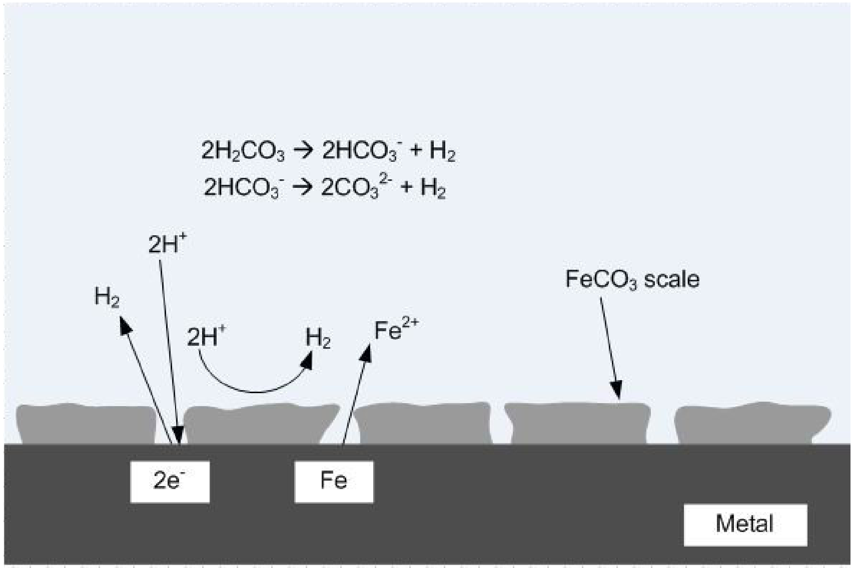

Figure 2.3. Schematic CO_2 corrosion of steel with $FeCO_3$ scale on metal surface[15]

Based on Figure 2.3 above, the surface covered by scale is not available for the anodic reaction. This is caused by the existence of scale, which prevent chemical reaction between surface and solution. In other hands it can be said that film formed have protected metal surface from corrosion process.

2.3. Factors Affecting CO_2 Corrosion

Many researchers described and investigated factors affecting CO_2 corrosion [1-8, 11,17,40]. In short, general and localized CO_2 corrosion are influenced by a number of factors, which is divided into interface-related, materials-related and medium-related parameters. Interface-related parameters include temperature, flow rate, condensation, and presence of scales. Materials-related parameters are alloy composition, microstructure and heat treatment. The influences of pH, CO_2 partial pressure, solution chemistry, and presence of oxygen belong to medium-related parameters. All parameters are interdependent and affect the CO_2 corrosion in different ways. Detail effect of each parameter would also been described in this chapter.

2.3.1. Temperature effect in CO_2 corrosion

The temperature strongly influences the CO_2 corrosion due to its effect on the rate of scale formation[18]. At low temperatures, corrosion rates increase because of high solubility of the $FeCO_3$ film. As temperature increases (around 60-80°C) the iron carbonate layer becomes more adherent to the metal surface and more protective in nature resulting in a decrease of the corrosion rate. Under this condition, dense crystalline films are formed which often give good protection. The effect film formation on corrosion rate at different temperatures is proposed by DeWaard and Milliams, shown in Figure 2.4 below.

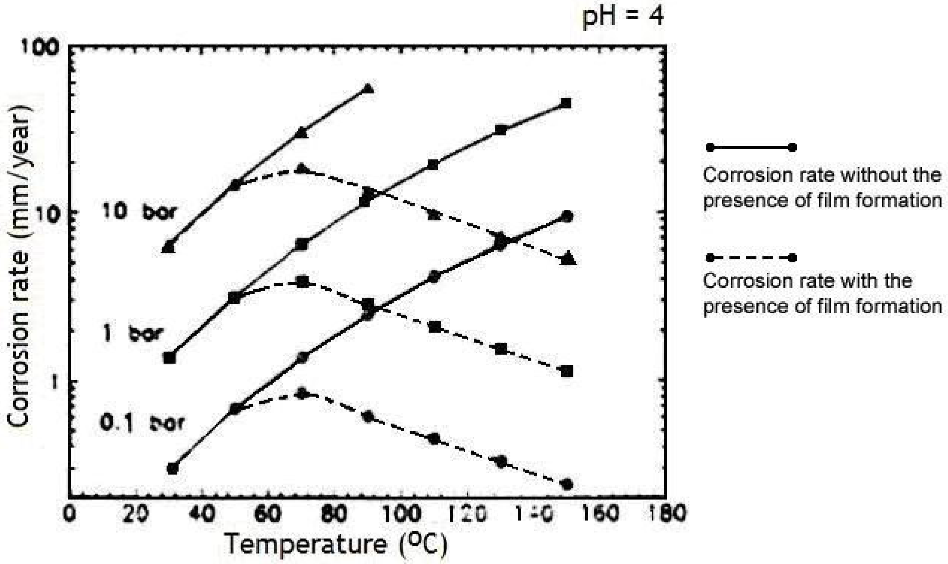

Figure 2.4. Effect of temperature on corrosion rate in CO_2 environment at pH 4 according to De Waard Milliams[18]

As shown in Figure 2.4, corrosion rate increases with increasing temperature. In the absence of $FeCO_3$ films, corrosion rate increases dramatically at high temperature. In condition where $FeCO_3$ film is favorable to form, corrosion rate reduces above 70°C due to the presence of film precipitation on the steel surface.

Many researchers also reported the correlation between temperature and corrosion rate. According to Crolet[20], at low temperatures, corrosion rate increase because of high solubility of $FeCO_3$ film. As temperatures increase (60-80°C), iron carbonate layer becomes more adherent to metal surface and more protective in nature yielding a decrease of corrosion rate. Ueda and Takabe[21] found that corrosion rate in CO_2 environment reach maximum at a critical temperature (T_{max}) and then decrease for both carbon and chromium steel. For carbon steel, temperature with highest corrosion rate was 80°C while for chromium steel temperature with highest corrosion rate was 100°C. In another paper, Takabe and Ueda[22] found that in CO_2 environment, the temperature with a maximum corrosion rate exists at around 100°C in carbon steel. This behavior is related to the formation of $FeCO_3$, which is the main corrosion product in CO_2 environments, and is classified into three types of corrosion namely below 60°C, at around 100°C and over 150°C. The first is a general corrosion type, the second is a ringworm or mesa corrosion type and the third is a corrosion resistant type through the formation of protective $FeCO_3$ film. CO_2 corrosion can be understood from the $FeCO_3$ formation behavior that the higher the temperature, the lower the solubility of $FeCO_3$.

Sun and Nesic[23] proposed that precipitation will occur if temperature is above 60°C, which corrosion rate had similar value as precipitation rate. This experiment was performed at pH 6, p_{CO_2} = 1 bar, $[Fe^{2+}]$ = 1 ppm, v = 1 m/s and temperature 20-90°C. No film formed at 20°C because supersaturation factor is less the 1, while at 60°C film precipitation started. By comparing the appearance of the iron carbonate layer for various temperatures, it was found that the surface coverage by the iron carbonate layer increased with the increase in temperature due to higher precipitation rate. In other paper, Nesic and Lee [24] revealed that at 50°C, corrosion rate at pH 6.6

remained high up to 30 hours of test. At 55^{o}C, corrosion rate started to decrease after 15 hours. While at 80^{o}C, corrosion rate directly decreased after few hours of test in the similar pH. This was caused by iron carbonate film resulting from the corrosion process. The increase in temperature enhanced $FeCO_3$ film by accelerating the kinetics of precipitation. Very protective films formed rapidly at 80^{o}C, while for lower temperatures (55 and 65^{o}C) kinetics of film formation was much slower. At 50^{o}C, kinetics was so slow that only some very porous film formation can be detected.

2.3.2. CO_2 partial pressure effect in CO_2 corrosion

The CO_2 partial pressure(p_{CO_2}) plays an important role in CO_2 corrosion both for film-free conditions (formation of non-protective films) and for film-forming conditions. In many publications[23,24,25,27,30], a relationship between CO_2 partial pressure and corrosion rate was established. However, higher CO_2 partial pressure does not mean necessarily also higher corrosion rates. This is a matter of environmental conditions.

Sun and Nesic [23] stated that increasing the CO_2 partial pressure from 4 to 18 bars under film-free conditions in a horizontal wet gas flow yields an increase of the corrosion rate from about 3 mm/year to about 8 mm/year. But an increase of the CO_2 partial pressure in the same flow system from 3.8 to 10.6 bar reduces the maximum corrosion rates from about 15 to 0.2 mm/year under conditions when semi protective films are formed, for example in the pH range below pH 5.2. Nesic and Lee[24] proposed that in the absence of protective films, an increase in CO_2 partial pressure will result in an increase of corrosion rate, because with increased CO_2 partial pressure, the direct reduction of H_2CO_3 to HCO_3^- will be accelerated due to an increase of H_2CO_3 concentration. However, when other conditions are favorable for formation of protective iron carbonate films, increased CO_2 partial pressure may help to facilitate the film formation. At a given high enough constant pH, an increase in CO_2 partial pressure results in an increase of CO_3^{2-} concentration and a higher supersaturation, thus speeding up precipitation and film formation.

According to Pursell[25], generally under film-free conditions higher CO_2 partial pressures result in higher corrosion rates by reducing the pH and increasing the rate of carbonic acid reduction. While according to Singer[27], partial pressure of CO_2 has little influence on the corrosion rate respectively at low temperature and high cooling, and at high temperature and low cooling. On the other hand, at high temperature and high cooling, the influence is more significant. It can be explained by the fact that at a low condensation rate it is easier to saturate the liquid film with corrosion products, increasing the pH and retarding the kinetics of the reaction of corrosion by CO_2. At a high condensation, it is impossible to saturate the liquid film and the pH could be more sensitive to the influence of the partial pressure of CO_2. The anodic reaction is practically unaffected when the CO_2 partial pressure is increased from 3 to 20 bar while the cathodic limiting current density is strongly increased due to a higher reservoir of carbonic acid. This again indicates that in CO_2 corrosion the pH is only an orientating parameter for assessing the corrosiveness. What really matters is the availability of carbonic acid and the surface sites for its reduction. Furthermore, in the case of scale-free CO_2 corrosion, an increase of p_{CO_2} typically leads to increase in the corrosion rate. The explanation is that by referring to Henry's Law, there is tendency of increasing CO_2 concentration in the solution. Hence, the concentration of carbonic acid also increases. This can increases cathodic reaction and ultimately corrosion rate. However, when other conditions are favorable for formation of ferrous carbonate layers, increased p_{CO_2} can have beneficial effect. At high pH, higher p_{CO_2} leads to an increase in bicarbonate and carbonate ion concentration and a higher supersaturation, which accelerates precipitation and protective layer formation.

In another case, Cabrini, *et.al* [30] observed an increase of the CO_2 partial pressure from 1 to 30 bar in an unbuffered 0.1 % NaCl solution yielded an increase of the corrosion rate of rotated low alloy steel probes from 2 to 4 mm/y at 40°C and from 1.5 to 2.5 mm/y at 90°C. Thus, the correlation between the corrosion rate of low alloy steels and the CO_2 partial pressure is quite complicated and by no means linear. So far, there is no model which can predict this correlation satisfactorily and needs to be further explored.

2.3.3. pH effect in CO_2 corrosion

pH affects the CO_2 corrosion of carbon steels by different mechanism. Increased pH values generally lead to a reduction of the corrosion rate by influencing the electrochemical mechanisms and the formation of protective iron carbonate film [3]. By an increase of pH, the cathodic reduction of H^+ is slowed down which decreases the anodic dissolution rate of iron. Furthermore at very high pH values, protective carbonate scales are formed on the surface that reduces the corrosion rate significantly with time[26,27]. This is due to the effect of decreasing the solubility of iron carbonate in the solution as shown on Figure 2.5.

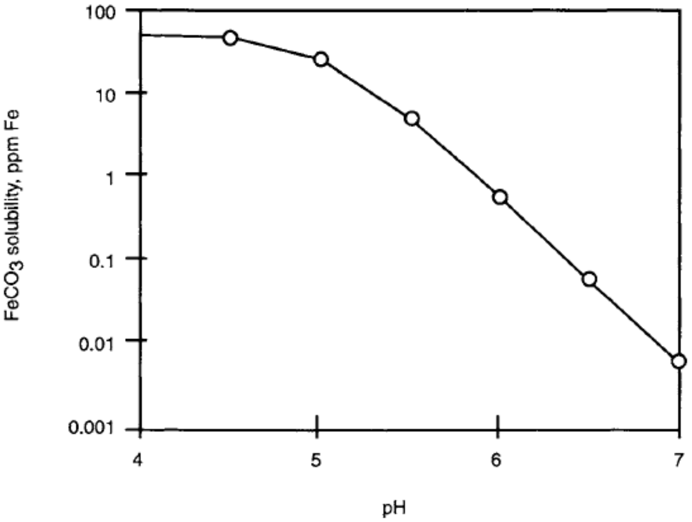

Figure 2.5 Effect of iron carbonate solubility at different pH[26]

According to Kun Lin[23] at higher pH (pH>5) and higher CO_2 partial pressure (≥1 bar) the cathodic reaction is controlled by the direct reduction of H_2CO_3, which is related to the amount of dissolved CO_2. The indirect effect of pH on the formation of protective films (such as iron carbonate) is the most important factor. Higher pH leads to a decreased solubility of iron carbonate and thus results in an increased precipitation rate, faster formation of protective films and hence reduction of the corrosion rate.

It was found that at lower temperatures, protective scales could only be formed when the pH 6 or more, while above 80°C protective scales are easily formed[32]. In another study[33], flow loop tests with carbon steel, protective scales only could be observed for pH greater than 5.0. Also at pH 5, reduction of H_2CO_3 was the dominant cathodic reaction. Reduction of H_2O was not affected by the presence of CO_2.

2.3.4. Effect of Surface Films in CO_2 Corrosion

In CO_2 corrosion, when the concentration of $FeCO_3$ exceeds the solubility limit, they combine to form iron carbonate films on the steel surfaces as mentioned above. Therefore, high saturation near surface is needed for the formation of protective films. Once the film is formed, it will remain protective at a much lower supersaturation. According to Schmitt and Hörstemeier[3], to get a successful protection, the film must be adherent and cover the whole surface. The protective properties of the surface scale depend on the characteristics of the material (metal composition, heat treatment/microstructure) and the environmental conditions (temperature, CO_2 partial pressure, pH)[4]. Temperature strongly influences the conditions needed to form protective iron carbonate layers. At lower temperatures (<60°C) the solubility of $FeCO_3$ is high and the precipitation rate is slow and protective films will not form unless the pH is increased. Furthermore, *in-situ* measurement of the conductivity of iron carbonate films revealed that iron carbonate films exhibit a very low electrical conductivity and act as an insulator[25]. Therefore, carbonate films can not act as cathodic sites, which mean they are not comparable with iron sulfides which exhibit electronic conductivity. This is also true when cementite is dispersed in the carbonate film.

The precipitation rate of $FeCO_3$ has been described as slow and temperature dependent process and even under supersaturated conditions, high corrosion rates can maintain for weeks until protective iron carbonate layers are formed, specifically at low temperatures. Furthermore, in flow systems corrosion films obviously can grow for months without giving protection unless the steel is exposed to stagnant or "wet" conditions [26]. During a few days stagnation, corrosion products can accumulate on the steel surface and form protective films. Thus, the kinetics of $\mathrm{FeCO_3}$ precipitation seems to be a controlling factor for the protectiveness of the corrosion product layer. At higher temperature, the $\mathrm{FeCO_3}$ solubility is reduced and the precipitation rate is much faster, thus allowing the formation of iron carbonate films.

Protective carbonate scales can be recognized already by its morphology and crystallinity. At temperatures ≥ 90°C the scale is composed of well-defined and well-packed cubes, while at lower temperatures a flat grain-type appearance is found[26]. However, the morphology of iron carbonate scales depends not only on the temperature, but also on the pH and the CO_2 partial pressure, as well. At higher pH values (>6.5), protective iron carbonate films can also form at room temperature [27,28]. Gulbrandsen[31] has found that the relative supersaturation is an important factor for film growth and the protectiveness of the film.

2.4. Iron Carbonate ($FeCO_3$) Film Formation

Iron carbonate ($\mathrm{FeCO_3}$) film formation is the main corrosion product in the CO_2 corrosion process. In case of blank CO_2 corrosion, when the concentrations of Fe^{2+} and $\mathrm{CO_3^{2-}}$ exceed the solubility limit, solid iron carbonate precipitates as follows:

$$\mathrm{Fe^{2+} + CO_3^{2-} \rightarrow FeCO_3} \tag{25}$$

$$\mathrm{Fe^{2+} + H_2CO_3 \rightarrow FeCO_3 + H_2} \tag{26}$$

The electrochemical reactions are often accompanied by the formation of films of $\mathrm{FeCO_3}$, which can be protective or non-protective depending on the conditions inside solution.

Iron carbonate precipitates at steel surface and decreases the corrosion rate by [5]:

- Presenting a diffusion barrier for the species involved in the corrosion process;
- Blocking a portion of the steel and preventing electrochemical reactions from occurring underneath it.

Mechanism of $FeCO_3$ film formation was well explained by Hunnik *et.al* [10]. The reduction of the corrosion process by $FeCO_3$ film can be visualized as follows: first stage is nucleation. Initiation of $FeCO_3$ sites develop arbitrarily. Second stage is the growth. Some of local sites grow continuously, while at the other sites, nucleation still exists. The films start to cover steel surface. The third stage is propagation. Iron carbonate film covers steel surface thoroughly and corrosion rate decreases due to coverage layer. After the layer establish, the reaction between metal surface and solution will stop.

The exact corrosion reduction is difficult to predict in view of the many factors involved, like the type of steel, the flow velocity (both shear stress and mass transport effects), temperature, CO_2 partial pressure and formation water composition. It is clear that a full description of the influence of precipitation on corrosion rate is far too complicated. However, prediction of the corrosion rate reduction may be possible under specific conditions. A further observation is that corrosion can only be reduced if the precipitation rate is of the order of the corrosion rate, If iron precipitation would be much slower than iron dissolution, steel surface would be corroded away before a protective, dense layer could form.

According to Nesic[15], corrosion rate was reduced at pH 6, T 50^oC, partial pressure of CO_2 2 bar with “extreme” thin films, suggesting the importance of the so-called surface coverage effect when a portion of the surface under the films becomes “unavailable” for corrosion. Electrochemical reactions do not occur at the locations of the surface where the film is attached to the metal.

The corrosion product, iron carbonate, may form a protective film or semi-protective film that controls the corrosion. Iron(II) acetate, which is more soluble than iron carbonate, interacts with the iron carbonate formation leading to an increase in corrosion rate. According to Hedges *et.al* [17], HCO_3^- was shown to decrease the corrosion rate, while CH_3COO^- in the form of CH_3COOH decreases the pH and increases the corrosion rate, and even greater than that predicted by some of the models. If the acetate ion presents, it will be converted to iron(II) acetate and eventually exhausted. At that time, the iron carbonate film starts to thicken and the corrosion rate reduces in the absence of CH_3COO^-. Thus, the mechanism by which acetic acid increases the corrosion rate may be explained by its ability to decrease the pH and solubilise Fe^{2+}, thus reducing the iron carbonate film thickness. This interaction between iron(II) acetate and iron carbonate film, however, not widely studied.

Ueda *et.al* [21] stated that the higher the temperature, the lower solubility of $FeCO_3$, it means corrosion product remains in the steel surface. This temperature dependent growth mechanism also has been observed in a number of experiments [1-11]. Experiments also have shown that an apparently dense corrosion film is formed directly on the metal surface when good protection is obtained, while a porous film, sometimes filled with iron carbonate in the outer part only, is formed when corrosion protection is obtained.

According to Ueda *et.al* [22], corrosion rate for 1% - 2% Cr steel increase until reach temperature (T_{max}) 75^oC and then decrease as the Fe^{2+} ion concentration on the steel exceed the solubility of $FeCO_3$. and the T_{max} shift to higher temperature following the addition of acetic acid. Therefore, it is thought that the reaction rate of $FeCO_3$ film formation reaction plays an important part in the corrosion behavior.

It is well recognized that the temperature strongly influences the conditions needed to form protective iron carbonate layers. At lower temperatures (<60°C) the solubility of $FeCO_3$ is high and the precipitation rate is slow and protective films will not form unless the pH is increased [16,21]. In this temperature range the corrosion rate increases with temperatures up to an intermediate range of 60 – 80 °C. Above 60°C the protectiveness of the iron carbonate layer increases with temperature due to the decrease of iron carbonate solubility and, thus, the corrosion rate is reduced.

The precipitation rate of $FeCO_3$ has been described as slow temperature dependent process and even under supersaturated conditions, high corrosion rates can maintain for weeks until protective iron carbonate layers are formed, especially at low temperatures. During a few days stagnation, corrosion products can accumulate on the steel surface and form protective films. Thus kinetics of $FeCO_3$ precipitation seems to be a controlling factor for the protectiveness of the corrosion product layer. At higher temperatures the $FeCO_3$ solubility is reduced and the precipitation rate is much faster, thus allowing the formation of iron carbonate films [23]. Protective carbonate scales can be recognized already by its morphology and crystallinity. At temperatures $\geq$ 90°C the scale is composed of well-defined and well-packed cubes, while at lower temperatures a flat grain-type appearance is found [26]. However, the morphology of iron carbonate scales strongly depends not only on the temperature, but on the pH and the CO_2 partial pressure, as well. At higher pH values (>6.5), protective iron carbonate films can also form at room temperature.

2.5. CO_2 Corrosion with Acetic Acid

The presence of acetic acid can have important effects on the CO_2 corrosion, and this subject has been investigated by several authors[1,3,5,6,11,13,15,17,19,40]. The open literature indicates that the presence of acetic acid in the liquid phase leads to an increase in the general corrosion rate. Detailed studies of organic acids in CO_2 production were first made in the 1980's by Crolet and co workers[1] who observed a significant increase of the CO_2 corrosion rate in the presence of acetic acid (CH_3COOH) at pH 4 while the effect vanished at pH 6 and higher. This could be explained by the dissociation of CH_3COOH, because at different pH values different amounts of undissociated acetic acid and Ac^- are present in the solution. With increasing pH values, the concentration of free acetic acid in the solution decreases. They also have proposed a classification where less than 60 ppm CH_3COOH is regarded to give only slightly increased risk of corrosion, while concentrations of more than 60 ppm significantly increase the corrosiveness. Acetic acid dissociates according to equation below:

$$CH_3COOH \rightleftharpoons H^+ + CH_3COO^- \tag{27}$$

And reaction between CH_3COOH and carbon steel yields iron(II) acetate ($Fe(CH_3COO)_2$)

$$Fe^{2+} + 2(CH_3COOH) \rightarrow Fe(CH_3COO)_2 + H_2 \tag{28}$$

It is believed that acetic acid influences the corrosion process in two ways [5]. First, the acetic acid acts as a provider of hydrogen ions and has a limited effect on the pH (acting as a buffer). Secondly, the free acetic acid is believed to be reduced directly on the metal surface in a similar way as carbonic acid. The contribution to the hydrogen ion reduction leads to an increase of the cathodic current. Gulbrandsen[10] found that at 80^oC the average corrosion rate increased with increasing CH_3COOH concentration, and corrosion attack was in uniform pattern. The existence of $Fe(CH_3COO)_2$ may reduce the driving force for protective $FeCO_3$ film formation, because of consuming Fe^{2+} ion and carried away to solution.

Hedges *et.al.*[17] showed that presence of acetate ion (CH_3COO^-) can increase corrosion rate even if pH increases. Also the presence of acetate ion only affects the corrosion rate and not the corrosion mechanism. The concentration of acetic acid has significant effect on the initial corrosion rate. The presence of 100 ppm CH_3COOH increases the corrosion rate after 1 hour from 3.8 mm/year to 9.1 mm/year. The presence of CH_3COOH made corrosion rate increases initially and rises to a maximum value. As concentration of CH_3COOH increased, the time taken to reach maximum corrosion rate increased as well. Eventually the corrosion rates decline and tend towards the values generated in the absence of CH_3COOH.

The presence of acetic acid could also affect the properties of the iron carbonate layer. Dugstad [18] tested 12 ppm acetic acid under film forming conditions at 80°C; ph 5.8, 2 bar CO_2 and 6-30 ppm Fe^{2+} and 0.1% *NaCl*. From the result, it was concluded that CH_3COOH caused more mesa attack. Corrosion films were more fragmented with pores and flaws. Additions of acetic acid reduces the protectiveness of the films which is attributed to a decrease of the pH and lower supersaturation of Fe^{2+} in the corrosion film and at the steel surface. This leads to a decrease of the film thickness resulting in higher corrosion rates. Furthermore, the acetate ion is assumed to attack existing iron carbonate films and make them thinner.

Recent studies revealed that the main cause of mild steel corrosion is the free acetic acid and not the acetate ion thus it is clear that acetic acid affects the corrosion rate only at lower pH values. Crolet et al[20] reported that in the presence of traces of free CH_3COOH, the majority of corrosion layers on bare metal were no longer $FeCO_3$, but iron(II) acetate ($Fe(CH_3COO)_2$), which had a much greater solubility. According to Ueda and Takabe[20], the presence of acetic acid significantly increasing corrosion rate for both pure iron and Cr steel compared to blank CO_2 corrosion. However, it was found that the temperature, which has highest corrosion rate, was similar for all materials with and without acetic acid. Nesic *et.al*[27] stated that, the acetic acid acts as a provider of hydrogen ions and has a limited effect on the pH (acting as a buffer). Secondly, the free acetic acid is believed reduces directly on the metal surface in a similar way as carbonic acid. This and the contribution to the hydrogen ion reduction lead to an increase of the cathodic current. But there is a misunderstanding about the role between acetic acid and carbonic acid. Acetic acid is often referred to as a stronger acid than carbonic acid. The dissociation constant (K_a) of H_2CO_3 expressed pK_a is about 3.5 at 25°C, which is lower than CH_3COOH, ($pK_a = 4.8$). Therefore H_2CO_3 is still the main cathodic reactant in CO_2 corrosion. A consequence of this, that H_2CO_3 has a higher reaction rate constant than CH_3COOH.

Recent studies of Nafday and Nesic[39] with different acetic acid concentrations revealed no significant effect on iron carbonate scale formation and its protectiveness on carbon steel. The measurements were performed in a glass cell at stagnant conditions deoxygenated with CO_2 in a 3% NaCl solution at 80°C and pH 6.6. The protectiveness of an iron carbonate scale depends primarily on the rate of precipitation what in turn is a function of temperature and supersaturation. Iron carbonate scale thickness, structure and crystal size are virtually unaffected by the presence of CH_3COOH.

George *et.al*[42] which using 0-850 ppm acetic acid, reported that anodic reaction was retarded. And also the limiting current of the cathodic reaction in the CO_2 environment was greatly increased with increasing concentration of acetic acid.

Joosten *et.al*[44] found that presence of acetic acid increases corrosion rate. The corrosion rate is also increased with increasing temperature of acetic acid. However, it is decreased above temperature of 70°C. It indicates the absence of protective iron carbonate film at the lower temperature and high solubility of Fe^{2+} ion.

Based on the above reviews, CO_2 corrosion still become an important issue and need further findings, especially with the presence of acetic acid and high temperature where $FeCO_3$ films is favorable to form. And experiments which are performed here at stagnant condition (without any effect of flow) and without any addition of Fe^{2+} which may differ from previous research. Hence, $FeCO_3$ films that precipitate at metal surface only come from the corrosion process itself.

CHAPTER III
METHODOLOGY

3.1. Experimental Procedures

Two types of experiments were performed for corrosion measurements and film formation characterization. Electrochemical corrosion measurement was performed to obtain corrosion rate data on various temperatures, pH and concentrations of acetic acid, and film formation test to obtain information regarding corrosion product layer at pH 5.5 and 90^{o}C. Sample with corrosion product as the result of film formation test was then carried for surface characterization. Experiments setup and sample preparation were conducted before running the entire tests.

3.1.1. Experimental setting

Corrosion rate test was performed using Quickfit glass cell with cover/cap and heater as shown in Figure 3.1. Initially the glass cell was assembled; a salt solution was prepared by filling 500 mL de-ionized water into 1-liter beaker, and then 30 grams NaCl was added into cell. The beaker was filled up again with de-ionized water until reach 1 liter. The water was then stirred with magnetic stirrer bar for mixing purpose. After 15 minutes, this salt solution was transferred into the glass cell. Next, glass cell was covered tightly and heated up to desired temperature (see test matrix Table 3.1) using hot plate and observed by a thermometer immersed into solution. The solution was deoxygenated by purging with 1 bar CO_2 gas continuously. Once desired temperature was reached, the pH of test solution was adjusted to 5.5 by adding 1 M sodium bicarbonate ($NaHCO_3$) solution. The pH meter was calibrated using pH 4 and pH 7 buffer solution, which was heated up according to experiment's parameters. The appropriate amount of acetic acid (according to parameter) was added into solution and purging period was prolonged for 1 hour. Working electrode, Metro-ohm Ag/AgCl reference electrode and platinum auxiliary electrode were immersed into the solution and all electrical connections were made for corrosion rate monitoring. Corrosion rate was recorded using ACM 1350V5 Gill 12 Weld Tester instruments with Linear Polarization Resistance software.

Schematic of glass cell, working electrode and other controller tools are shown on Figure 3.1 below:

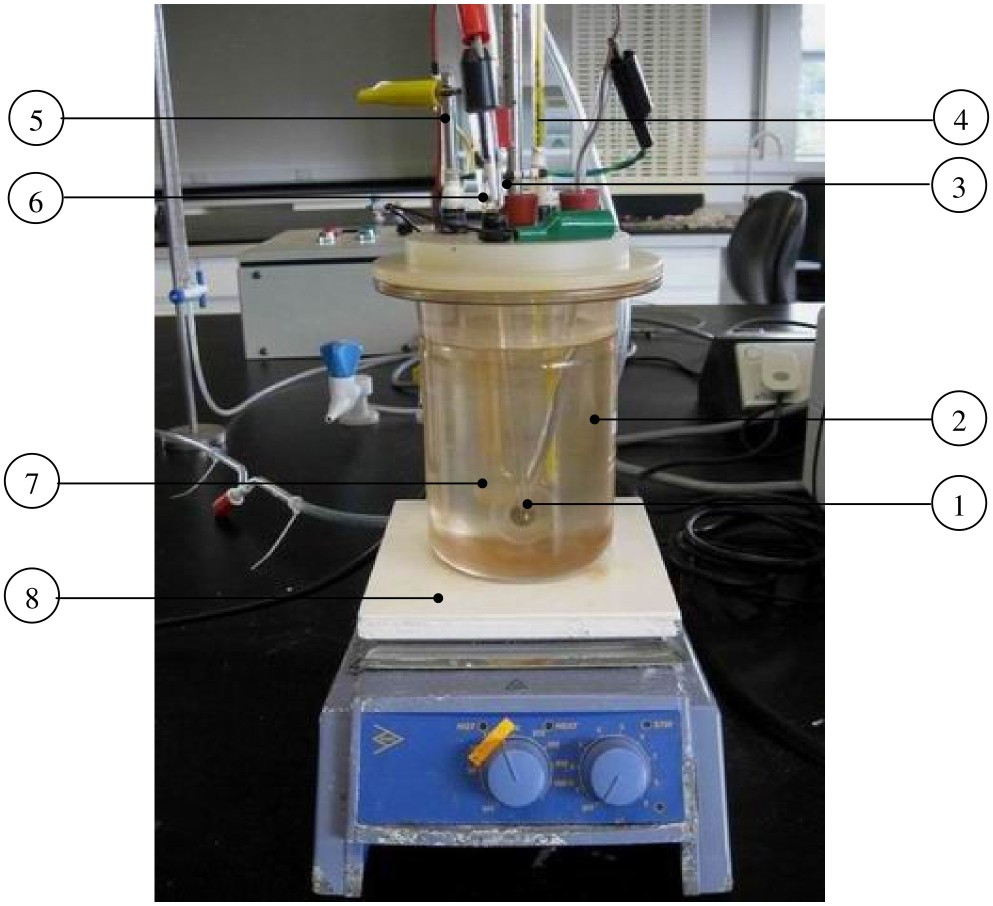

Figure 3.1 Schematic of glass cell equipment

1.working electrode; 2. glass cell; 3. pH probe; 4. thermometer; 5. platinum auxiliary electrode; 6. Ag/AgCl reference electrode; 7. CO_2 bubbler; 8. hot plate

3.1.2. Material and preparation

The working electrode was made from low carbon steel as received with diameter of 12 mm. Detailed chemical composition of the carbon steel is given in Table 3.1.

Table 3.1. Chemical composition of BS 970 (wt %)[40]

C	Si	Mn	P	S	Cr	Mo	Ni	Fe
0.148	0.175	0.799	0.010	0.032	0.069	0.014	0.065	Balance

Sample was made by cutting the steel rod 8 mm height each. Then the sample was connected with 20-cm-long copper wire to deliver current during test. Small diameter plastic hose covers copper wire to avoid interference or contact with solution during test. Next step was mounting the sample with epoxy resin and leaving one open lateral side as primary object of this research. Prior to immersion, the specimen surface was polished with 400 to 2400 grit SiC paper, and rinsed with ethanol.

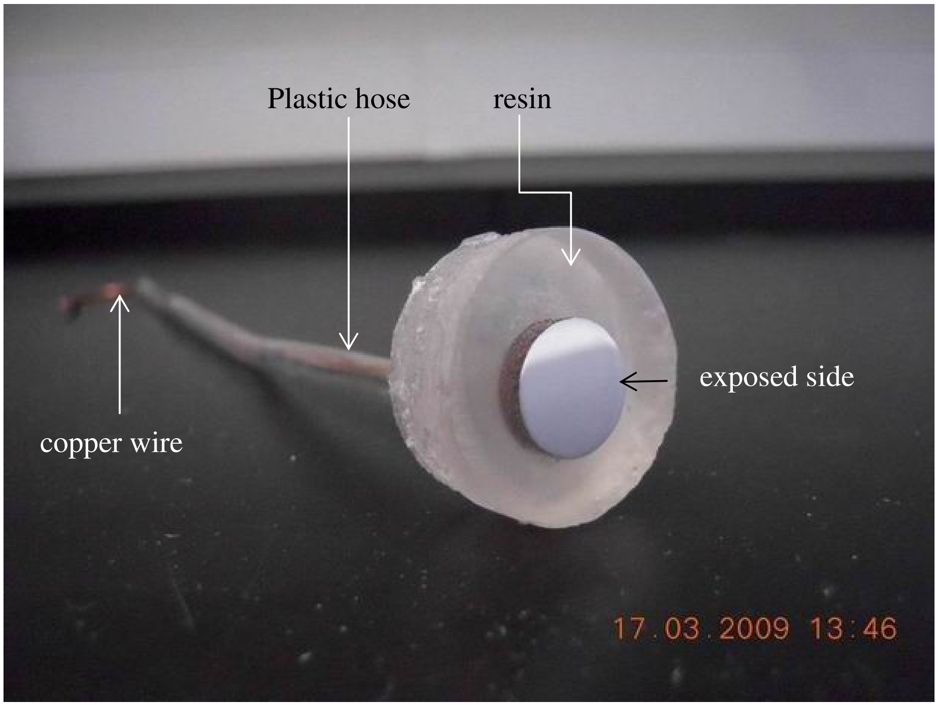

Figure 3.2. LPR test sample covered with epoxy resin

3.2. Electrochemical Corrosion Measurements

Corrosion measurement was performed using Linear Polarization Resistance (LPR) test and potentiodynamic polarization sweeps. LPR test was performed to obtain corrosion rate data, while polarization sweep was performed to obtain information regarding mechanism and kinetic of corrosion process.

3.2.1. Linear Polarization Resistance test

Linear Polarization Resistance (LPR) test was conducted with sweep every 1 hour, starting immediately after specimen immersed into the solution. All measurements were performed using ACM Instruments Weld Tester monitoring system and analyzed using the accompanying software. Test matrix of preliminary LPR test is presented in Table 3.2 below.

Table 3.2. Test Matrix of preliminary LPR test

Parameters	**Remarks**
Solution	3 % NaCl
Gas	CO_2
pH	5.5
Total CH_3COOH (ppm)	0, 10, 20, 60, 100, 400
Length of test	24 hours
Temperature (°C)	70, 80, 85, 90
Sweep rate	20 mV/min
Potential range	±10 mV
Rotational Velocity of magnetic stirrer bar (rpm)	0/ stagnant

Corrosion rate was measured hourly and then plotted graphically. The corrosion rate plot would be used to determine temperature tendency of $FeCO_3$ film formation. Then, second LPR test under filming condition at 90^oC was performed, with and without acetic acid and different periods. Matrix of film formation LPR test is presented in Table 3.3, while duration of film formation LPR test is presented in Table 3.4. The purpose of film formation test was to produce precipitated iron carbonate film on steel surface during corrosion process.

Table 3.3. Test Matrix of film formation LPR test

Parameters	**Remarks**
Solution	3 % NaCl
Gas	CO_2
pH	5.5
Total CH_3COOH (ppm)	0, 10, 20, 60, 100, 400
Length of test	6 - 96 hours
Temperature (°C)	90
Sweep rate	20 mV/min
Potential range	±10 mV
Rotational Velocity of magnetic stirrer bar (rpm)	0/ stagnant

Table 3.4 Film formation LPR test duration with 0-400 ppm acetic acid

CH_3COOH added (ppm)	**Duration of LPR test (hours)**			
	Sample 1	**Sample 2**	**Sample 3**	**Sample 4**
0	6	24	96	-
10	6	24	96	-
20	6	24	96	-
60	6	12	24	96
100	6	12	24	96
400	6	12	24	96

To anticipate evaporation of solution during 96 hours test, additional solution was added accordingly every 24 hours with identical composition and treatment as main solution.

3.2.2. Potentiodynamic polarization sweeps

The polarization sweeps were conducted at a sweep rate of 100 mV/min and sweep range ±300 mV. The sweep was started after 1 hour of immersion, continuously from -300 mV below the corrosion potential to 300 mV above corrosion potential. Each sample was tested separately with new solution according to acetic acid concentration. Prior to the sweeps, the solution and sample was prepared similarly to Linear Polarization Resistance test. Polarization sweep was performed at pH 5.5, CO_2 pressure 1 bar and temperature 90^oC.

3.3. Surface Characterization

Samples with corrosion product film (result of film formation test) were next examined to identify the type and observe the morphology of film. Three methods were used, which are X-Ray Diffraction (XRD), Scanning Electron Microscope (SEM) and EDAX examination. These tests were performed immediately after film formation test end to avoid reaction with environment.

3.3.1. X-Ray Diffraction (XRD) analysis

X-Ray Diffraction analysis was performed to identify type of corrosion product film formed on steel surface. There were 3 samples examined with XRD, first was the base material as received. The second was sample, which tested in 0 ppm acetic acid and the third was sample, which tested in 400 ppm acetic acid. All samples were carried out into X-Ray Diffraction equipment directly after LPR test ended according to Table 3.4. to minimize reaction with atmospheric environment.

Figure 3.3 Sample for X-Ray Diffraction test, mounted with ∅ 5 cm resin

X-Ray Diffraction analysis was performed using Bruker D8 Advance system (see Figure 3.4) with maximum voltage 60 kV and maximum current 80 mA.

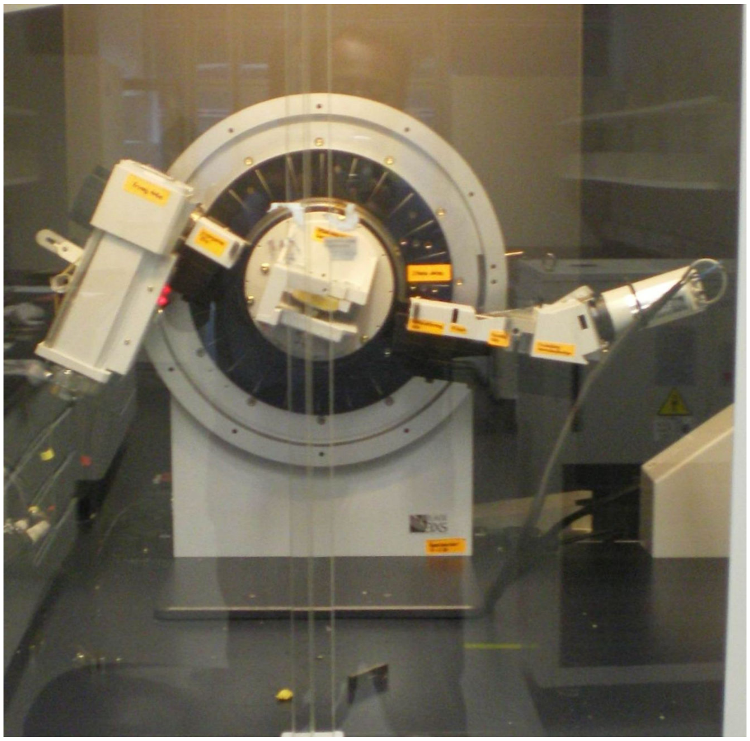

Figure 3.4. Bruker D8 X-Ray Diffraction test equipment

3.3.2. Scanning Electron Microscope (SEM) and EDAX examination

Scanning Electron Microscope (SEM) and EDAX examination was performed after each LPR test, refer to Table 3.3. Each sample was cut into 2 pieces to facilitate the testing. The magnifications were ranged from 500X to 1000X. During SEM test, surface and film profile (size of film, distribution) was captured to obtain information about morphology of corrosion product. EDAX examination was performed directly after image capturing to determine chemical composition of the sample and film formed.

Figure 3.5. INCAx-sight OXFORD test equipment

Scanning Electron and EDAX examination was performed using INCAx-sight OXFORD Instruments with maximum voltage 30 keV.

CHAPTER IV

RESULTS AND DISCUSSIONS

CO_2 corrosion research with the presence of acetic acid in natural filming condition were performed experimentally and analyzed theoretically. The tests consist of electrochemical and surface characterization techniques. Theoretical analysis of the film formation covers calculation of the kinetics and precipitation. Results and analysis of each experiment are described in sub-chapters below.

4.1. Linear Polarization Resistance (LPR) Test Results

Preliminary experiment is performed using LPR with parameters and method explained in the previous chapter. Corrosion rate was recorded for 24 hours and calculated to obtain average corrosion rate. Plot of average corrosion rate with different acetic acid concentration is presented below:

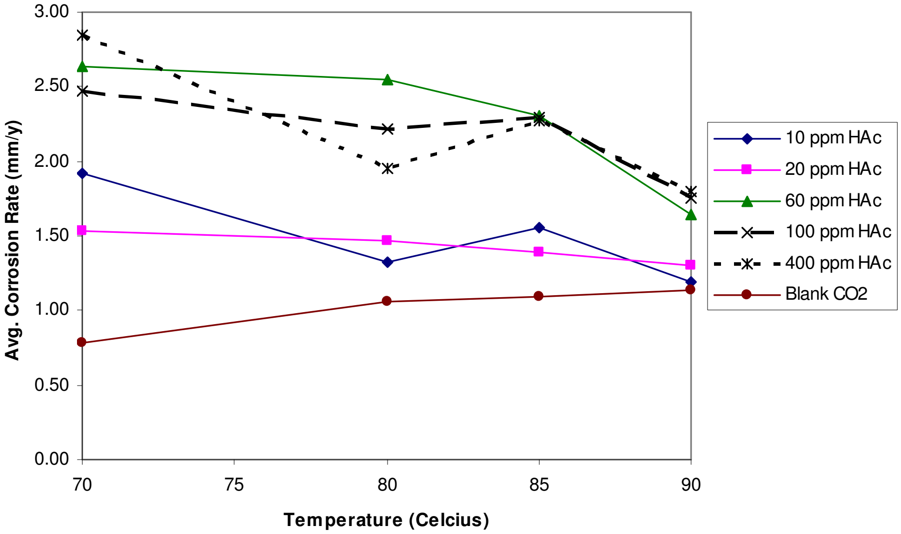

Figure 4.1 Average corrosion rate at pH 5.5; 70-90°C; CO_2 pressure = 1 bar; 0-400 ppm acetic acid in CO_2 environment.

Figure 4.1 shows trend of corrosion rate at different temperatures, where corrosion rate decreases at high temperature. Increasing in temperature will enhance kinetic of reaction for all species. This might causes faster corrosion reaction and faster $FeCO_3$ film formation as well. The presence of acetic acid increases corrosion rate by providing hydrogen ion (H^+) and acetate ion for chemical reaction with Fe^{2+} ion. For blank CO_2 corrosion, average corrosion rate increases slightly and at 90°C corrosion rate has the highest value. While for CO_2 corrosion with acetic acid, average corrosion rate was split in to two groups. First group consist of corrosion rate for 10 and 20 ppm acetic acid. While for second group, consist of corrosion rate data for 60, 100 and 400 ppm. The second group shows higher value compared to both blank and 10-20 ppm acetic acid CO_2 corrosion. In addition, it can be seen that, increase of temperature followed by decreasing of average corrosion rate, although at 85°C, some of corrosion rate values slightly increase. This behavior is in accordance with previous findings[4], that above 70°C corrosion rate tends to decrease which can be caused by scale or film formation and affecting corrosion rate.

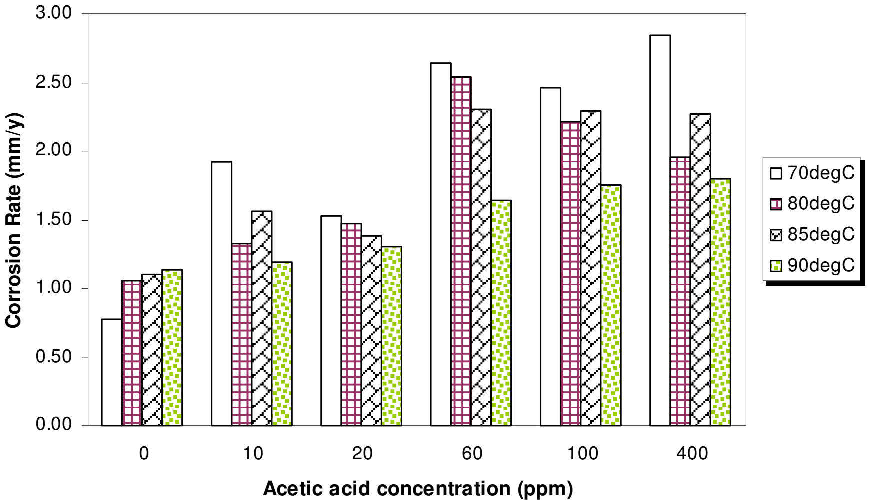

Figure 4.2 Average corrosion rate plot at pH 5.5; p_{CO_2} 1 bar; with 0-400 ppm acetic acid at different temperatures in CO_2 environment

Figure 4.1 can be re-arranged into Figure 4.2 above, which shows average corrosion rate vs. acetic acid concentration. Corrosion rate increases as acetic acid concentration increases. As explained previously, 10 ppm and 20 ppm acetic acid yield slightly higher corrosion rate compared to blank CO_2 corrosion. While for 60-400 ppm acetic acid, corrosion rate significantly increases. This result in accordance with previous finding[18], which stated that acetic acid above 60 ppm in concentration would give significant increase in corrosion rate of steel.

Investigation of film formation at 90^oC shows that corrosion rate tends to decrease with time (Figure 4.3). Blank CO_2 corrosion result is also used as comparison to acetic acid added test results. Figures 4.4 below shows hourly corrosion rate for 96 hours at 90^oC, which was recorded by software:

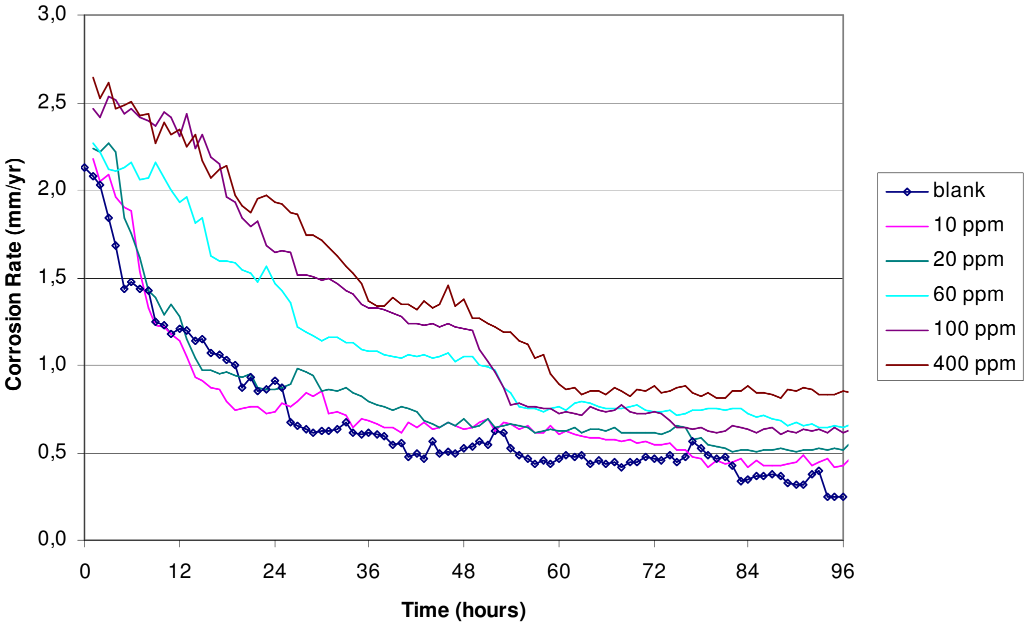

Figure 4.3 Corrosion rate for 96 hours test, 90^oC, p_{CO_2} 1 bar, pH 5.5 and 0-400 ppm acetic acid

In order to observe the effect of acetic acid on corrosion rate, plot of blank CO_2 corrosion (as baseline data) vs different concentrations of acetic acid is splitted in to individual graph which is presented on Figure 4.4 (a-e).

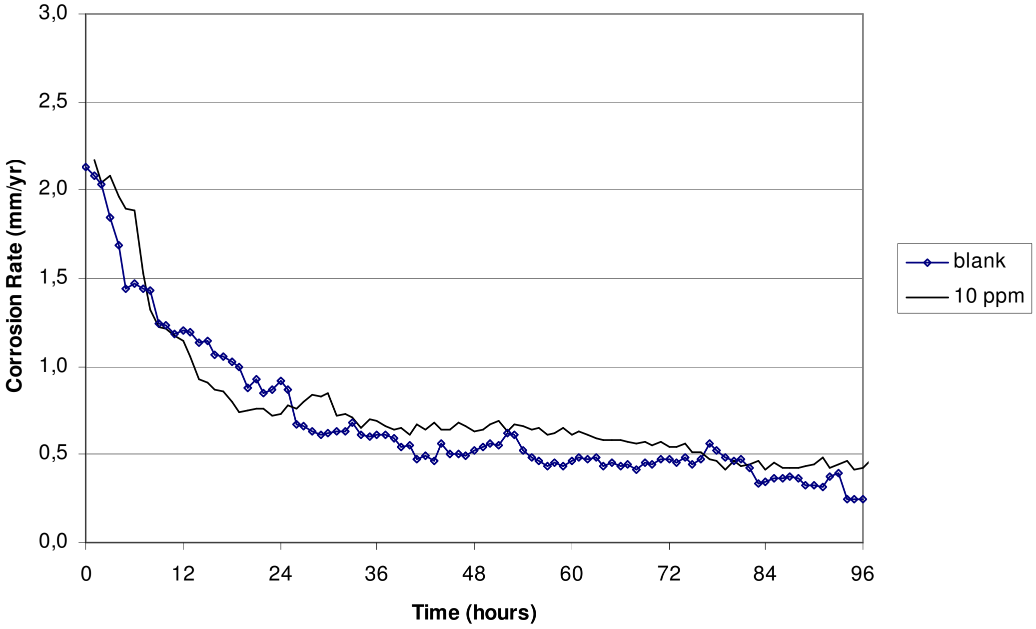

Figure 4.4a Corrosion rate between blank CO_2 corrosion and 10 ppm acetic acid

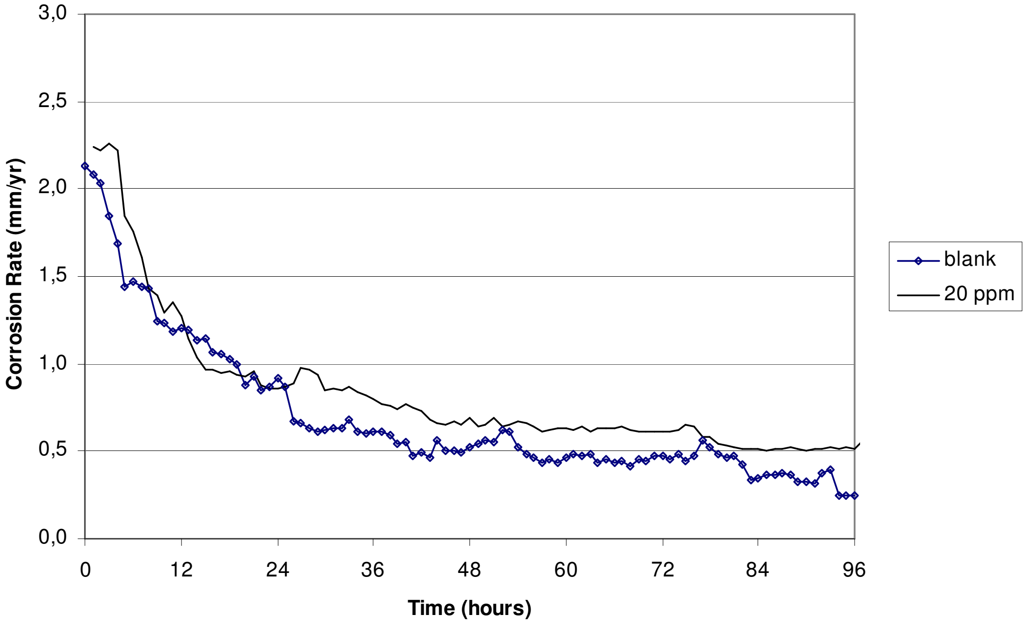

Figure 4.4b Corrosion rate between blank CO_2 corrosion and 20 ppm acetic acid

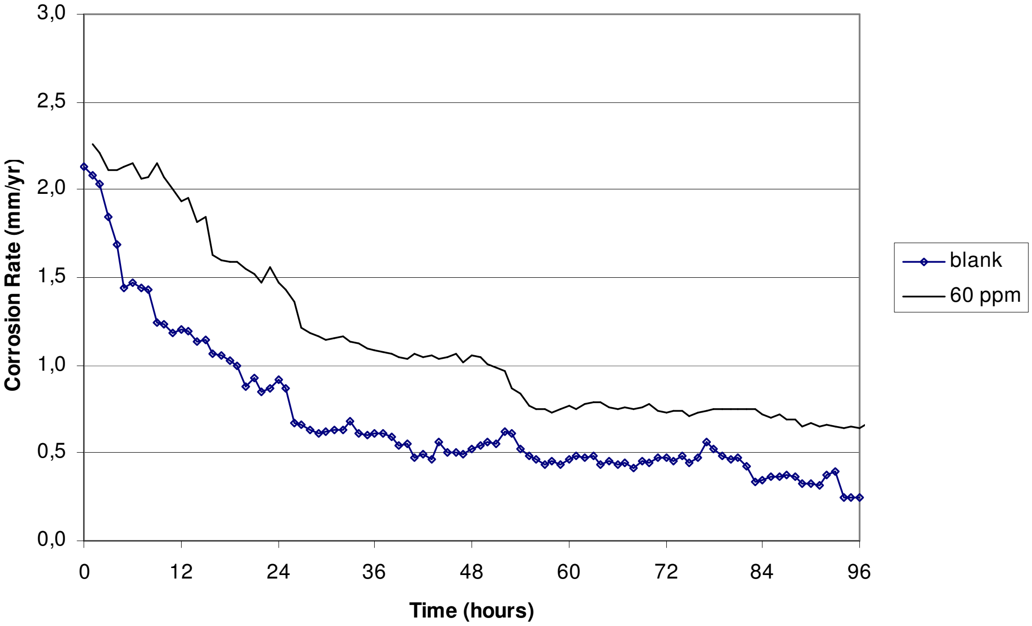

Figure 4.4c Corrosion rate between blank CO_2 corrosion and 60 ppm acetic acid

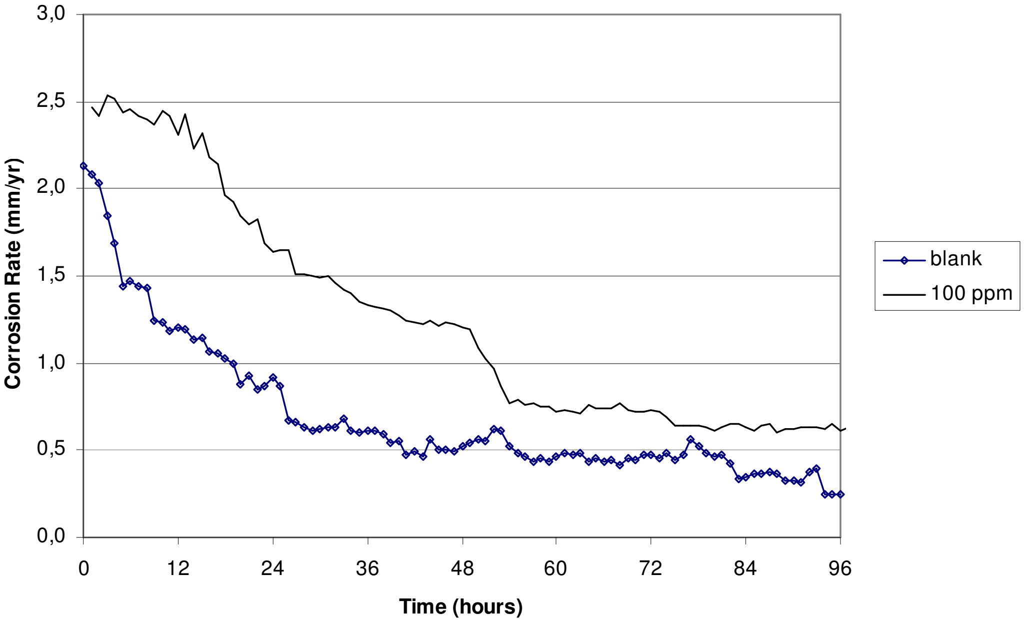

Figure 4.4d Corrosion rate between blank CO_2 corrosion and 100 ppm acetic acid

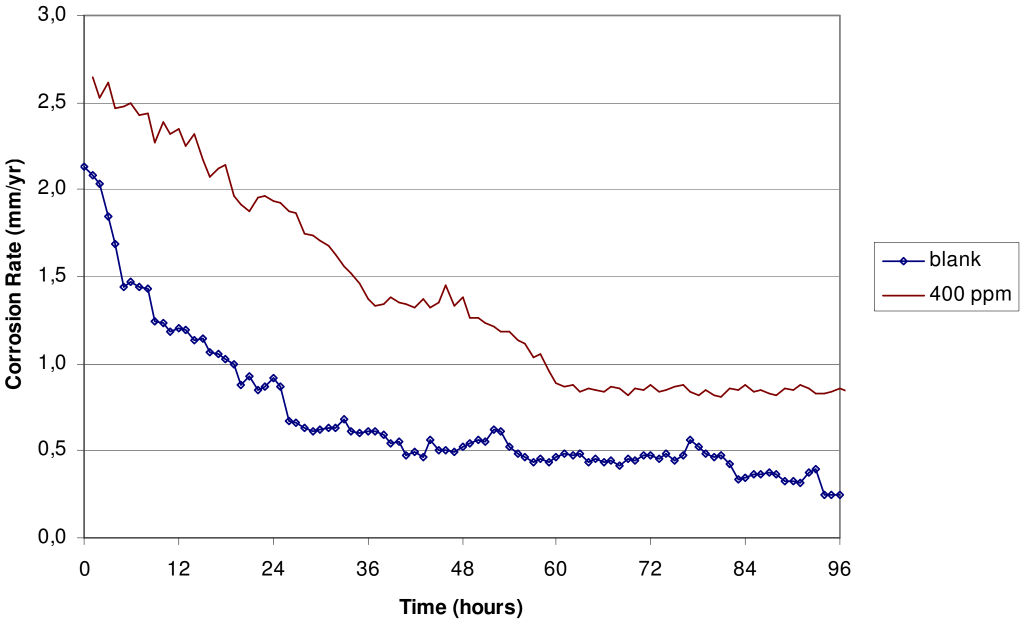

Figure 4.4e Corrosion rate between blank CO_2 corrosion and 400 ppm acetic acid

Figure 4.4 (a-e) show corrosion rates of both blank CO_2 corrosion and acetic acid added CO_2 corrosion. Linear Polarization Resistance (LPR) result showed that blank test without acetic acid had corrosion rate of 2.13 mm/yr and decreased to 0.25 mm/yr at the end of the test. The presence of small amount of acetic acid below 60 ppm did not change corrosion rate significantly as compared to blank condition. Corrosion rate of samples with 10 and 20 ppm acetic acid were 2.18 and 2.24 mm/year at the beginning, lower than blank test and stable in few hours at range 0.47 to 0.56 mm/yr (higher than blank test). Significant effect of acetic acid was observed with 60, 100 and 400 ppm acetic acid, where corrosion rate of 2.26 to 2.65 mm/yr at the beginning of the test and decreased to 0.62 to 0.84 mm/yr. Corrosion rate increases as acetic acid concentration increases compared to blank CO_2 corrosion. It is observed that time needed to reach stability of corrosion rate is different among all parameters. Corrosion rate with 60 ppm or more acetic acid remains high after several hours of test. The reason of this condition was thinning effect by acetate ion (CH_3COO^-). Acetate ions react with ion Fe^{2+}, as well as carbonate and bicarbonate ions. The existence of acetic acid 60 ppm or more delay corrosion rate stability and yields delaying of $FeCO_3$ film formation. Corrosion rate with 400 ppm acetic acid has the longest time to reach stability with 60 hours of test.

4.2. Polarization Test Result and Discussion

The polarization sweep results for sample tested at 90°C with different acetic acid concentration is shown on Figure 4.5

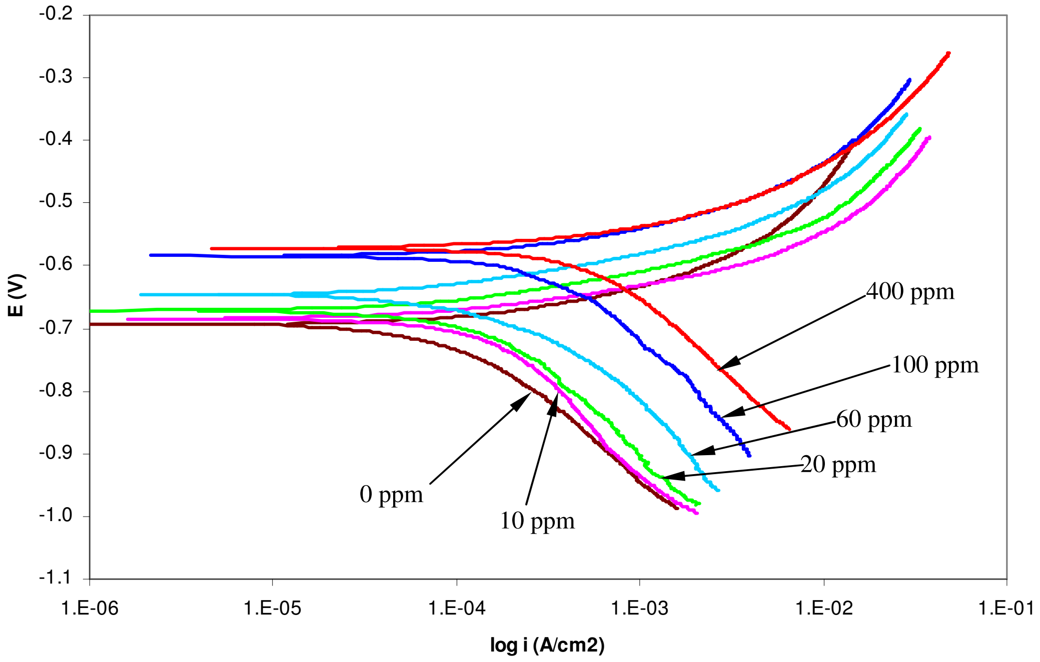

Figure 4.5. Potential sweep result different acetic acid concentration, T 90°C, CO_2 pressure 1 bar, pH 5.5 and 0-400 ppm acetic acid

Corrosion current density (i_{corr}) is observed increase with increases of acetic acid concentration. Samples with 10 and 20 ppm acetic acid show similar cathodic and anodic curves compared to blank CO_2 corrosion (0 ppm acetic acid). It can be said that small acetic acid concentration almost does not give significant contribution to corrosion process. While for sample with 60-400 ppm acetic acid, cathodic curve show an increasing of hydrogen evolution compared to blank CO_2 corrosion. An increasing of acetic acid concentration is followed with a shift of cathodic curve to right side. The mechanism of CO_2 corrosion rate with the presence of acetic acid does not change, however, the kinetic of corrosion changes with the presence of more than 60 ppm of acetic acid.

4.3. Surface Characterization Results and Discussion

Surface morphology of corroded samples are examined with X-Ray Diffraction (XRD), Scanning Electron Microscope (SEM) and EDAX techniques. Detail of examination and results are described in the next sub chapter

4.3.1. Energy Dispersive X-Ray Spectroscopy (EDAX) examination results

Sample is examined using EDAX to identify the chemical composition exists on surface. This test is performed directly after LPR test finished and the results are presented on figures below.

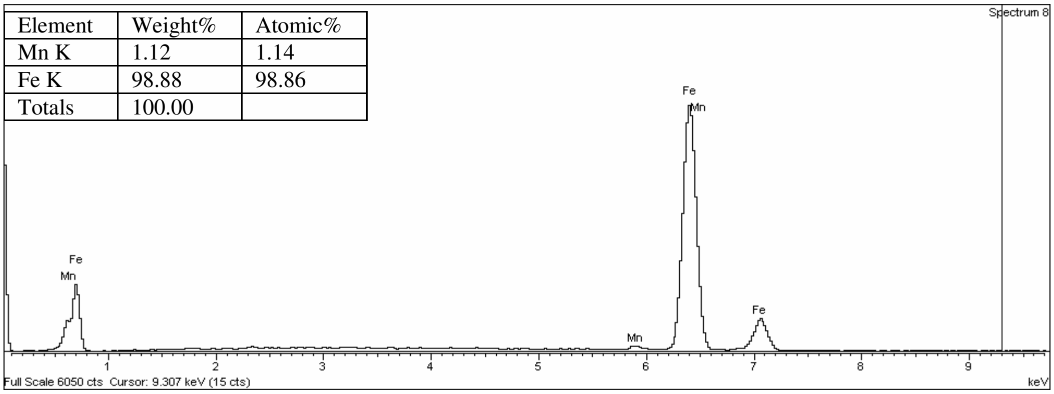

Element	Weight%	Atomic%
Mn K	1.12	1.14
Fe K	98.88	98.86
Totals	100.00	

Figure 4.6 EDX spectrum of BS970 mild steel surface as polished

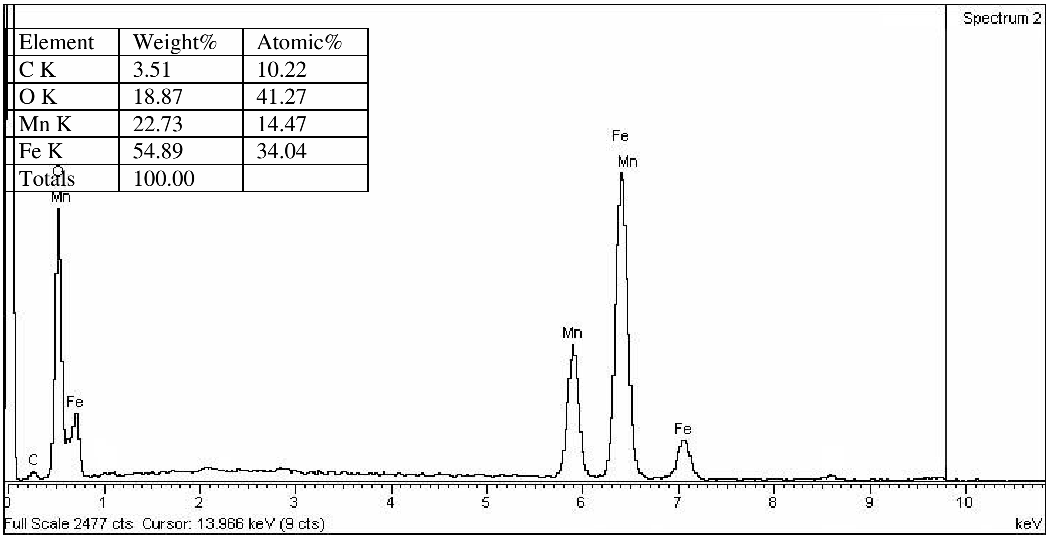

Element	Weight%	Atomic%
C K	3.51	10.22
O K	18.87	41.27
Mn K	22.73	14.47
Fe K	54.89	34.04
Totals	100.00	

Figure 4.7 EDX spectrum of $FeCO_3$ film on corroded sample, which exposed under blank CO_2 corrosion

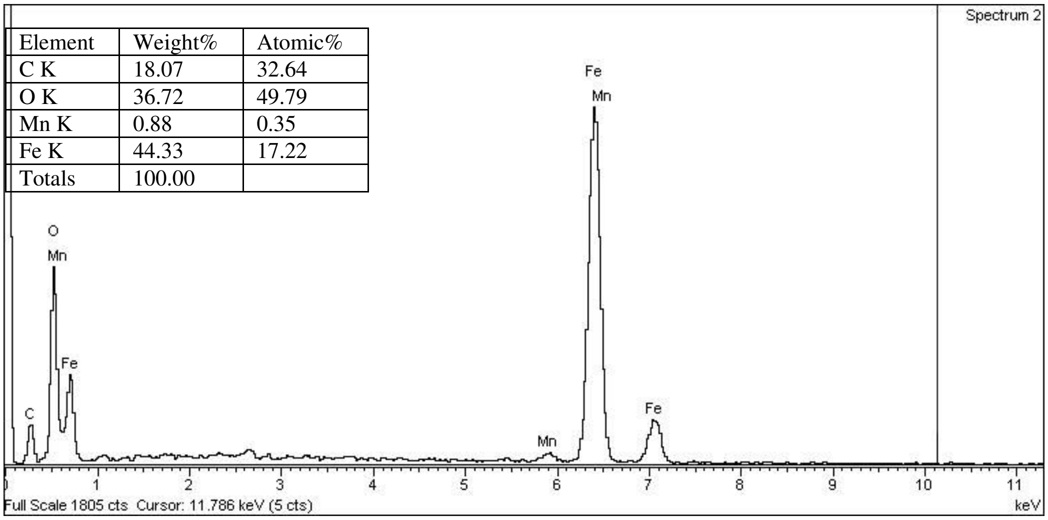

Element	Weight%	Atomic%
C K	18.07	32.64
O K	36.72	49.79
Mn K	0.88	0.35
Fe K	44.33	17.22
Totals	100.00	

Figure 4.8 EDX spectrum of $FeCO_3$ film on corroded sample, which exposed under CO_2 corrosion with 400 ppm acetic acid

Refer to EDX graph above, composition of material used for this test is in accordance with the chemical composition of base material (Figure 4.6). For corroded material samples (Figure 4.7 and 4.8), there is no evidence the existence of Cl^- ion which comes from the solution (NaCl). There are only main elements for composing corrosion product, which are Fe, O and C.

4.3.2. X-Ray Diffraction Examination Result

Corroded sample also been tested using X-Ray Diffraction to verify type of film formed on steel surface. Consist of base material as polished without electrochemical testing, sample tested with 0 ppm acetic acid and sample tested with 400 ppm acetic acid. The results are presented in figures below.

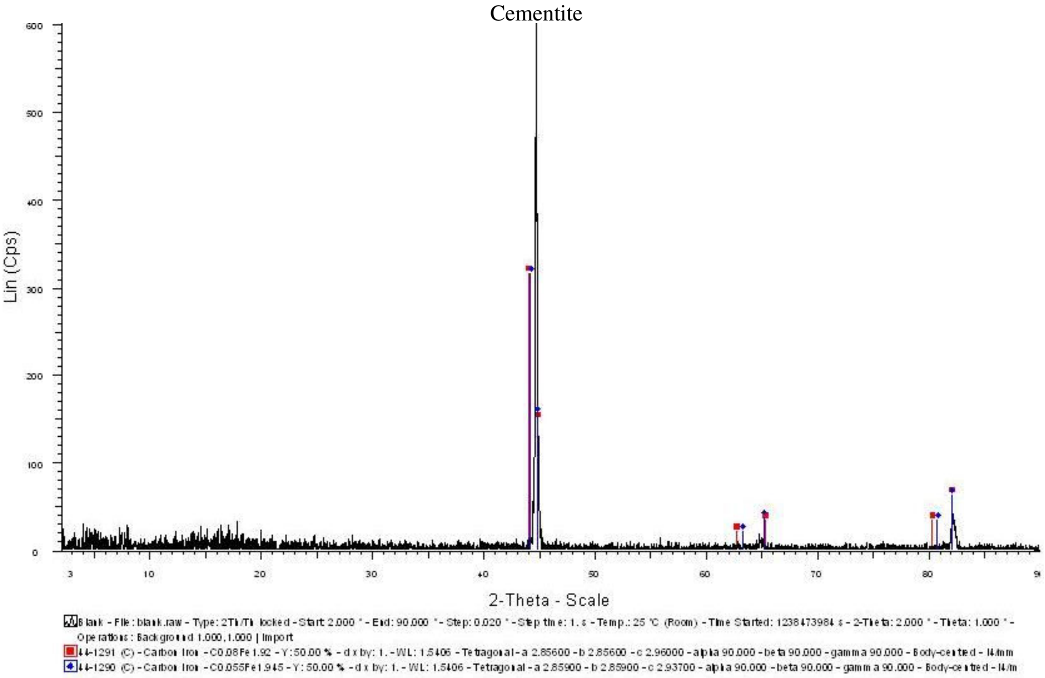

Figure 4.9 XRD diffractogram of polished base material as received

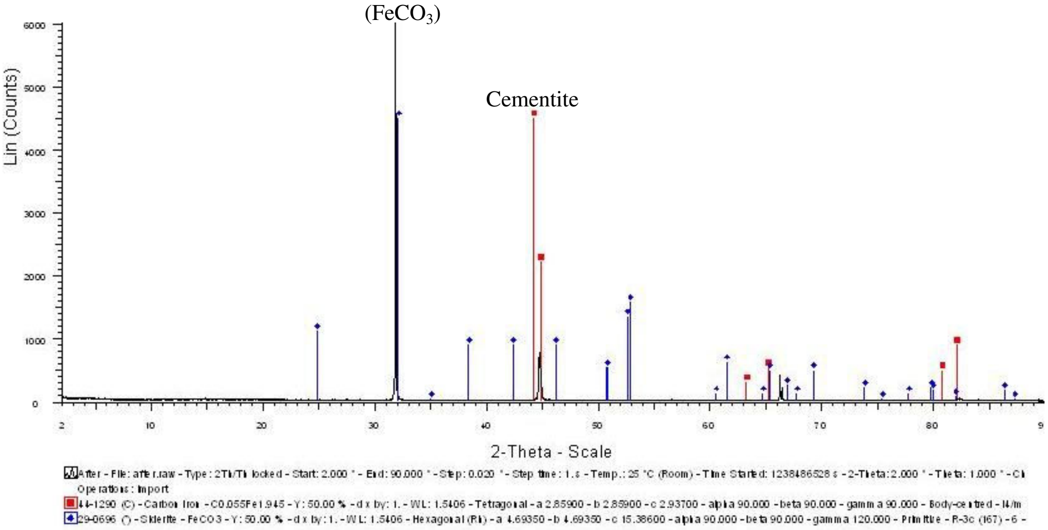

Figure 4.10 XRD diffractogram of corroded sample after 96 hours LPR test; T = 90°C, pH 5.5, 0 ppm of acetic acid, showing the existence of $FeCO_3$ (siderite) film on steel surface

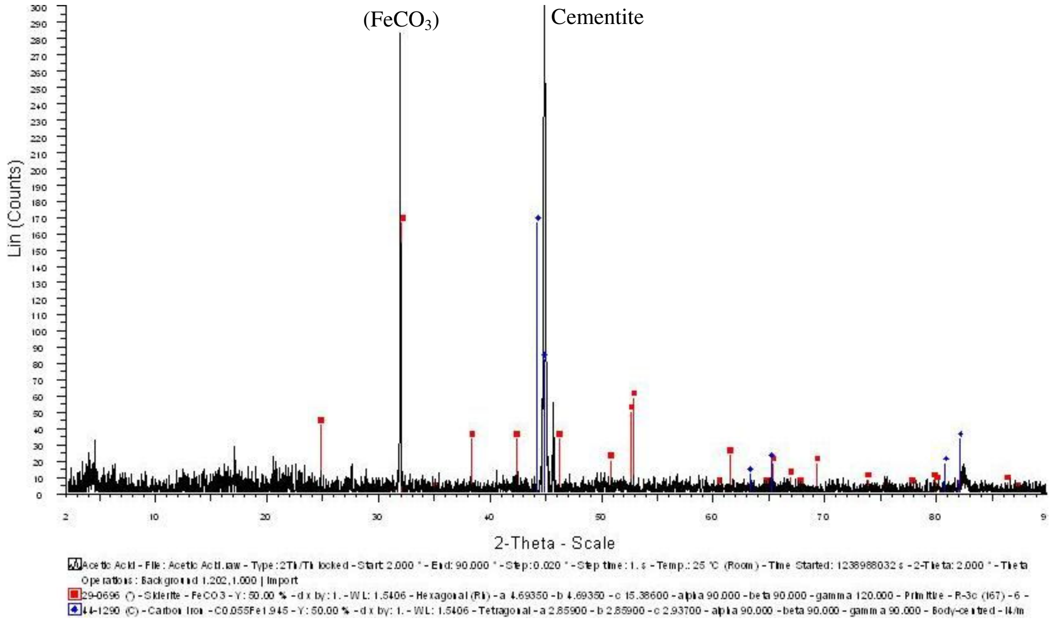

Figure 4.11. XRD diffractogram of corroded sample after 96 hours LPR test; T = 90°C, pH 5.5, 400 ppm acetic acid, showing the existence of $FeCO_3$ film on steel surface.

Figure 4.10 and Figure 4.11 show the existence of $FeCO_3$ as main corrosion product in the CO_2 corrosion with and without acetic acid. It is represented by peak at and confirmed by the database. There is no evidence or detection of iron(II) acetate $Fe(CH_3COO)_2$ precipitation on metal surface. Iron(II) acetate is another CO_2 corrosion product as the result of reaction between acetate ions and Fe^{2+} ions. The absence of $Fe(CH_3COO)_2$ does not mean that species is not produced. Since solubility of $Fe(CH_3COO)_2$ considered high ($pK_{Fe(CH_3COO)_2} = 1.9$), the precipitated $Fe(CH_3COO)_2$ on steel surface cannot be found.

4.3.3. Scanning Electron Microscope (SEM) examination result and discussion

Scannning Electron Microscope (SEM) test results consist of face view and cross sectional view. Face view observation results are taken from samples, which immersed on film formation test with different exposed time as described in Table

3.4. While for cross sectional view, all figures captured are coming from samples which previously immersed for 24 and 96 hours.

4.3.3.1. SEM result for blank CO_2 corrosion sample

Surface image of base material BS 970 as polished is taken as comparison to samples tested with acetic acid. The result is presented in the figures below:

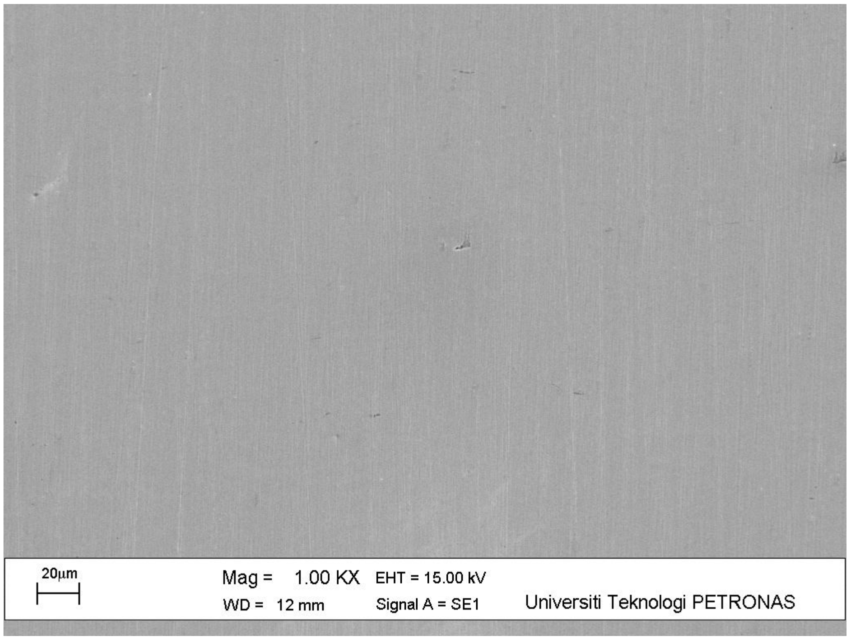

Figure 4.12. SEM picture of polished base material as received.

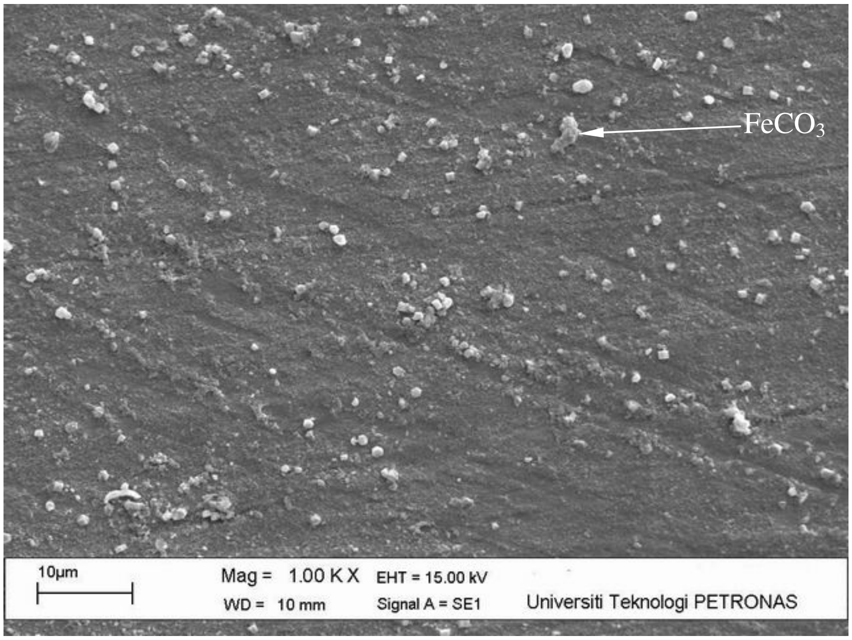

Figure 4.13. Face view of blank CO_2 corrosion sample after 6 hours showing small amount of $FeCO_3$ precipitates on steel surface

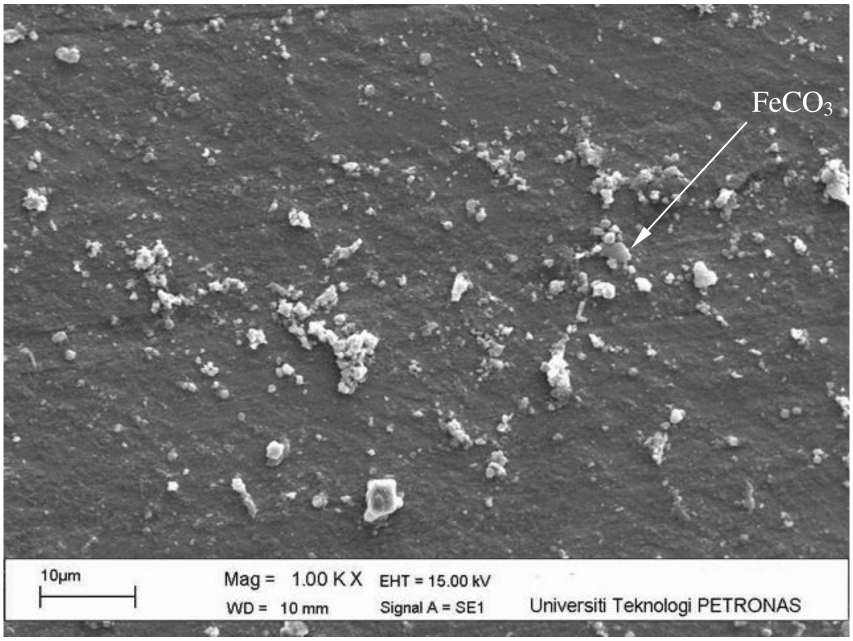

Figure 4.14. Face view of blank CO_2 corrosion sample after 24 hours, showing more $FeCO_3$ compared to 6 hours immersion

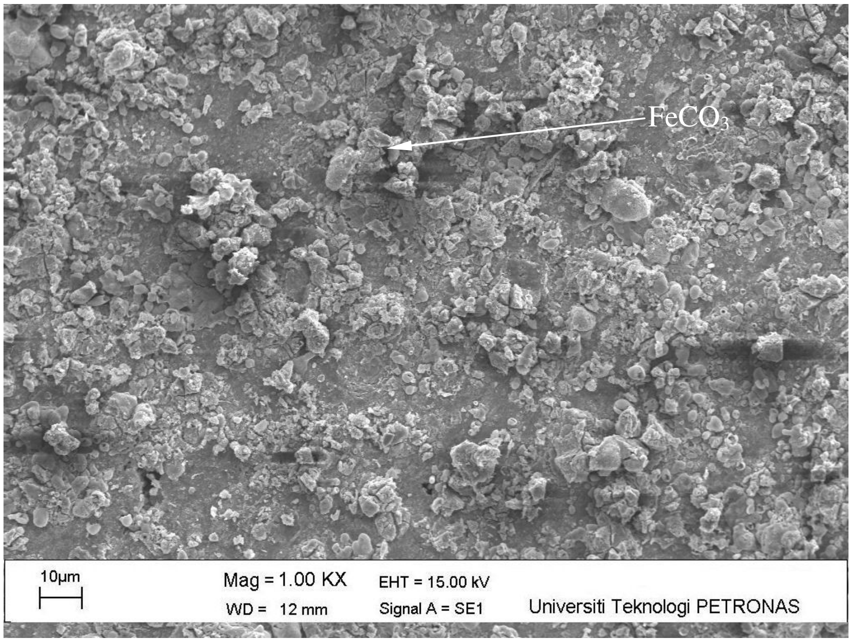

Figure 4.15. Face view of blank CO_2 corrosion sample after 96 hours showing large amount of $FeCO_3$ film covering steel surface partially

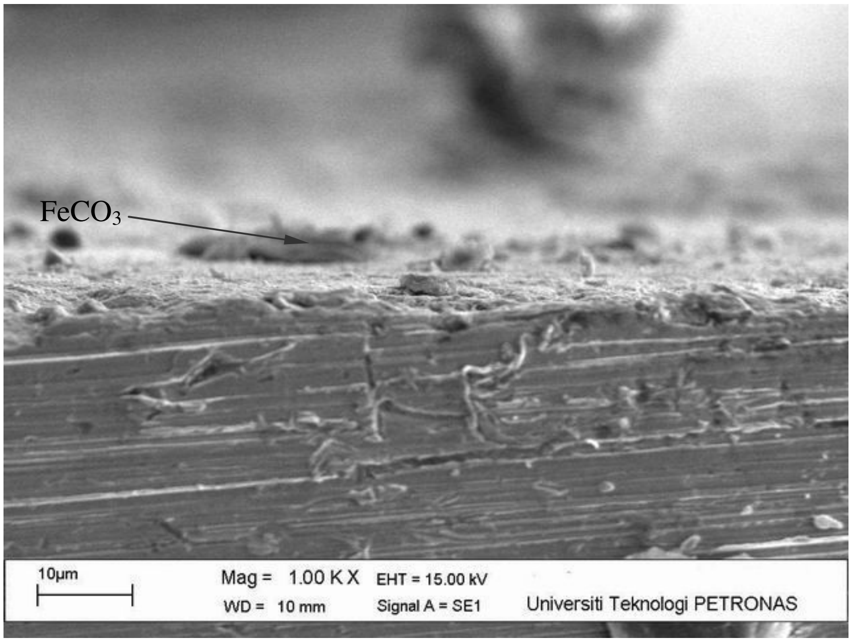

Figure 4.16. Cross section view of blank CO_2 corrosion sample after 24 hours

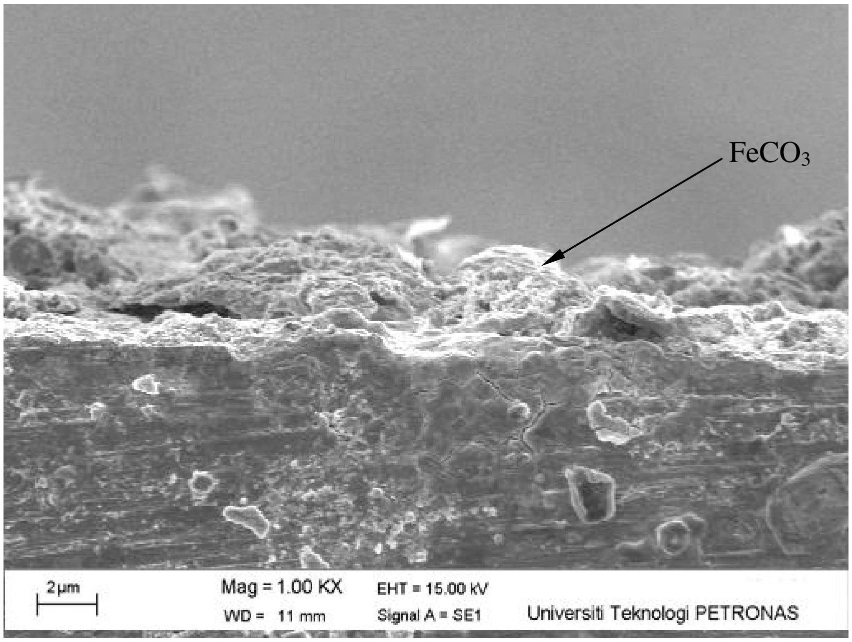

Figure 4.17. Cross section view of blank CO_2 corrosion sample after 96 hours, showing non uniform thickness of $FeCO_3$ film

The formation of iron carbonate ($FeCO_3$) film is found on steel surface (identified by XRD). However, since corrosion rate values in 24 hours decreases gradually, there is only small amount of $FeCO_3$ precipitates in that period. After 96 hours of test, number of $FeCO_3$ precipitates on steel surface increases significantly, in spite of it does not covers the entire surface. Film free area still appears on Figure 4.14 to Figure 4.15.

4.3.3.2. SEM results for 10 and 20 ppm acetic acid CO_2 corrosion samples

Face and cross sectional views of 10 and 20 ppm acetic acid samples are shown on Figure 4.18 to 4.27 below.

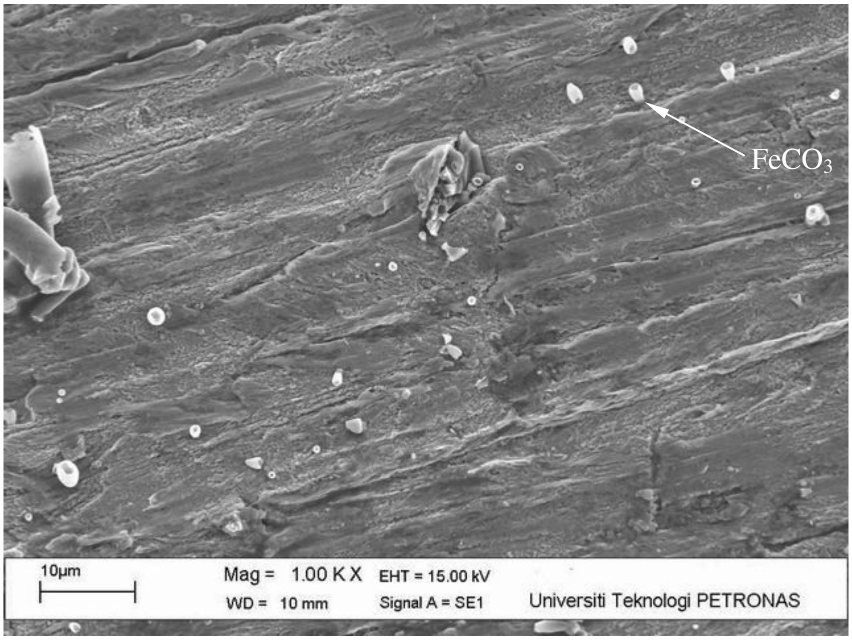

Figure 4.18. Face view of 10 ppm acetic acid added sample after 6 hours

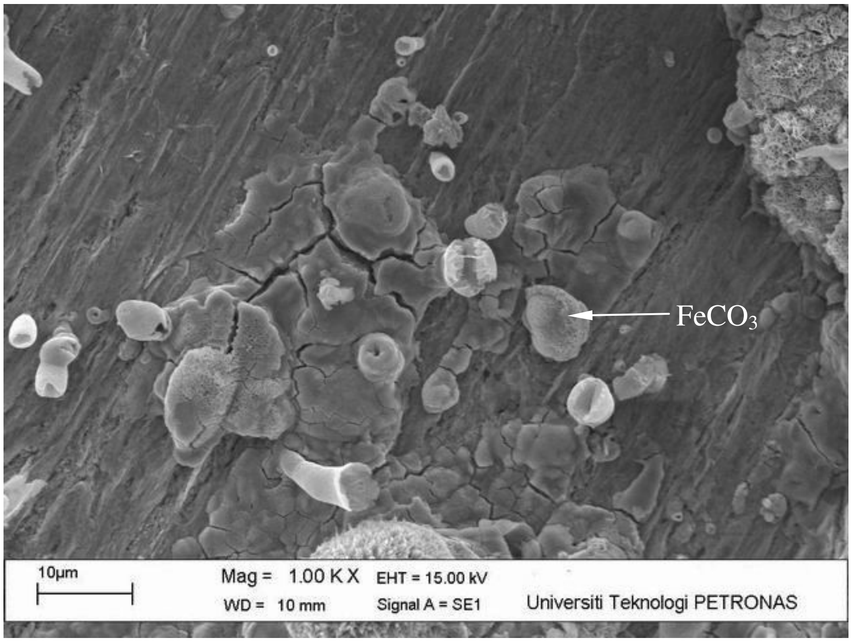

Figure 4.19. Face view of 10 ppm acetic acid added sample after 24 hours

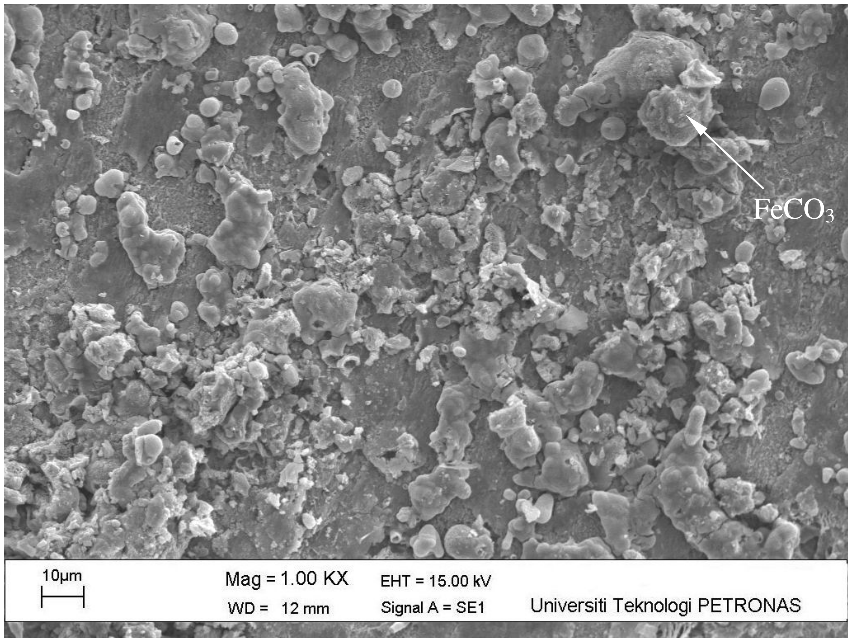

Figure 4.20. Face view of 10 ppm acetic acid added sample after 96 hours

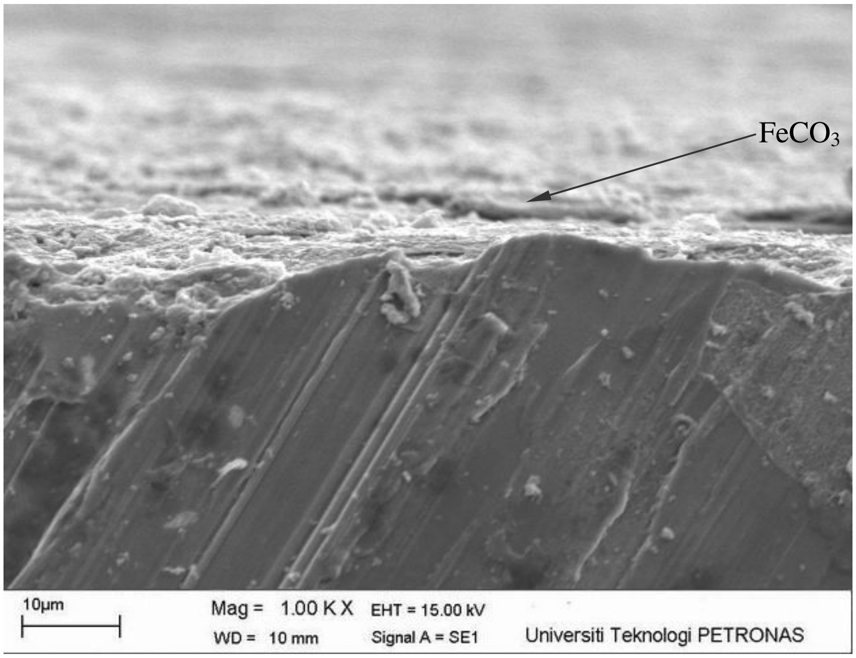

Figure 4.21. Cross section view of 10 ppm acetic acid added sample after 24 hours

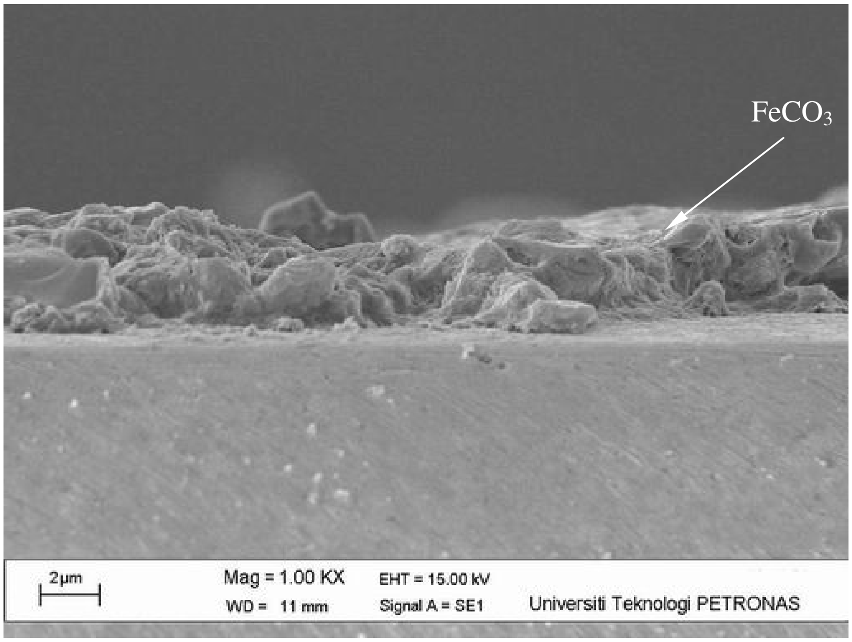

Figure 4.22. Cross section view of 10 ppm acetic acid added sample after 96 hours

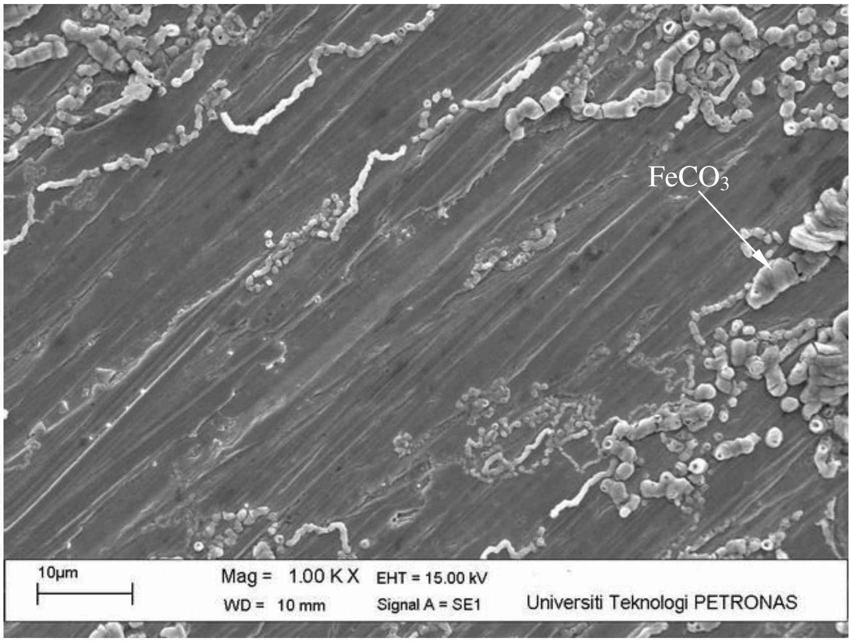

Figure 4.23. Face view of 20 ppm acetic acid added sample after 6 hours

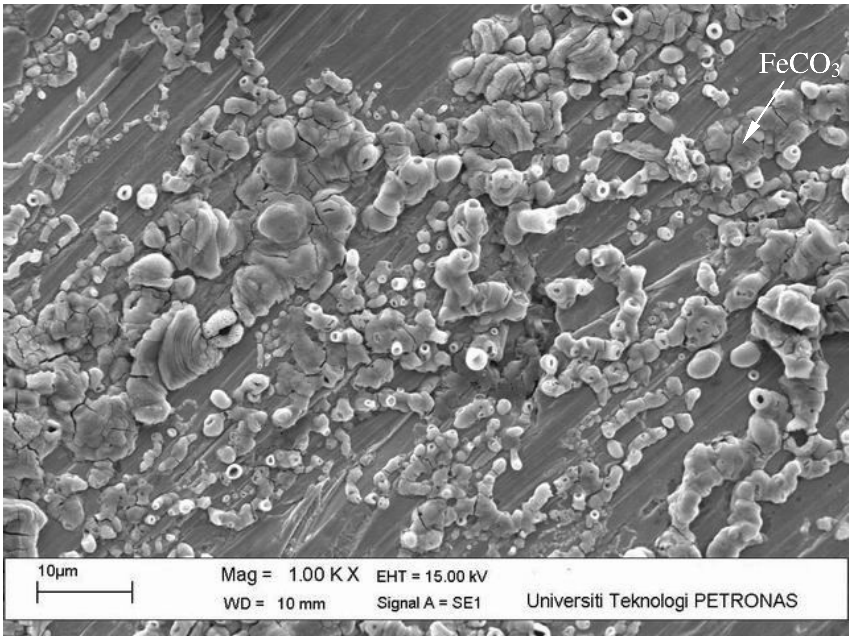

Figure 4.24. Face view of 20 ppm acetic acid added sample after 24 hours

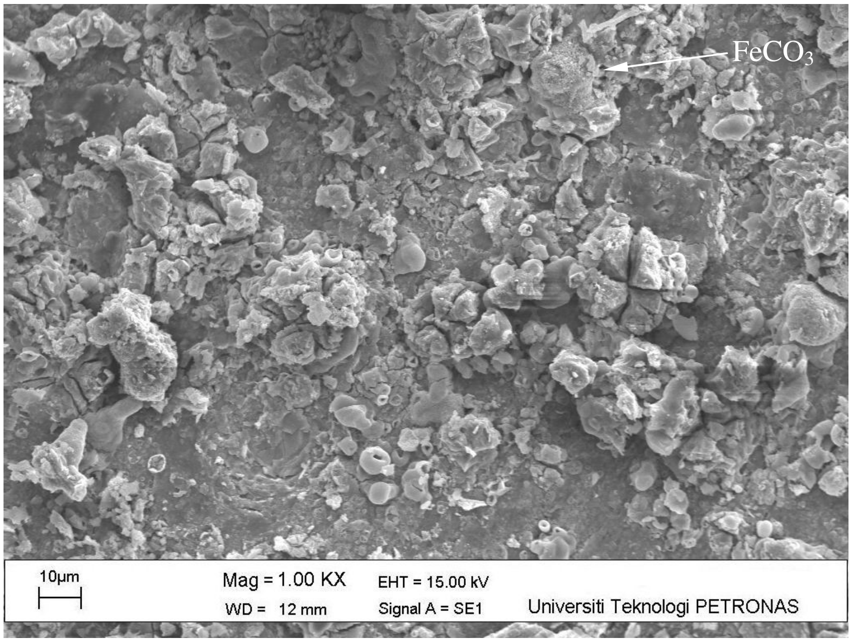

Figure 4.25. Face view of 20 ppm acetic acid added sample after 96 hours

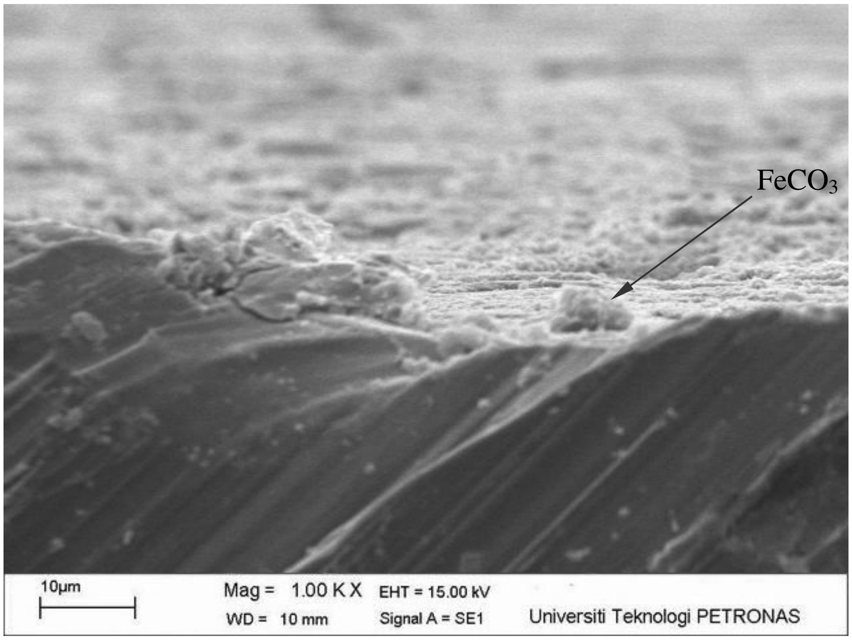

Figure 4.26. Cross section view of 20 ppm acetic acid added sample after 24 hours

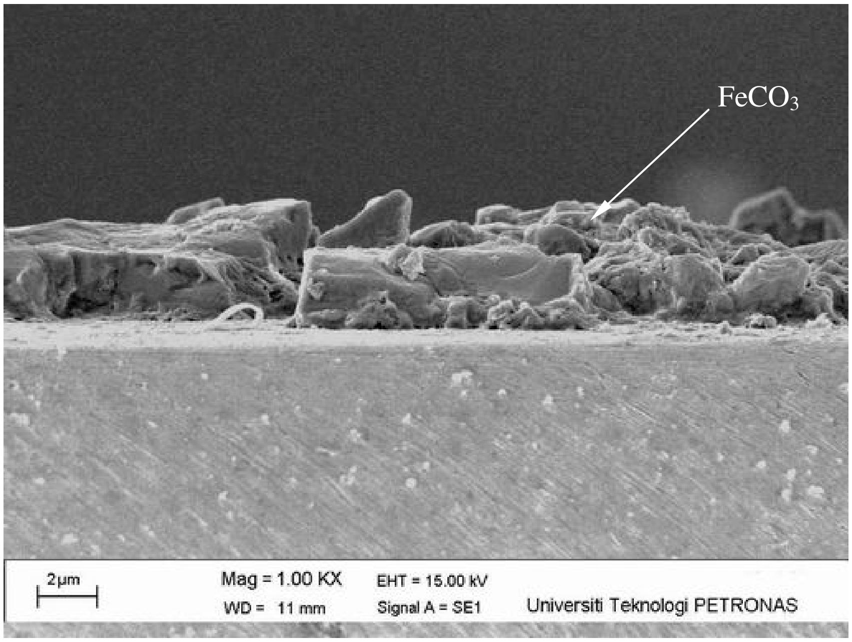

Figure 4.27. Cross section view of 20 ppm acetic acid added sample after 96 hours

Figure 4.18 to 4.22 show face and cross sectional view of steel surface after LPR test with 10 acetic acid. After 6 hours of test, CO_2 corrosion for sample with 10 ppm acetic acid yields only small amount of $FeCO_3$ film as well as blank CO_2 corrosion (Figure 4.18). Precipitated $FeCO_3$ film slightly denser compared to blank CO_2 corrosion after 24 hours test (Figure 4.19). $FeCO_3$ film for sample immersed in 24 hours show denser crystal cluster compared to sample immersed in 6 hours. At the end of test, $FeCO_3$ film grows and become larger and wider at some sites (Figure 4.20). The thickness of film formed after 96 hours approximately 2 μm (Figure 4.22).

Figure 4.23 to 4.27 show surface condition of corroded samples immersed in solution containing 20 ppm acetic acid. After 6 hours test, $FeCO_3$ film starts precipitate and there are many film initiations at corroded surface as shown in Figure 4.23. The film initiates at random location and form parallel lines. After 24 hours, film becomes denser and grows along surface (Figure 4.24). Line pattern found at the beginning of test almost disappear. After 96 hours of test (Figure 4.25), surface condition of this sample is almost similar compared to sample with 10 ppm acetic acid. $FeCO_3$ film grows in some sites and leaving small amount of open sites uncovered. The thickness of film layer increases significantly after 96 hours compared to 24 hours (Figure 4.26 and 4.27) in range of 2-4 μm.

4.3.3.3. SEM results for 60, 100 and 400 ppm acetic acid CO_2 corrosion samples

Figure 4.28 to 4.54 below show SEM observation both cross sectional and face view of sample with 60, 100 and 400 ppm acetic acid.

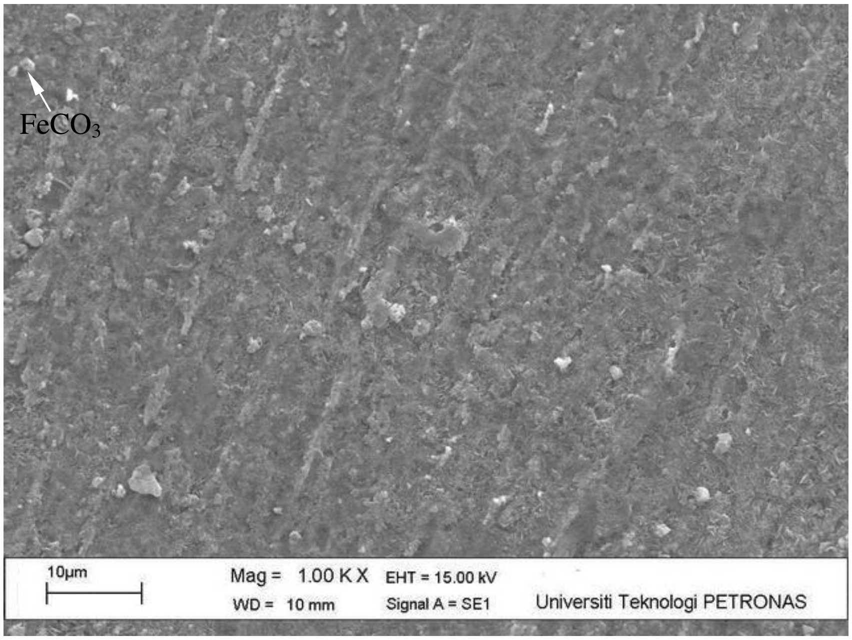

Figure 4.28. Face view of 60 ppm acetic acid added sample after 6 hours

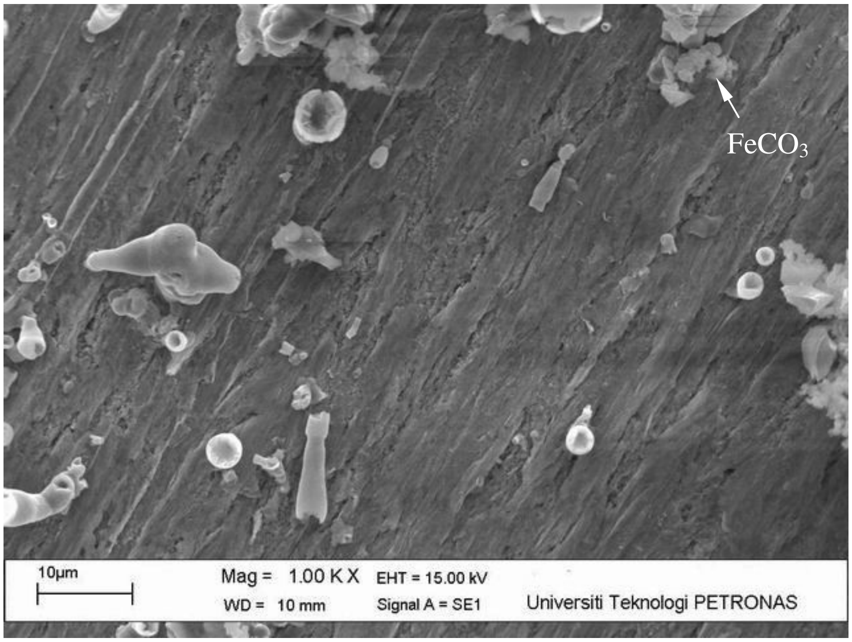

Figure 4.29. Face view of 60 ppm acetic acid added sample after 12 hours shows growth of $FeCO_3$ crystal cluster

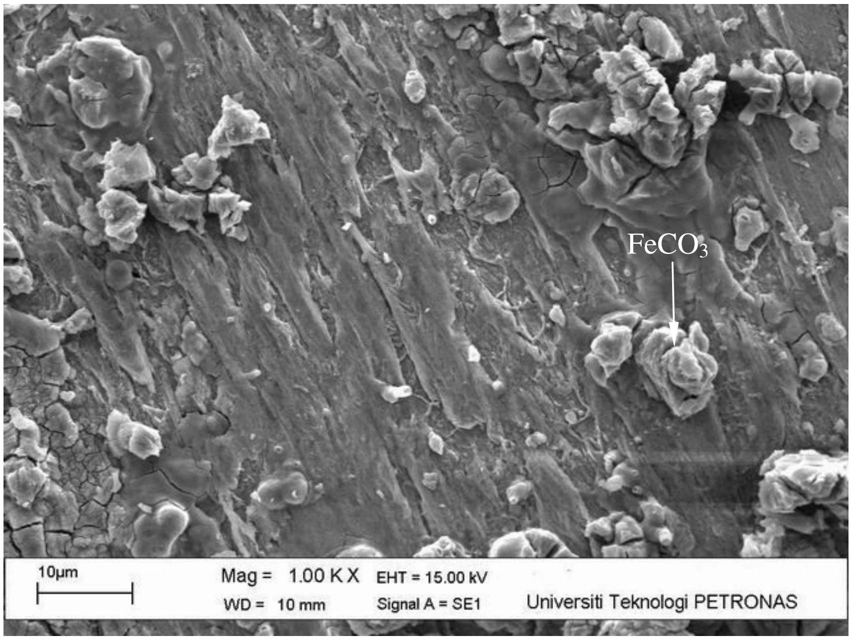

Figure 4.30. Face view of 60 ppm acetic acid added sample after 24 hours shows larger of $FeCO_3$ film at some sites

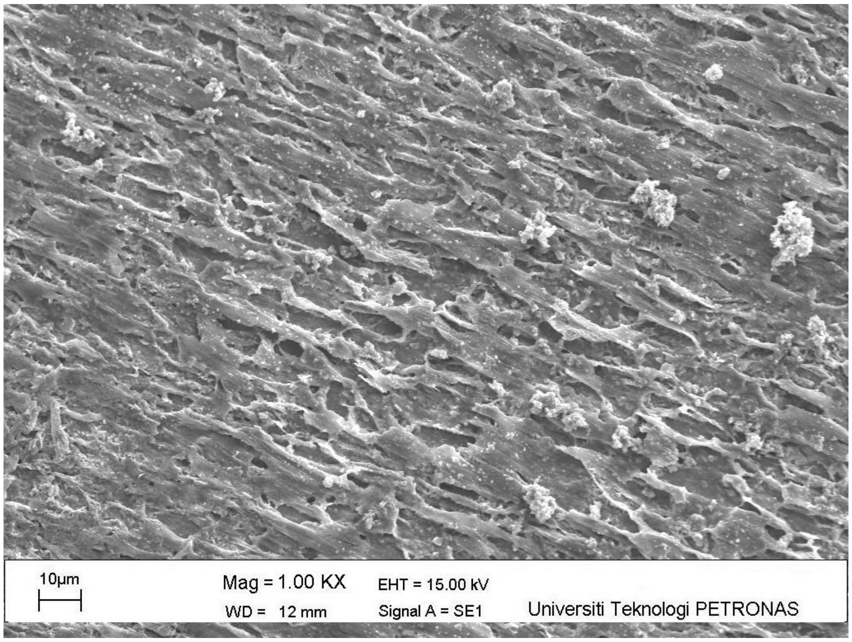

Figure 4.31. Face view of 60 ppm acetic acid added sample after 96 hours shows dense $FeCO_3$ film covers almost all steel surface

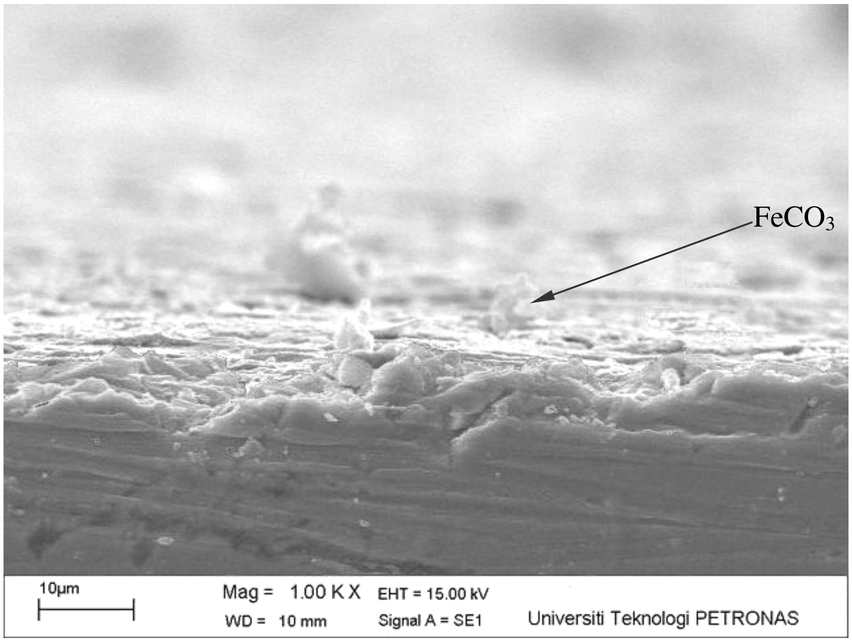

Figure 4.32. Cross section view of 60 ppm acetic acid added sample after 24 hours

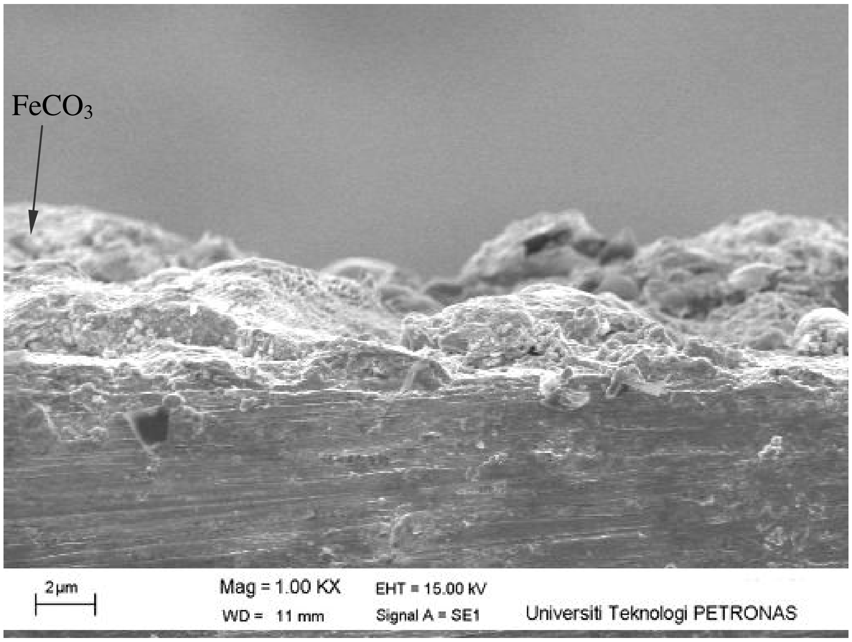

Figure 4.33. Cross section view of 60 ppm acetic acid added sample after 96 hours

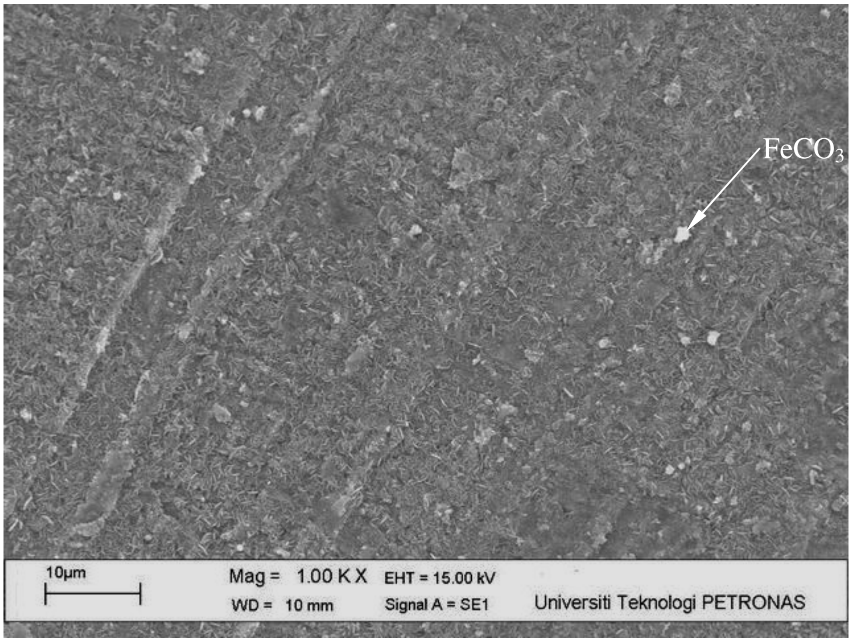

Figure 4.34. Face view of 100 ppm acetic acid added sample after 6 hours

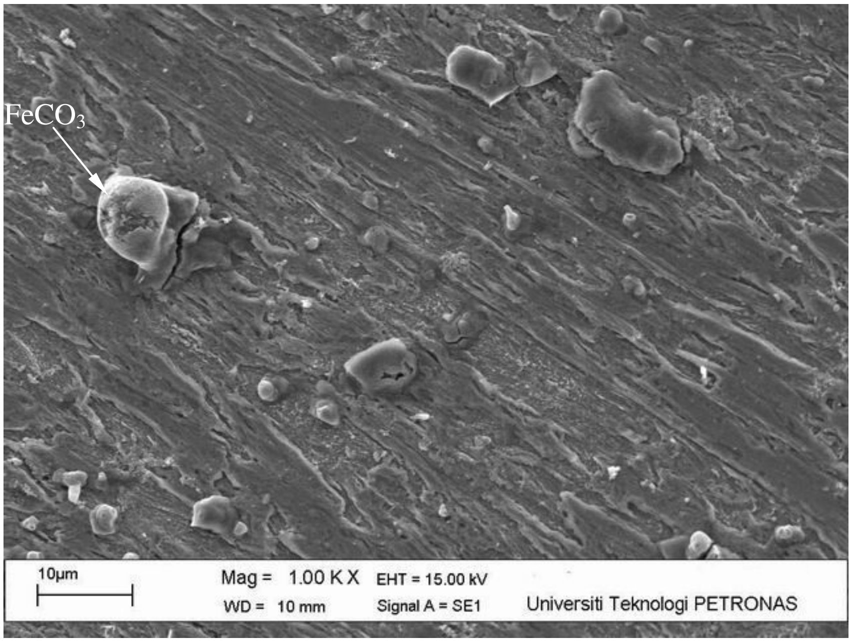

Figure 4.35. Face view of 100 ppm acetic acid added sample after 12 hours

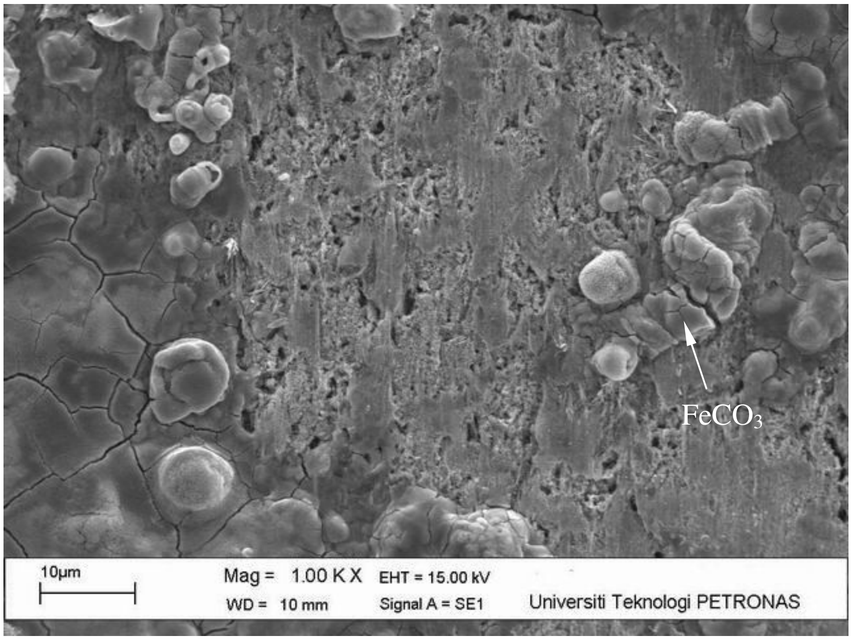

Figure 4.36. Face view of 100 ppm acetic acid added sample after 24 hours

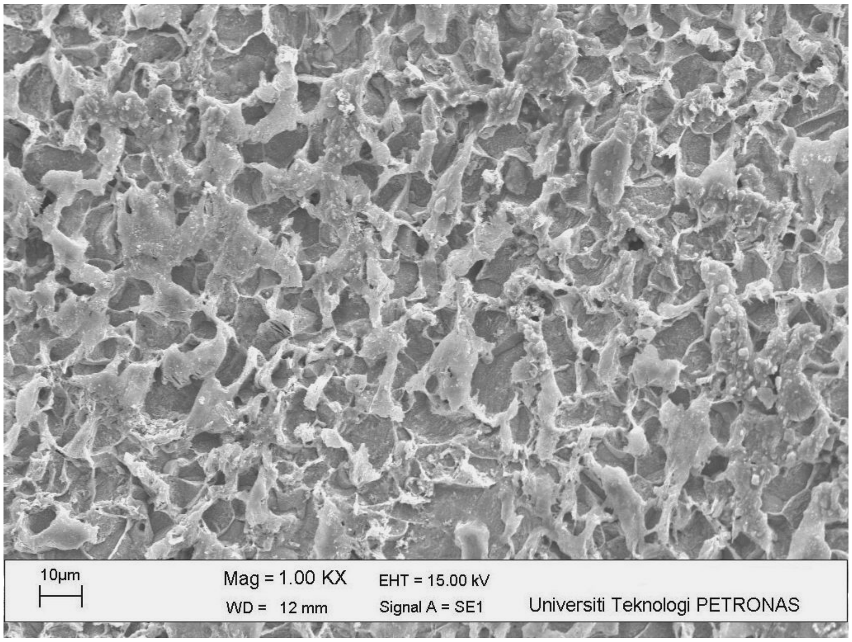

Figure 4.37. Face view of 100 ppm acetic acid added sample after 96 hours shows growth of FeCO$_3$ film covers steel surface

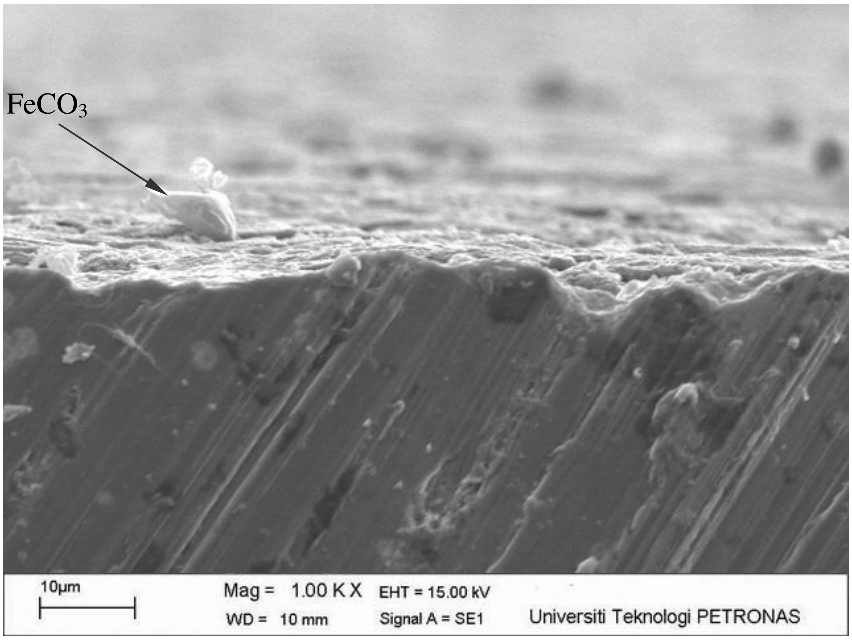

Figure 4.38. Cross section view of 100 ppm acetic acid added sample after 24 hours

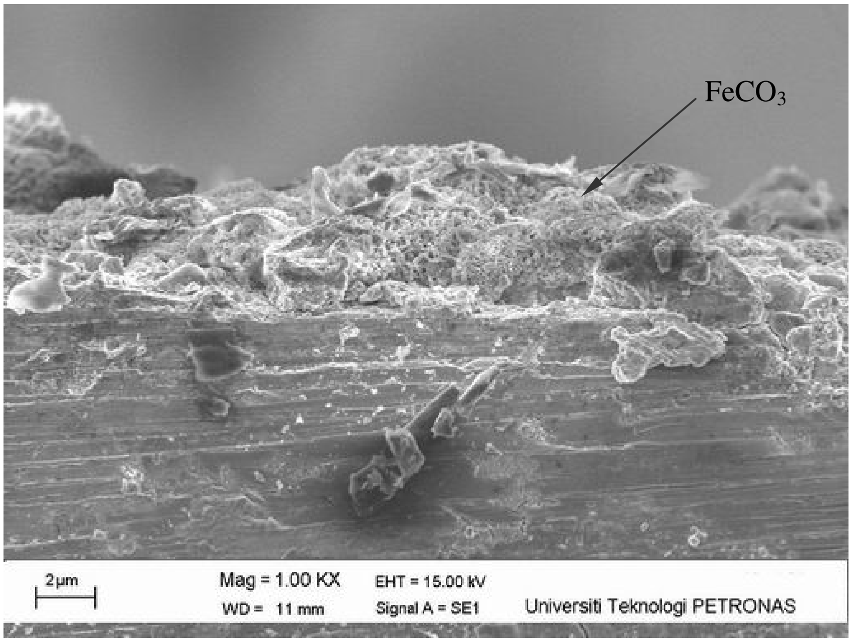

Figure 4.39. Cross section view of 100 ppm acetic acid added sample after 96 hours

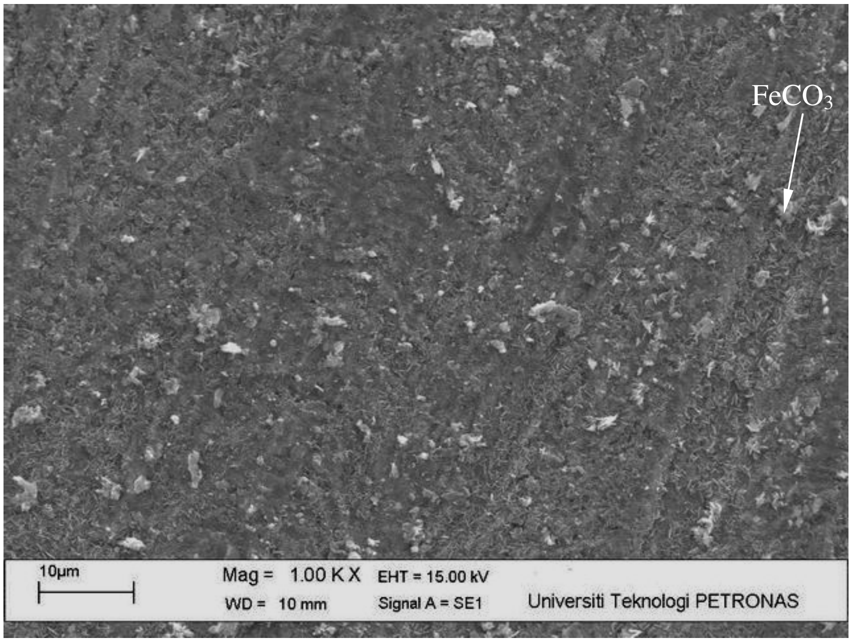

Figure 4.40. Face view of 400 ppm acetic acid added sample after 6 hours

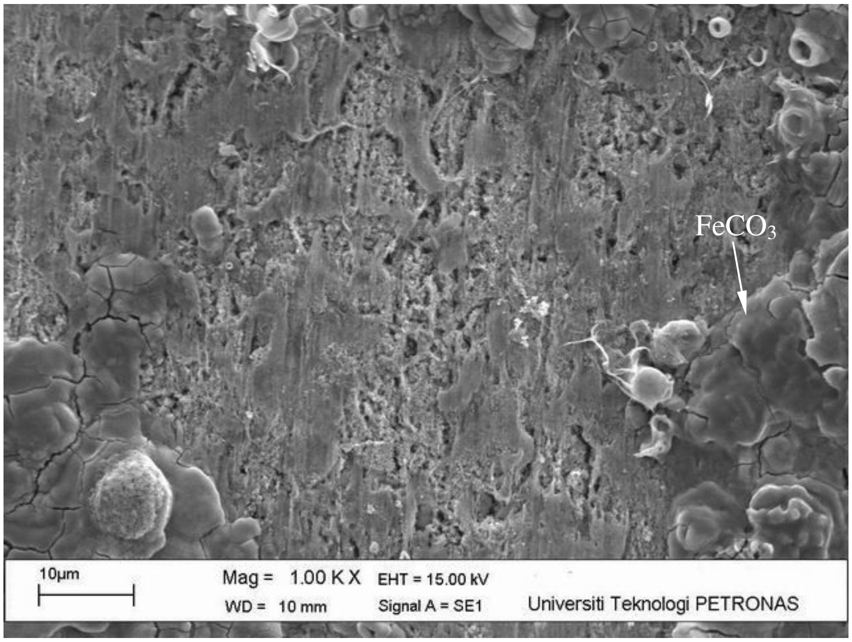

Figure 4.41. Face view of 400 ppm acetic acid added sample after 12 hours

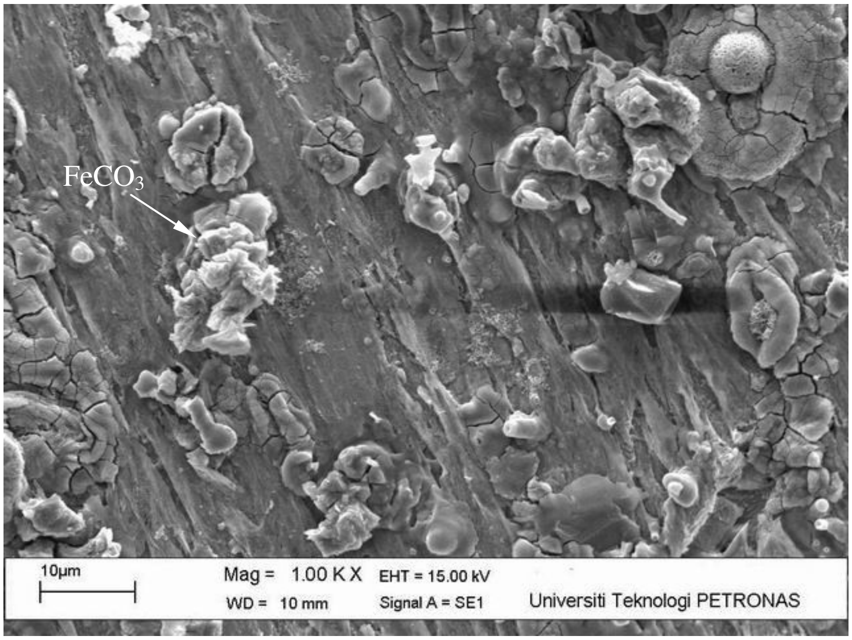

Figure 4.42. Face view of 400 ppm acetic acid added sample after 24 hours

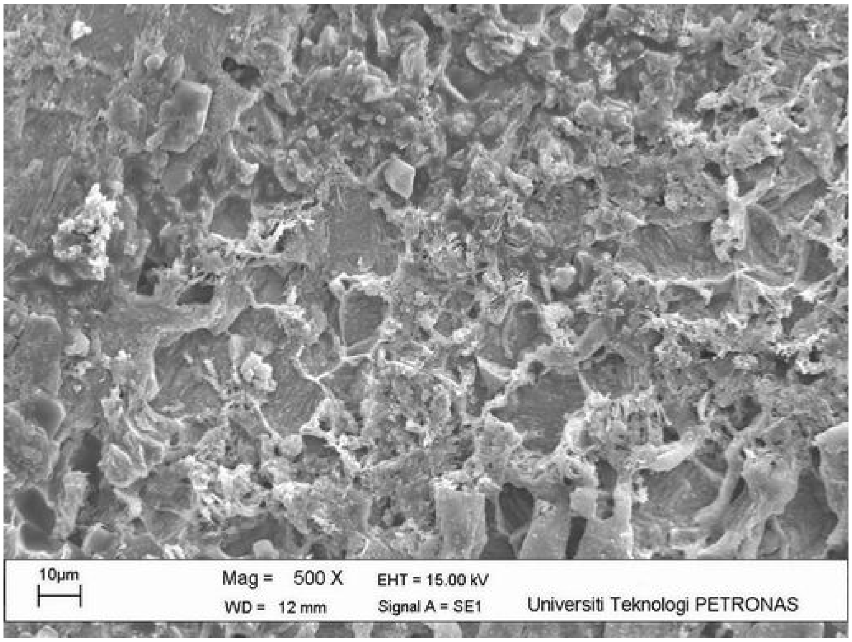

Figure 4.43. Face view of 400 ppm acetic acid added sample after 24 hours shows growth of FeCO$_3$ film on steel surface

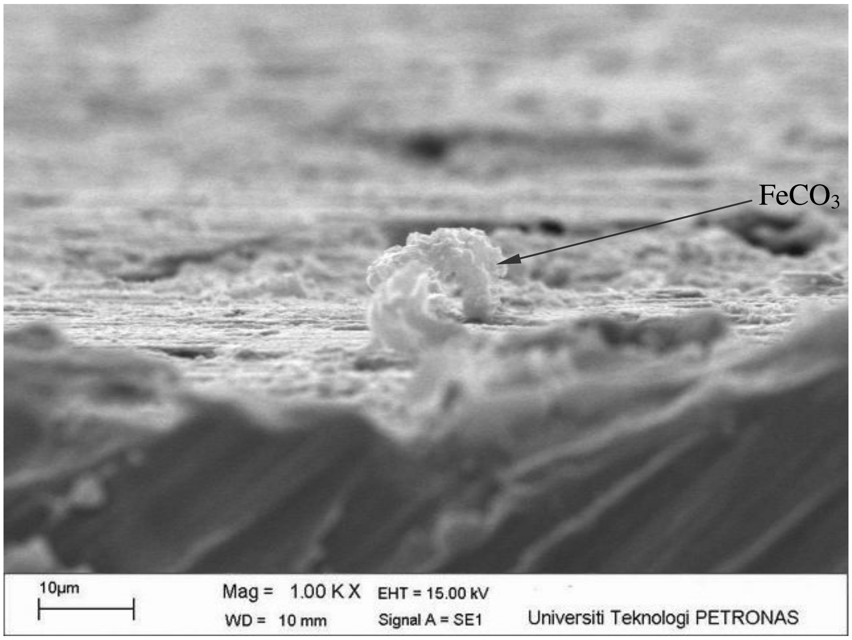

Figure 4.44. Cross section view of 400 ppm acetic acid added sample after 24 hours

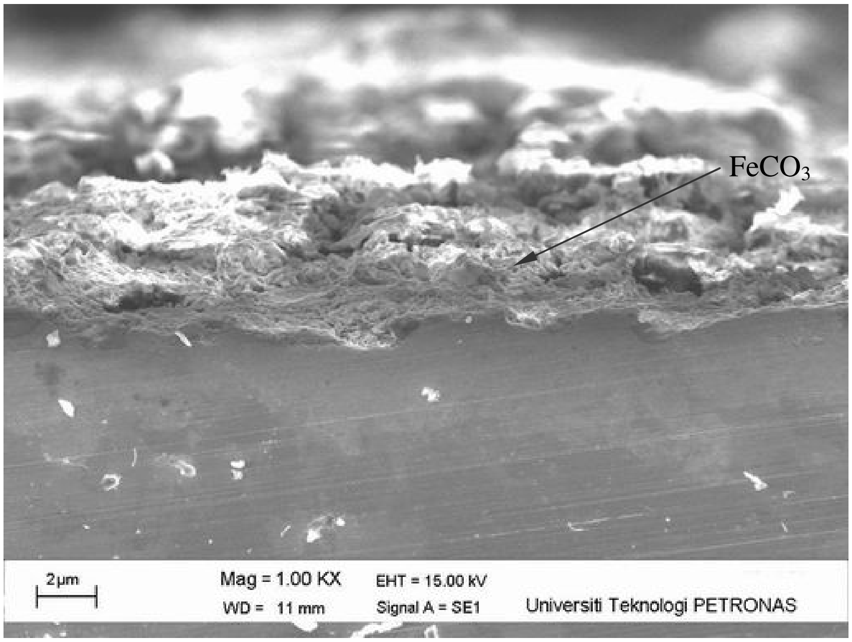

Figure 4.45. Cross section view of 400 ppm acetic acid added sample after 96 hours

For 60 ppm acetic acid added sample (Figure 4.28 to 4.33), first sample which immersed for 6 hours shows few numbers of film initiation, only few spots appear on steel surface. After 12 -24 hours of corrosion process, more $FeCO_3$ precipitate and grow on steel surface compared to 6 hours test. At the end of test (96 hours), $FeCO_3$ film almost covers the surface and thickness of film increases significantly in range 2 to 4 μm.

Figure 4.34 to 4.39 show SEM examination of 100 ppm acetic acid added corrosion samples. Similar with previous sample (60 ppm acetic acid), the steel surface still clean after 6 hours of test. There are some small spots appear on Figure 4.34, less compare with 10 and 20 ppm samples. Film initiation starts to precipitate after 12 hours of test (Figure 4.35). However, the film forms at some sites only which means there is still possibility for corrosion process at uncovered surface. Dense $FeCO_3$ film forms on 24 hours to 96 hours of test samples (Figure 4.36 and 4.37). $FeCO_3$ film precipitates and grows covering almost entire surface. The thickness of film is in range 3 to 5 μm.

At last, face view of 400 ppm acetic acid added samples are presented on Figure 4.40 to 4.45. After 6 hours immersion, iron carbonate does not precipitate significantly on steel surface even though corrosion rate is high (Figure 4.40). After 24 hours, dense $FeCO_3$ film exists and grows on steel surface. However, there are some uncovered area remain exist (Figure 4.42). At the ends of 96 hours test (Figure 4.43), $FeCO_3$ film covers and grows on almost entire surface and leaving small area uncovered. This result is in accordance with Gulbrandsen [10] which found that the existence of $Fe(CH3COO)_2$ may reduce the driving force for protective $FeCO_3$ film because of consuming Fe^{2+} ion and carried away to solution. The thickness of film is in range 2-6 μm as shown in Figure 4.45.

Based on those figures, $FeCO_3$ film precipitates on steel surface during film formation test. However, film growth is only dominated by 60, 100 and 400 ppm acetic acid samples, mainly between 24-96 hours. Dense $FeCO_3$ film forms earlier compared to the previous three samples (blank, 10 and 20 ppm samples). However, the dense of film does not decrease corrosion rate to low level as well as blank CO_2 corrosion. Corrosion rate reaches stability at high value. Blank CO_2 corrosion, 10 ppm and 20 ppm samples do not show good coverage of $FeCO_3$ film, only precipitation exists. Besides, corrosion rate for blank, 10 ppm and 20 ppm samples drop into low level after few hours of corrosion test. Hence, the amount of $FeCO_3$ film precipitates on steel surface is considered low as well. If cross section view picture compared with face view picture on similar parameter, it is seen that $FeCO_3$ film tends to form new nuclei or grows along steel surface rather than make the film thicker.

Precipitation of iron carbonate goes through two phases: nucleation and crystal growth. The behavior of film growth is unpredictable since the initiation or nucleation of film is in random order. Crystal grows from large number of nuclei, which join each other at existing crystal. In other words, film tends to grows where there is an existing nuclei as similar phenomena of crystal growth. It is obvious that size of film, which forms earlier getting larger, while for the other area, nucleation just begin (small size of film) and the rest, blank site still appears. During growth, new nuclei will remain precipitate at blank site. However, these secondary nuclei formed will grow slower than primary nuclei as corrosion rate already decreased (film-covered factor).

Since the film formed does not cover entire metal surface, it is difficult to carry this result as quantitative parameter for calculation purpose. The reason is that the film growth prediction or modeling is made based on increasing of dense film thickness during corrosion process (one-dimensional prediction) while based on SEM test, there is still uncovered area exists which make the calculation develop to three dimensional with uncertainties. Hence all SEM pictures above remain as qualitative result and only could be compared each other in this scope.

As shown from experiments, $FeCO_3$ film is formed in natural filming condition. And it is also observed that there is a small film-free area found on some sites. In the next discussion, theoretical analysis is presented to determine saturation condition and precipitation rate of the $FeCO_3$ film formation.

4.4. Theoretical Calculation of Film formation in Natural Condition

Prior to discussion about kinetic of $FeCO_3$ film with and without acetic acid, it is necessary to determine equilibrium condition of the species in the solution during corrosion process. Equilibrium constants and chemical reactions are described in table below. Based on experimental parameters; temperature 90°C (363 K); pH 5.5 and pressure of CO_2 is 1 bar, concentration of CO_2, H_2CO_3, HCO_3^- and CO_3^{2-} are calculated as follow:

Table 4.1 Equilibrium constant of species involved in CO_2 corrosion

Description :	Dissolution of carbon dioxide
Reaction :	$CO_2(g) \rightleftharpoons CO_2(aq)$ (17)
Equilibrium constant :	$K_d = \frac{[CO_2(aq)]}{pCO_2}$ (18)
$\log K_d = 108.3865 + 0.01985076T - \frac{6919.53}{T} - 40.45154 \log T + \frac{669365}{T^2}$ (Plummer) (29)	
Description :	Hydration of CO_2
Reaction :	$CO_2 + H_2O \rightleftharpoons H_2CO_3$ (19)
Equilibrium constant :	$K_{hyd} = \frac{[H_2CO_3]}{[CO_2]}$ (30)
$K_{hyd} = 0.00258$ (31)	
Description :	Dissociation of carbonic acid
Reaction :	$H_2CO_3 \rightleftharpoons H^+ + HCO_3^-$ (20)
Equilibrium constant :	$K_{a1} = \frac{[H^+][HCO_3^-]}{[H_2CO_3]}$ (32)

Table 4.1 (cont'd)

<table>
<tr><td colspan="2">$\log K'_{a1} = \frac{29688.2}{T} + 81.84\ln(T) - 0.0896488T - \frac{2046790}{T^2} - 522.461$ (33)
$K_{a1} = K'_{a1}\left(K_{hyd} + \frac{1}{K_{hyd}}\right)$ (34)</td></tr>
<tr><td>Description :</td><td>Dissociation of bicarbonate</td></tr>
<tr><td>Reaction :</td><td>$HCO_3^- \rightleftharpoons H^+ + CO_3^{2-}$ (21)</td></tr>
<tr><td>Equilibrium constant :</td><td>$K_{a2} = \frac{[H^+][CO_3^{2-}]}{[HCO_3^-]}$ (35)</td></tr>
<tr><td colspan="2">$\log K_{a2} = -\frac{2730.7}{T} - 0.02199T + 5.388$ (36)</td></tr>
<tr><td>Description :</td><td>Precipitation of Iron carbonate</td></tr>
<tr><td>Reaction :</td><td>$Fe^{2+} + CO_3^{2-} \rightarrow FeCO_3$ (25)</td></tr>
<tr><td>Equilibrium constant :</td><td>$K_{sp} = [Fe^{2+}][CO_3^{2-}]$ (37)</td></tr>
<tr><td colspan="2">$\log K_{SP} = -59.3498 - 0.041377 - \frac{2.1963}{T} + 24.5724\log(T) + 2.518I^{0.5} - 0.657I$ (38)</td></tr>
<tr><td>Description :</td><td>Dissociation of acetic acid</td></tr>
<tr><td>Reaction :</td><td>$CH_3COOH \rightleftharpoons H^+ + CH_3COO^-$ (27)</td></tr>
<tr><td>Equilibrium constant :</td><td>$K_{HAc} = \frac{[H^+][CH_3COO^-]}{[CH_3COOH]}$ (39)</td></tr>
<tr><td colspan="2">Kharaka: $\log K_{HAc} = -6.66104 + 0.0134916T - 2.37856\times10^{-5}T^2$ (40)
At 90^oC, $K_{HAc} = 1.265\times10^{-5}$ molar</td></tr>
</table>

Using experiments parameters, result of each calculation is presented below:

- Dissolution of carbon dioxide

  $[CO_2]$ = 0.01143 mol/L

- Carbon dioxide hydration

  $[H_2CO_3]$ = 2.948 x 10^{-5} mol/L

- Carbonic acid dissociation

  $[HCO_3^-]$ = 1.6027 x 10^{-3} mol/L

- Bicarbonate dissociation

$$\left[CO_3^{2-}\right] \quad = 3.8716 \times 10^{-8} \text{ mol/L}$$

If similar equations are applied in pH range 4-7, plot of species concentration can be displayed as in Figure 4.46

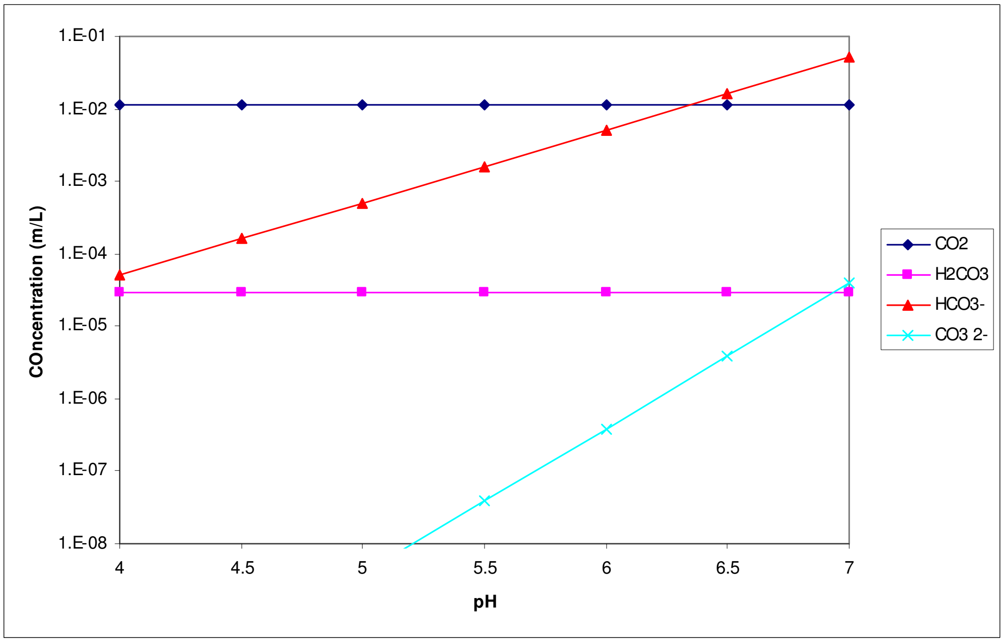

Figure 4.46. Concentration of species involved in CO_2 corrosion environment in range pH 4-7 at 90°C; pressure 1 bar

Water chemistry calculation for acetic acid added solution is similar to the previous calculation. The only difference is that there is one additional species reacts with metal surface, which is acetate ion (CH_3COO^-).

Total CH_3COO^- concentration in solution is obtained from acetic acid and sodium acetate (CH_3COONa) added during experiment setup. According to experimental parameter with pH 5.5, acetic acid added were 10 ppm, 20 ppm, 60 ppm, 100 ppm and 400 ppm. Total CH_3COO^- concentration can be calculated using equilibrium condition method and Henderson-Hesselbalch equation.

$$\mathrm{pH} = \mathrm{pK_a} + \log \frac{[\mathrm{CH_3COO^-}]}{[\mathrm{CH_3COOH}]} \tag{41}$$

With pH 5.5, pKa at 90^{o}C = 4.898 (equation 25) and known concentration of $\mathrm{CH_3COOH}$, the results is tabulated at table below:

Table 4.2 Initial concentration of total acetate ion in the solution

$[\mathrm{CH_3COOH}]$		$[\mathrm{CH_3COONa}]$	**Total** $[\mathrm{CH_3COO^-}]$ **(mol/L)**
(ppm)	**mol/L**	**mol/L**	
10	1.667E-04	6.669E-04	6.700E-04
20	3.333E-04	1.334E-03	1.337E-03
60	1.000E-03	4.001E-03	4.004E-03
100	1.667E-03	6.669E-03	6.672E-03
400	6.667E-03	2.668E-02	2.668E-02

Concentration of acetic acid and sodium acetate as shown in Table 4.2 above will be used to determine accumulated Fe^{2+} ion during precipitation process.

4.5. Kinetic of $FeCO_3$ Film Precipitation

4.5.1. Accumulated Fe^{2+} ion calculation

As explained in the literature review, $FeCO_3$ is the main product of CO_2 corrosion. Film formation is complex process and the precipitation rate of iron carbonate is the main controlling factor in this environment. When the concentration of Fe^{2+} and CO_3^{2-} exceed solubility limit (K_{sp}) in aqueous solution, iron carbonate precipitates on steel surface. Saturation is needed for the formation of full protective film. Once film forms, it will grows and covers steel surface from further corrosion process.

Chemical reaction involved during corrosion process with and without acetic acid is already described in previous chapters, such as:

$$Fe^{2+} + CO_2(aq) + H_2O \rightleftharpoons FeCO_3(s) + H_2 \quad (23)$$

$$Fe^{2+} + 2(CH_3COOH) \rightarrow Fe(CH_3COO)_2 + H_2 \quad (28)$$

For blank CO_2 corrosion, corrosion product is only $FeCO_3$, while with the presence of acetic acid/ acetate, there is another corrosion product which is $Fe(CH_3COO)_2$. Since entire experiments using pH < 7, CO_3^{2-} is a minority species, Mendoza and Turgoose[13] proposed that HCO_3^- has to be included as the precipitable ion. Then the formation of iron carbonate becomes:

$$Fe^{2+} + HCO_3^- \rightleftharpoons FeCO_3 + H^+ \quad (24)$$

With modification of equilibrium constant :

$$\frac{K_{SP}}{K_{a2}} = \frac{[Fe^{2+}][HCO_3^-]}{[H^+]} \quad (42)$$

The value of K_{SP} is the function of temperature and ion activity and it has been calculated and compared by Wei Sun and Nesic[38]. Final K_{sp} equation is:

$$\log[K_{SP}] = -59.3498 - 0.041377 - \frac{2.1963}{T} + 24.5724\log(T) + 2.518I^{0.5} - 0.657I \quad (38)$$

Which at 90°C the value of $K_{SP}\ FeCO_3 = 4.35154 \times 10^{-12}$ mol/L

According to above equilibrium formula, concentration of Fe^{2+} needed for precipitation process at pH 5.5 without acetic acid is

$$\left[Fe^{2+}\right] = \frac{K_{SP}\left[H^{+}\right]}{K_{a2}\left[HCO_3^{-}\right]} \tag{43}$$

$$= \frac{\left(4.35154\times10^{-12}\right)\left(10^{-5.5}\right)}{\left(7.639\times10^{-11}\right)\left(1.6027\times10^{-3}\right)}$$

$$= 1.124 \text{ x } 10^{-4} \text{ mol/L}$$

Total equilibrium concentration of Fe^{2+} with the presence of acetic acid is determined by concentration of HCO_3^{-} and CH_3COO^{-}. Equation from Gulbrandsen and Bilkova[14] can be used to quantify concentration of Fe^{2+} ion.

$$\left[Fe^{2+}\right] = \frac{\left[Ac^{-}\right]+\left[HCO_3^{-}\right]}{2} \tag{44}$$

Hence, using above equation, concentration Fe^{2+} needed for precipitation for blank and with the presence of acetic acid can be calculated and the result is tabulated in table below:

Table 4.3. Concentration of Fe^{2+} required to reach saturated condition with presence of acetic acid

[Ac^-] total	**[HCO_3^-]**	**[Fe^{2+}] min for precipitation**
mol/L	**mol/L**	**mol/L**
0	0.001603	0.00080
0.000670	0.001603	0.00114
0.001337	0.001603	0.00147
0.004004	0.001603	0.00280
0.006672	0.001603	0.00414
0.026679	0.001603	0.01414

The entire calculation results above shows minimum Fe^{2+} concentration needed for film formation (saturated condition) under equilibrium for both blank CO_2 corrosion and with the presence of acetic acid.

The amount of Fe^{2+} released during LPR test was not directly measured. However, it still can be calculated from corrosion rate equation as guided by ASTM G102 about calculating mass loss. The result is presented in figure below:

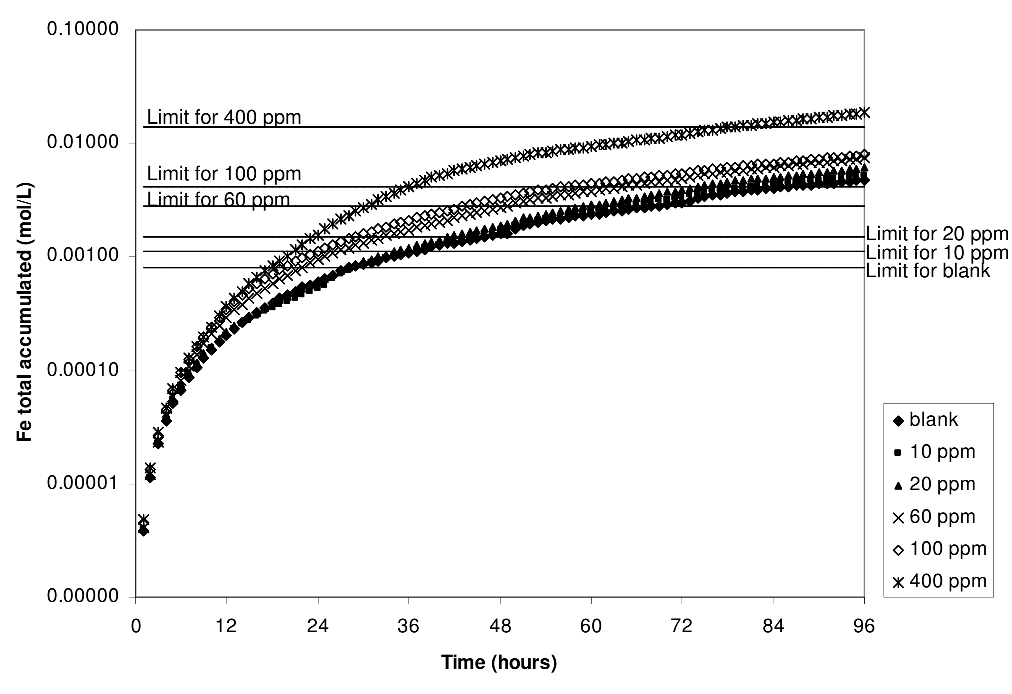

Figure 4.47. Accumulated Fe^{2+} ion during CO_2 corrosion process, with and without acetic acid (T 90°C; pH 5.5; p 1 bar)

According to Figure 4.47 above, Fe^{2+} ion reach the limit for precipitation for all condition. However, the time needed to reach saturation varies among them. Sample with 400 ppm acetic acid has the longest time to reach the limit for precipitation (approximately 78 hours). While the shortest time needed for precipitation is presented by blank CO_2 corrosion sample. However, based on cross sectional SEM pictures, $FeCO_3$ film formed remains thin at the end of test (Figure 4.17) because of low corrosion rate since beginning of LPR testing. On the other hand, the thickness of $FeCO_3$ film for sample with 400 ppm acetic acid is almost similar with 60 and 100 ppm samples. It is understandable since the saturation limit for this sample is the highest compare to others. Saturation of 400 ppm acetic acid is reached after 78 hours of test. Hence, it only has 18 hours until ends of test to precipitate on steel surface.

4.5.2. Precipitation rate calculation

Film growth depends primarily on the kinetics of scale formation and it changes with time as the corrosion and precipitation rate change. Semi empirical expressions have been used to represent the precipitation process. Johnson and Tomson proposed semi-empirical equation to develop precipitation rate (PR) equation, which will be used here[27]:

$$PR = .k_r.K_{sp}\left\{S^{0.5}-1\right\}^2 \ (\text{mol/m}^3\text{s}) \qquad \text{or}$$

$$PR = e^{54.8-\frac{123\text{kJ/mol}}{RT}} K_{sp}\left\{S^{0.5}-1\right\}^2 \tag{46}$$

which :

PR = precipitation rate $\left(\text{mol/m}^3\text{s}\right)$

k_r = Arrhenius equation $= e^{54.8-\frac{123\text{kJ/mol}}{RT}} \left(\text{kg}^2/\text{mol}\,\text{m}^2\text{s}\right)$

K_{SP} = solubility product limit $\left(\text{mol}^2/\text{kg}^2\right)$

S = saturation of corrosion product $= \dfrac{\left[Fe^{2+}\right]\left[CO_3^{2-}\right]}{K_{sp}}$

$\left[Fe^{2+}\right]$ = concentration of Fe^{2+}

$\left[CO_3^{2-}\right]$ = concentration of CO_3^{2-}

R = constant

T = temperature in Kelvin

As proposed by Mendoza and Turgoose, since CO_3^{2-} is minority species, saturation equation above is slightly modified into:

$$S = \frac{[Fe^{2+}][HCO_3^-]K_{a2}}{[H^+]K_{sp}} \tag{47}$$

By entering Fe^{2+} resulted from accumulated Fe^{2+} calculation previously, precipitation rate for every hour can be presented on graph below:

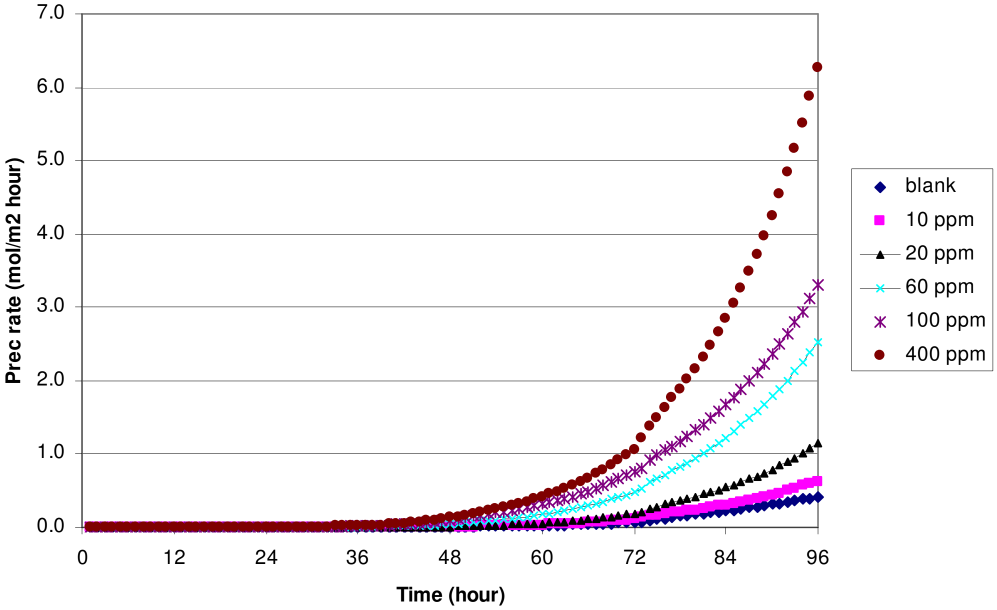

Figure 4.48 Precipitation rate of Fe^{2+} on CO_2 corrosion with and without acetic acid (T 90°C; pH 5.5; p 1 bar)

According to Figure 4.48 above, precipitation rate for 0, 10 and 20 ppm CO_2 corrosion sample tends to constant from beginning to 60 hours of test. For CO_2 corrosion with 60, 100 and 400 ppm acetic acid, precipitation rate is constant from beginning to 40 hours of test. The slopes of precipitation rate also shows different trends among 0, 10 and 20 ppm acetic acid samples compared to sample with 60, 100 and 400 ppm acetic acid which have steeper slope or higher precipitation rate. It establishes the fact that 10 and 20 ppm in concentration of acetic acid do not affect corrosion rate and $FeCO_3$ film formation significantly.

4.6. Comparison between Experiment Results and Prediction Model

Determining corrosion rate in the service is more complex compared to laboratory experiment. This is because of lot of factors related to operating parameter involved. Some prediction model tools are proposed to determine corrosion rate of the pipeline and other production and exploration equipments. Experimental results obtained have been compared with Cassandra[49], Norsok[50] and ECE prediction tool[51]. The calculation with prediction tools here uses similar parameter with experiment parameters and simplified to generate possible results. However, there are some experiments parameters, which cannot be accommodated by the software, which is the flow or the velocity of solution. Comparison on corrosion rate between experiments and prediction tools are presented on figures below:

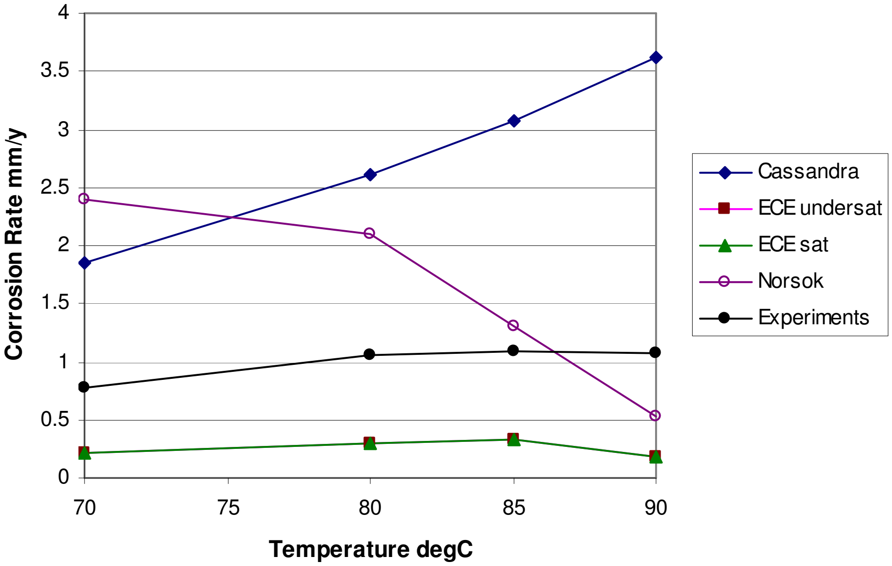

Figure 4.49. Corrosion rate between experiments and prediction tools at 70-90°C; pH 5.5, CO_2 pressure 1 bar and 0 ppm acetic acid

Based on Figure 4.49 above, for blank CO_2 corrosion, Cassandra tool is showing an increasing of corrosion rate with the increase of temperature, while ECE and Norsok results show slight increase and the values are far below Cassandra. Experiment result is in between those prediction tool and decreases with the increase of temperature. For ECE, there is no difference between the saturated or undersaturated of dissolved Fe^{2+} ion in the solution (inline graph). There is a similarity in trend between experiment and ECE-Norsok prediction tool, which is the tendency of decreasing of corrosion rate at high temperatures.

For corrosion rate with the presence of acetic acid, experiment result is only compared with ECE prediction tool since there is no complete information about acetic acid parameter used in Cassandra and Norsok. Corrosion rate, which is calculated using ECE, is divided in to two result, undersaturated and saturated Fe^{2+} ion. All data with various ppm of acetic acid are presented in the figures below:

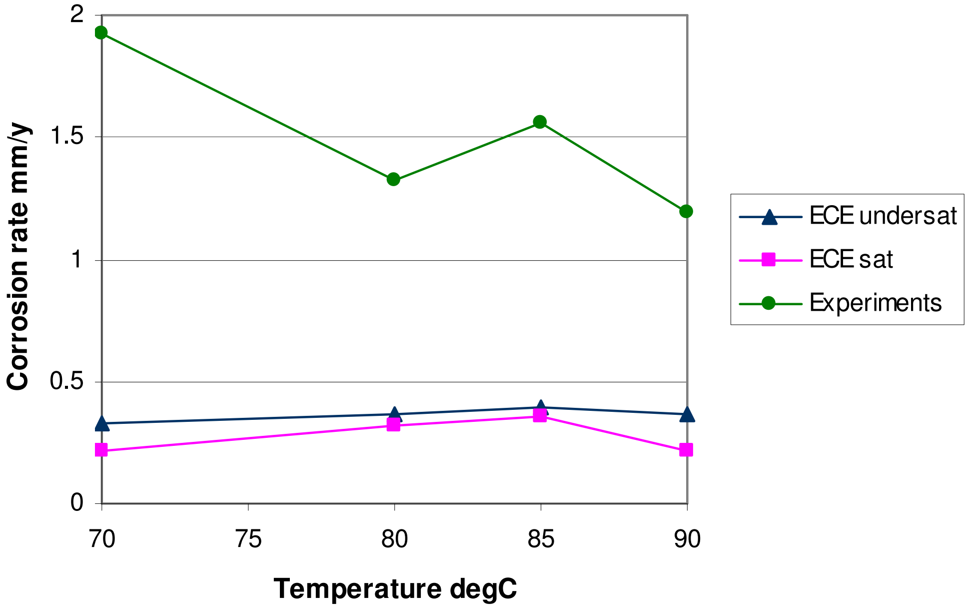

Figure 4.50. Corrosion rate between experiments and prediction tool at 70-90°C; pH 5.5; CO_2 pressure 1 bar and 10 ppm acetic acid

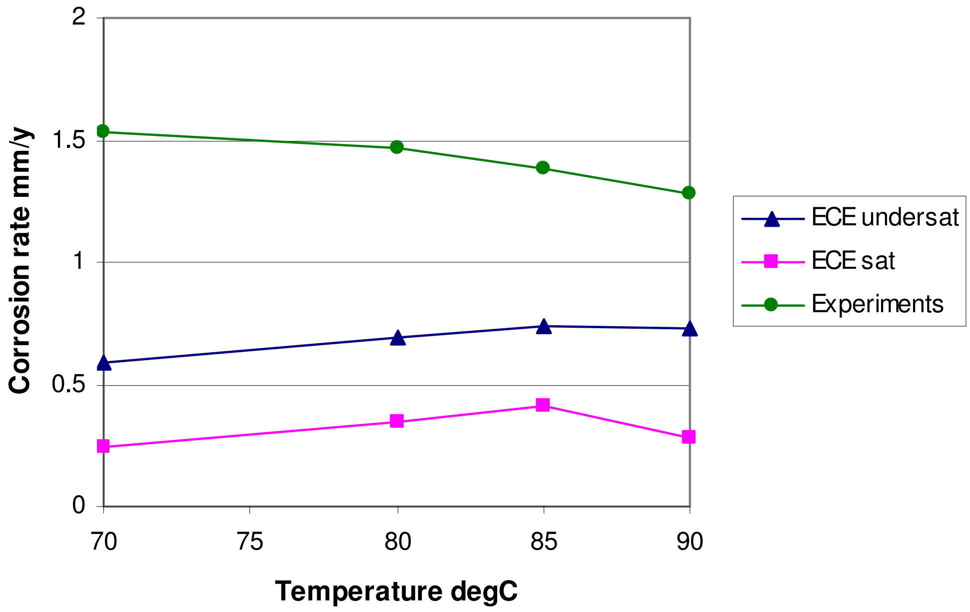

Figure 4.51. Corrosion rate between experiments and prediction tool at 70-90°C; pH 5.5; CO_2 pressure 1 bar and 20 ppm acetic acid

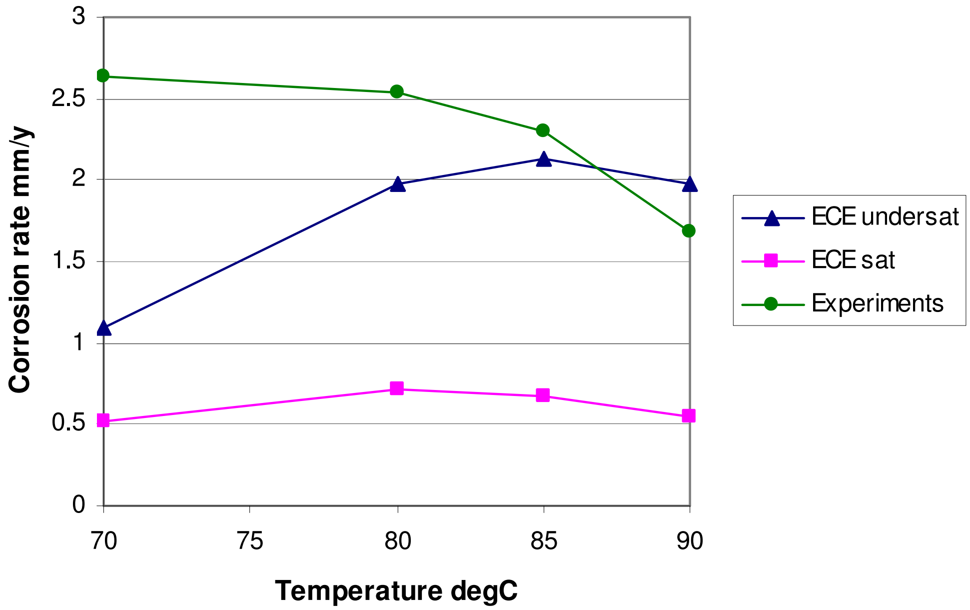

Figure 4.52. Corrosion rate between experiments and prediction tool at 70-90°C; pH 5.5; CO_2 pressure 1 bar and 60 ppm acetic acid

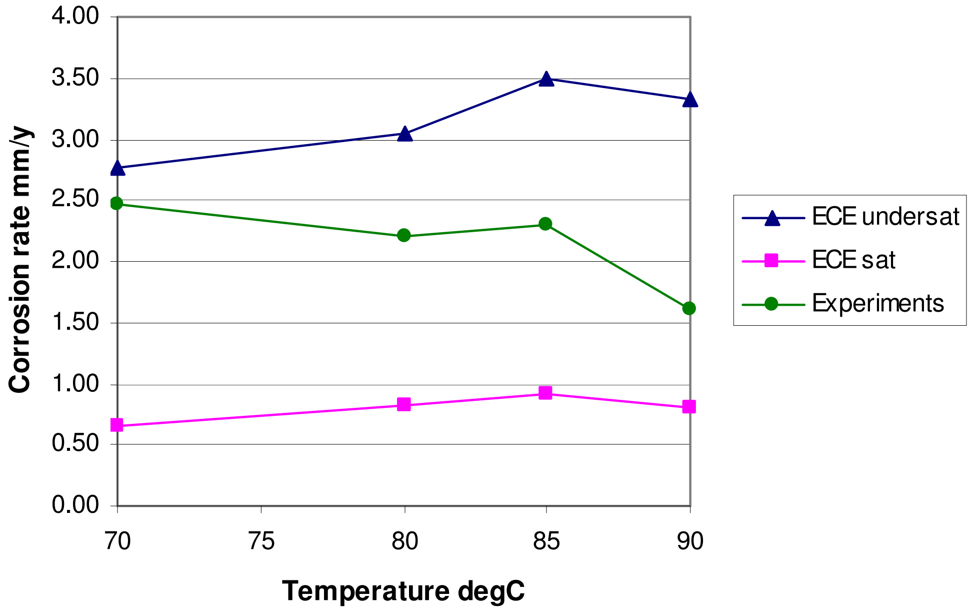

Figure 4.53. Corrosion rate between experiments and prediction tool at 70-90^{o}C; pH 5.5; CO_2 pressure 1 bar and 100 ppm acetic acid

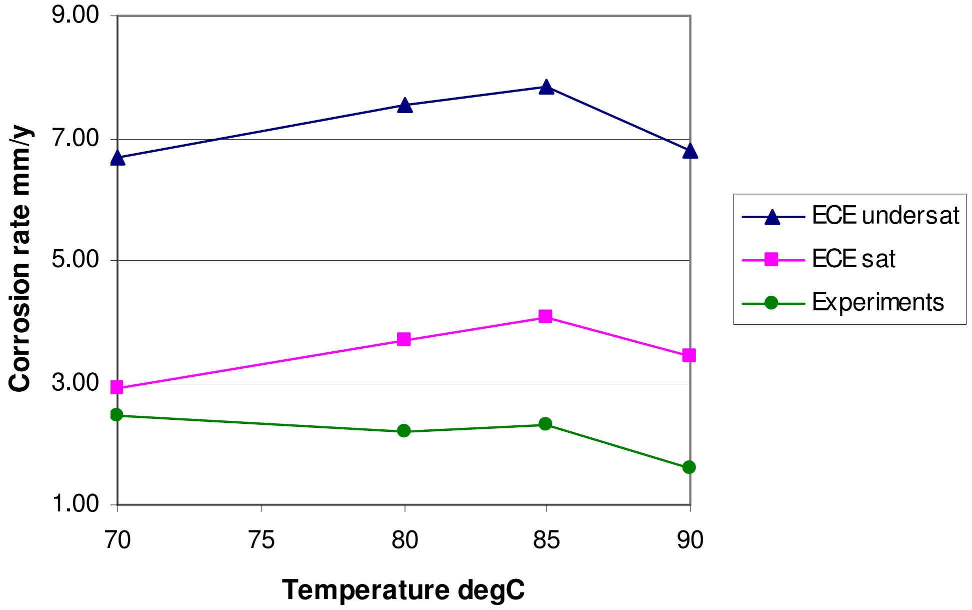

Figure 4.54. Corrosion rate between experiments and prediction tool at 70-90^{o}C; pH 5.5; CO_2 pressure 1 bar and 400 ppm acetic acid

Figure 4.50 to 4.54 above show the comparison between experiment and ECE prediction tool for corrosion rate with the presence of acetic acid. Corrosion rate calculated with ECE in undersaturated and saturated condition shows similar trend compared to experiment results for all acetic acid samples. Corrosion rate tends to decreases at 90^{o}C for both methods. It can be seen that higher acetic acid concentration, lower the corrosion rate for experiments result, compared to ECE prediction tool While in saturated condition, ECE prediction tool show lower corrosion rate for entire acetic acid concentration. However, there is no enough information from the prediction tool about the factors cause decreasing of corrosion rate at high temperature (for example film formation effect). The only information gained from the tool is only conformity about corrosion rate trends with experiments.

CHAPTER V
CONCLUSIONS

5.1. Conclusions

The presence of acetic acid increases corrosion rate of mild steel in CO_2 environment significantly above 60-ppm in concentration, while for 10-20 ppm in concentration, there is only small effect to corrosion rate and $FeCO_3$ film formation. With less than 60 ppm acetic acid, corrosion rate drops in to low level in few hours, as well as blank CO_2 corrosion. Acetic acid affects corrosion process by competition with bicarbonate ions to react with Fe^{2+} ions. This yields a delay of corrosion rate stability, mainly above 60 ppm acetic acid.

There is no evidence the existence of precipitated iron(II) acetate ($Fe(CH_3COO)_2$) on steel surface due to high solubility of iron(II) acetate. The only product of CO_2 corrosion, which precipitates on steel surface, is iron carbonate ($FeCO_3$). Saturation of Fe^{2+} ion is reached for both blank CO_2 corrosion and with the presence of acetic acid. However, time needed to reach saturation of Fe^{2+} ion is different among all acetic acid concentration. With 400 ppm of acetic acid, it needs 78 hours to reach saturation limit. Hence it is understandable if the film thickness relatively similar compared to corrosion with 60 and 100 ppm in concentration. The thickness of $FeCO_3$ film is in range 2-6 μm. High density and growth of iron carbonate film are obtained with more than 60-ppm acetic acid.

Comparison between experiment result and prediction tools shows an agreement about trend of corrosion rate with increases of temperature. However, there is no sufficient information on prediction tool regarding the effect of film formation to corrosion rate. Overall, the existence of $FeCO_3(s)$ film precipitation covers steel surface and leave small amount area uncovered. This condition is considered semi-protective for further corrosion process.

5.2. Recommendations

The extension for LPR testing is highly recommended to observe corrosion rate stability and iron carbonate film growth in long term condition. This recommendation is for measuring and calculating film thickness purpose, since recent work could not meet significant thickness for measurements. In addition, it is recommended to perform an investigation of CO_2 corrosion on flow loop to represent of pipeline system. Addition of other gas for example hydrogen sulfide and addition of inhibitor are still possible to investigate.

REFERENCES

1. Crolet J.L., N. Thevenot and A. Dugstad, (1999), "Role of Free Acetic Acid on the CO_2 Corrosion of Steels", Corrosion/99, Paper No. 24, NACE International, Houston, Texas.
2. Fajardo, V., Canto, C., Brown, B., and Nesic, S., (2007), "Effect of Organic Acid in CO_2 Corrosion", Corrosion/2007, Paper No. 07319, NACE International, Houston, Texas.
3. Schmitt, G., Hörstemeier, M., (2006), "Fundamental Aspects Of CO_2 Metal Loss Corrosion – Part II: Influence of Different Parameters on CO_2 Corrosion Mechanism", Corrosion/06, Paper No. 06112, NACE International, Houston, Texas.
4. Ueda, M. and Takabe, H. (1999), Effect of Environmental Factor and Microstructure on Morphology of Corrosion Products in CO_2 Environments. Corrosion/99, Paper No. 13, NACE International, Houston, Texas.
5. Sun, Y., George, K. and Nesic, S., (2003), "the Effect of Cl^- and Acetic Acid on Localized CO_2 Corrosion in Wet Gas Flow", Corrosion/2003, Paper No. 03327, NACE International, Houston, Texas.
6. Nesic, S. and Nafday, O.A. (2005), Iron Carbonate Scale Formation and CO_2 Corrosion in the Presence of Acetic Acid. Corrosion/2005, Paper No. 05295, NACE International, Houston, Texas.
7. Gulbrandsen, E., Morard, J.H. and Crolet, J.L. (1999), Study of The Possible Mechanism of Steel Passivation in CO_2 Corrosion. Corrosion/99, Paper No. 624, NACE International, Houston, Texas.
8. Nesic, S., Nordsveen, M., Nyborg, R. Stangeland, A., (2001) "A Mechanistic Model for CO_2 Corrosion with Protective Iron Carbonate Films", Corrosion/01, Paper No. 40, NACE International, Houston, Texas.
9. Shreir L.L., Jarman, R.A., Burstein, G.T., "Corrosion Volume I: Metal/ Environment Reactions", 3rd ed, (2002), Butterworth-Heinemann

10. Hunnik, E.W.J., Pots, B.F.M. and Hendriksen, E.L.J.A. (1996), "The Formation of Protective $FeCO_3$ Corrosion Product Layers in CO_2 Corrosion", Corrosion/96, Paper No. 6, NACE International, Houston, Texas.
11. Gulbrandsen, E. and Bilkova, K., (2006), "Solution Chemistry Effects on Corrosion of Carbon Steels in Presence of CO_2 and Acetic Acid", Corrosion/06, Paper No. 06364, NACE International, Houston, Texas.
12. Stumm, W. and Morgan, J.J., (1995), "Aquatic Chemistry. Chemical Equilibria and Rates in Natural Waters", Wiley – Interscience Publication, John Wiley & Sons, Inc., New York.
13. Nordsveen M., Nesic S., Nyborg R. and Stangeland A., (2003), "A Mechanistic Model for Carbon Dioxide Corrosion of Mild Steel in the Presence of Protective Iron Carbonate Films – Part 1: Theory and Verification", Corrosion/01, Paper No. 01040, NACE International, Houston, Texas.
14. Mora-Mendoza, J.L., Turgoose, S., (2002), "Fe_3C Influence on The Corrosion Rate of Mild Steel in Aqueous CO_2 Systems Under Turbulent Flow Conditions", Corrosion Science 44, Elsevier Science Ltd.
15. Nesic S., Nordsveen M., Nyborg R. and Stangeland A., (2003), "A Mechanistic Model for Carbon Dioxide Corrosion of Mild Steel in the Presence of Protective Iron Carbonate Films – Part 2: A Numerical Experiment", Corrosion Science, Corrosion Vol. 59 No.6, NACE International, Houston, Texas.
16. Dayalan, E., de Moraes, F.D., Shadley, J.R., Shirazi, S.A. and Rybicki, E. F., (1998), "CO_2 Corrosion Prediction in Pipe Flow under $FeCO_3$ Scale-Forming Conditions", Corrosion/98, Paper No. 98051, NACE International, Houston, Texas.
17. Hedges, B. and McVeigh, L., (1999), "The Role of Acetate in CO_2 Corrosion: The Double Whammy", Corrosion/99, Paper No. 21, NACE International, Houston, Texas.
18. Dugstad, A., (2006), "Fundamentals Aspects of CO_2 Corrosion. Part I: Mechanism", Corrosion/06, Paper No. 06111, NACE International, Houston, Texas.
19. Garsany, Y. and Pletcher, D., (2002), "The Role of Acetate in CO_2 Corrosion of Carbon Steel: Has the Chemistry been Forgotten?", Corrosion/02, Paper No. 02273, NACE International, Houston, Texas.

20. Crolet, J.L., Thevenot, N. and Nesic, S. (1996), Role of Conductive Corrosion Products in the Protectiveness of Corrosion Layers. Corrosion/96, Paper No. 4, NACE International, Houston, Texas.
21. Ueda, M. and Takabe, H. (1998), “Effect of Organic Acid on CO_2 Corrosion of Carbon and Cr Bearing Steel”, Corrosion/98, Paper No. 35, NACE International, Houston, Texas.
22. Ueda M., Ikeda A., (1996), “Effect of Microstructure and Cr Content in Steel On CO_2 Corrosion”, Corrosion/96, Paper No.13, NACE International, Houston, Texas.
23. Sun, W. and Nesic, S., (2008) “Kinetics of Corrosion Layer Formation. Part 1 - Iron Carbonate Layers in Carbon Dioxide Corrosion”, Corrosion Science Section, Corrosion – April 2008, NACE International, Houston, Texas.
24. Nesic S., Lee K. L. John, (2003), “A Mechanistic Model for Carbon Dioxide Corrosion of Mild Steel in the Presence of Protective Iron Carbonate Films – Part 3: Film Growth Model”, Corrosion Science Section, NACE International.
25. Pursell M.J., Selman C. and Nielsen M.F., (1999), “Corrosion Risk Assessment and Risk Based Inspection for Sweet Oil and Gas Corrosion – Practical Experience”, Corrosion/99, Paper No. 9, NACE International, Houston, Texas.
26. Dugstad A., (1998), “Mechanism of Protective Film Formation During CO_2 Corrosion of Carbon Steel”, Corrosion/98, Paper No. 31, NACE International, Houston, Texas.
27. Singer, M., Nesic, S. and Gunaltun, Y., (2004), “Top of the Line Corrosion in Presence of Acetic Acid and Carbon Dioxide”, Corrosion/2004, Paper No. 04377, NACE International, Houston, Texas.
28. Johnson M.L. and Thomson M.B., (1991), “Ferrous Carbonate Precipitation Kinetics and its Impact on CO_2 Corrosion”, Corrosion/1991, Paper No. 268, NACE International.
29. Sun W. and Nesic S., (2005), “Basics Revisited : Kinetics of Iron Carbonate Scale Precipitation in CO_2 Corrosion”, Corrosion/2005, Paper No. 05195, NACE International, Houston, Texas.
30. Cabrini M., Hoxha G., Kopliku A. and Lazzari L., (1998), “Prediction of CO_2 Corrosion in Oil and Gas Wells. Analysis of Some Case Histories”, Corrosion/98, Paper No. 24, NACE International, Houston, Texas.

31. Gulbrandsen, E., (2007), "Acetic Acid and Carbon Dioxide Corrosion of Carbon Steel Covered with Iron Carbonate", Corrosion/06, Paper No. 07322, NACE International, Houston, Texas.

32. Oddo, J.E. and Tomson, M.B., (1999), "The Prediction of Scale and CO_2 Corrosion in Oil Field Systems", Corrosion/99, Paper No. 41, NACE International, Houston, Texas.

33. Dugstad, Lunde, L. and Nesic, S., (1994), "Control of Internal Corrosion in Multi-phase Oil and Gas Pipelines", Prevention of Pipeline Corrosion Conference, Marriot Houston Westside Hotel, Houston, Texas.

34. Nesic S., Postlethwaite J., and Olsen S., (1996), "An Electrochemical Model for Prediction of Corrosion of Mild Steel in Aqueous Carbon Dioxide Solutions", Corrosion Science, NACE International, Houston, Texas.

35. Nesic S., Thevenot N., Crolet J.L. and Drazic D.M., (1996), "Electrochemical Properties of Iron Dissolution in the Presence of CO_2 - Basics Revisited", Corrosion/96, Paper No. 3, NACE International, Houston, Texas.

36. Méndez, C., Singer, M., Camacho, A., Hernández, S., Nesic, S., Gunaltun, Y., Joosten, M., Sun, Y., Gabbetta, P., (2005), "Effect of Acetic Acid, pH and MEG on The CO_2 Top of The Line Corrosion", Corrosion/2005, Paper No. 05278, NACE International, Houston, Texas.

37. de Moraes, F.D., Shadley, J.R., Chen, J. and Rybicki, E.F., (2000), "Characterization of CO_2 Corrosion Product Scales Related to Environmental Conditions", Corrosion/2000, Paper No. 00030, NACE International, Houston, Texas.

38. Nyborg, R., (2002), "Overview of CO_2 Corrosion Models for Wells and Pipelines", Corrosion/02, Paper No. 02233, NACE International, Houston, Texas.

39. Nafday., O.A., (2004), "Film Formation and CO_2 Corrosion in The Presence of Acetic Acid", Thesis, Department of Chemical Engineering and the Russ College of Engineering and Technology, Ohio University, 2004.

40. Ismail, M.C., (2005), "Prediction of CO_2 Corrosion with the Presence of Acetic Acid", Thesis, School of Materials, Corrosion and Protection Centre, University of Manchester, UK.

41. Garsany, Y., Pletcher, D. and Hedges, B., (2002), “Speciation and electrochemistry of brines containing ion and carbon dioxide”, Journal of Electroanalytical Chemistry, no. 538-259, Elsevier Science, B.V.
42. George, K.S. and Nesic, S., (2007), “Investigation of Carbon Dioxide Corrosion of Mild Steel in The Presence of Acetic Acid – Part 1: Basic Mechanisms”, Corrosion Science Section, Corrosion – February 2007, NACE International, Houston, Texas.
43. Sun, W., Nesic. S. and Papavinasam, S., (2008), “Kinetics of Corrosion Layer Formation. Part 2 - Iron Sulfide and Mixed Iron Sulfide/Carbonate Layers in Carbon Dioxide/Hydrogen Sulfide Corrosion”, Corrosion Science Section, Corrosion – July 2008, NACE International, Houston, Texas.
44. Pots., B.F.M., John, R.C., Rippon, I.J., Thomas, M.J.J.S., Kapusta, S.D., Girgis, M.M. and Whitham, Tim, (2002), “Improvements on de Waard-Milliams Corrosion Prediction and Applications to Corrosion Management”, Corrosion/02, Paper No. 02235, NACE International, Houston, Texas.
45. Joosten, M.W., Kolts, J. and Hembree, J.W. (2002), Organic Acid Corrosion in Oil and Gas Production. Corrosion 2002, Paper No. 02294, NACE International, Houston, Texas.
46. Baboian, R., (2005), “Corrosion Tests and Standards: Application and Interpretation-Second Edition”, ASTM International, USA.
47. Atkins, P., Paula, J.D., (2002), "Physical Chemistry for the Life Sciences", Oxford University Press; 7th edition (January 2002), New York.
48. Lide, D.R., (2005), "CRC Handbook of Chemistry and Physics ", CRC Press, Boca Raton, Florida.
49. Hedges, B., Casandra, (2001), BP Corrosion, Inspection & Chemicals (CIC).
50. "CO_2 Corrosion Rate Calculation Model", NORSOK standard No. M-506, (1998), http://www.nts.no/norsok, (Oslo: Norwegian Technology Standards Institution).
51. Electronic Corrosion Engineer© (ECE©) program, Intetech Ltd. Salmon Court, Rowton, CHESTER CH3 6AT, UK
52. Fatah, M.C., Ismail, M.C., Kurniawan, B.A., (2008), “Comparison of CO_2 Corrosion Prediction Models Based on Field and Experimental Data”, International Conference on Plant Equipment and Reliability (ICPER), Selangor

APPENDIX A

DETAIL CALCULATION OF SPECIES IN THE SOLUTION

- Dissolution of carbon dioxide

$$CO_{2(g)} \Leftrightarrow CO_{2(aq)} \text{ and } K_d = \frac{[CO_2]}{p_{CO_2}}$$

at 90°C, K_d = 0.01143 mol/L.atm

Hence $[CO_2] = K_{sol}.p_{CO_2}$

= 0.1421 mol/L.atm x 1 atm

= 0.01143 mol/L

- Carbon dioxide hydration

$$CO_2 + H_2O \leftrightarrow H_2CO_3 \text{ and } K_{hyd} = \frac{[H_2CO_3]}{[CO_2]}$$

K_{hyd} = 0.00258

$[H_2CO_3] = K_{hyd}.[CO_2]$

= 0.00258 x 0.01143 mol/L

= 2.948×10^{-5} mol/L

- Carbonic acid dissociation

Carbonic acid dissociates in to two steps:

$$H_2CO_3 \leftrightarrow H^+ + HCO_3^- \text{ and } K_{a1} = \frac{[H^+][HCO_3^-]}{[H_2CO_3]}$$

K_{a1} = 1.7191×10^{-4} mol/L

Since solution's pH = 5.5, initial $[H^+] = 10^{-5.5}$

$$[HCO_3^-] \qquad = K_{a1}\frac{[H_2CO_3]}{[H^+]}$$

$$= 1.7191\times10^{-4}\times\frac{\cdot\,2.948\times10^{-5}}{10^{-5.5}}$$

$= 1.6027 \text{ x } 10^{-3}$ mol/L

- Bicarbonate dissociation

$$HCO_3^- \leftrightarrow H^+ + CO_3^{2-} \text{ and } K_{a2} = \frac{[H^+][CO_3^{2-}]}{[HCO_3^-]}$$

K_{a2} $= 7.639 \text{ x } 10^{-11}$

$$[CO_3^{2-}] \qquad = K_{a2}\frac{[HCO_3^-]}{[H^+]}$$

$$= 7.639\times10^{-11}\times\frac{1.6027\times10^{-3}}{10^{-5.5}}$$

$= 3.8716 \text{ x } 10^{-8}$ mol/L